ANALYSIS OF FISSIONABLE MATERIAL BY DELAYED EMISSIONS

A THESIS

Presented to

The Faculty of the Graduate Division

by

John McCloskey Jamieson

In Partial Fulfillment

of the Requirements for the Degree

Doctor of Philosophy

in the School of Nuclear Engineering

Georgia Institute of Technology

February, 1976

D-254

ANALYSIS OF FISSIONABLE MATERIAL BY DELAYED EMISSIONS

Approved:

G. G. Eichholz, Chairman

J. D. Clement

D. S. Harmer

W. W. Graham, III

K. W. Carlson

M. V. Davis

Date approved by Chairman: 2-19-74

ACKNOWLEDGMENTS

Through the course of this work, a number of people have contributed to its successful completion. I would like to express my gratitude to all concerned.

I would like to thank my advisor, Dr. Geoffrey Eichholz, for the guidance, encouragement, patience, and impatience that contributed immeasurably to the forward progress of this research. In addition, I wish to thank Dr. Waverly Graham, who got me started in this line of research and who has supplied advice and encouragement since, and the other members of my reading committee, Dr. Roger Carlson, Dr. Joseph Clement, Dr. Monte Davis, and Dr. Don Harmer, for making time in their busy schedules to follow the progress of this work.

I am indebted to the Georgia Tech Research Reactor staff for their cooperation in carrying out the experimental phases of this research. Mr. Fred Apple and Mr. Robert Kirkland supplied valuable assistance in setting up the experiment in the beam port, and Mr. Dean McDowell, Mr. Sam Kirbo, and Mr. Dave Cox helped greatly in the collection of data. I am grateful to Mr. Bob Boyd and Mr. Jerry Taylor for assuring the safe operation of the experiment. Mr. Mike Burke's expertise as a machinist was a great help in putting together the cycle generator and I appreciate his aid. As important as the technical abilities of these gentlemen have been, their friendship and interest have been equally important, and for that I am very grateful.

Also, I thank Mrs. Lydia Geeslin for a fine job of preparing the final manuscript.

I would like to express my gratitude to and appreciation of my wife, Barbara, for her love and encouragement through the course of this work, and for her evenings and weekends spent helping with drafts of this dissertation.

TABLE OF CONTENTS

TABLE OF CONTENTS (Concluded)

LIST OF TABLES

LIST OF ILLUSTRATIONS

LIST OF ILLUSTRATIONS (Concluded)

SUMMARY

The assay of nuclear fuel has become a topic of current interest with the increasing use of nuclear fission to generate electric power and the possibility of plutonium fuel cycles being used in fission reactors. In this dissertation, a method of analyzing nuclear material for different fissile nuclides is proposed and an experiment is described that has tested the method for analysis of uranium-235 and plutonium-239, alone and in combination.

The method of analysis is based on the differences in the abundances and half-lives of delayed neutron groups between the various fissile nuclides. Laplace transforms are used to show that the steady state response to a cyclic activation is independent of activation cycle period at short periods, decreases exponentially with period at long periods, and has a break point, or knee, where the response changes from constant to exponential at a specific period that is a function of the half-life of the characteristic emitters. When more than one half-life is present in the response, as in the case of fissile nuclides which have six or more delayed neutron groups, the total response is the superposition of the responses resulting from each different half-life, and has a break point for each half-life in the response.

In the experiment cyclic activation was accomplished by moving the samples containing fissile material cyclically through a thermal neutron beam from the Georgia Tech Research Reactor, out of the beam and through a delayed neutron detector, back through the beam, etc. The

delayed neutron response was recorded at activation cycle periods ranging from 0.1 to 100 seconds for samples containing varying amounts of uranium-235 and plutonium-239. Deviations in the responses of the samples containing both uranium-235 and plutonium-239 from the response of standards containing only uranium-235 or plutonium-239 were determined to infer the uranium-235 to plutonium-239 ratio. After the ratio of the two fissile nuclides present was obtained, the delayed neutron response at short cycle periods was used to estimate the mass of each fissile nuclide present in the sample.

For samples containing about one gram of fissile material, accuracies of one percent were obtained for uranium-235 and five percent for plutonium-239 when the fissile nuclides were present in about equal portions. Accuracies were dependent on uranium-235 to plutonium-239 ratio and on total mass of fissile material present.

The data taken for the assay experiment were also used to look for the existence of any delayed neutron group with a half-life shorter than about 0.2 second. No delayed neutron groups were found with half-lives between 0.01 and 0.2 second.

CHAPTER I

INTRODUCTION

To meet the world's energy needs for the next fifty years, heavy reliance must be placed on nuclear power. By 1980 the United States may depend on nuclear fission for the production of 15 percent of its electricity. This figure may be as high as 25 percent by the year 2000.[1] To support this nuclear-electric generating capability increasingly large amounts of fissionable materials must be produced, handled, and accounted for in the next few years. The commercial and intrinsic value of these materials, plutonium, uranium-233, and enriched uranium, insures that vendors and consumers will desire an accurate accounting of each transaction. In addition, the toxicity of these materials, particularly plutonium, and the potential for creating nuclear explosives with relatively small quantities of some fissionable materials has motivated the development of a nuclear safeguards system by the Nuclear Regulatory Commission and its counterparts in other countries that are developing or using nuclear generating facilities. "Safeguards" is a collective term that comprises those measures designed to guard against the diversion of materials such as source and special nuclear materials* from uses permitted by law or treaty, and

---

*"Source materials" are uranium containing the mixture of isotopes occurring in nature, uranium depleted in the isotope 235, or thorium, or ores containing these materials; and "special nuclear materials" are plutonium or uranium enriched in the isotopes 233 or 235.

to give timely indication of possible diversion, or credible assurance that no diversion has occurred.[2]

The monetary values of plutonium-239, reactor grade plutonium, and uranium-235 are compared to values of some other materials in Table 1. Some materials have required the development of extensive systems of control and accountability for purely economic reasons. Materials considered hazardous, such as narcotics and alcohol, are usually tightly controlled whether or not such control is warranted by their value. In exchanges of gold or other precious metals, both parties require accurate determination of mass and purity because a large amount of money can be involved in small shipper-receiver discrepancies. Transactions involving valuable nuclear materials involve similar financial considerations. In addition, the composition of fuel is important in planning the operation of a reactor. Fuel element worth and total heat value of the fuel are important parameters for determining fuel element placement in reactor cores and predicting the frequency of reactor shutdown for removing spent fuel. When spent fuel is returned to the processor, both the fuel user and processor need an accurate analysis to determine the credit due the fuel user. The processor also needs to know the isotopic content of the returned material for efficient handling, such as proper planning of separative work for enrichment from mixed feed. Not only are fissionable materials toxic, nuclear explosives can be constructed from plutonium, uranium-235 and -233 metal, and oxides of these materials.[3] In fact, only 5 to 10 kilograms of plutonium-239 or 20 to 30 kilograms of uranium-235 are necessary to construct an explosive.[4] This is a very small percentage

Table 1. Relative Values of Some Commonly Traded Materials

	$/kg
Plutonium	6,000
Gold	5,000
Penicillin	13,000
Heroin	2,000
Natural Uranium (U_3O_8)	33
Coal	0.03

of the total amount of fissionable material that will be handled in the United States or other countries with nuclear power programs. Explosives can be made with plutonium having any of the various isotopic compositions contemplated for nuclear reactors. To make weapons of predictable yield, the concentration of plutonium-240, which decays by spontaneous fission, must be kept low.[5] Plutonium generated in fast breeder reactors is suitable for high quality nuclear explosives because it contains low percentages of the isotopes ^{240}Pu and ^{242}Pu.[35] Weapons-grade uranium is usually considered to be enriched in uranium-235 or uranium-233 by 90 percent. However, explosives can be made from uranium enriched to as little as 20 or 30 percent.[4] While HTGR and fast breeders are fueled with uranium of weapons grade, the slightly enriched fuel used in commercial light water reactors can not be fabricated into explosives. Light water reactor fuel is not without military importance, though, since much of the separative work required to produce weapons-grade uranium has already been accomplished in enriching uranium for reactor fuel.[5] An enrichment plant can produce considerably more 90 percent enriched uranium using low enrichment reactor fuel instead of natural uranium as feed material.[5]

Safeguard procedures have been, and are being, developed to detect and prevent the diversion or accidental loss of special nuclear materials. Diversions may be attempted on scales ranging from a single employee stealing valuable material from his employer to conspiracies involving national governments removing nuclear material from an internationally sponsored peaceful program to produce nuclear weapons. To stem the spread of nuclear weapons and the concomitant threat of nuclear war, nations that have

not developed fission explosives may agree not to do so with the understanding that their neighbors, also NPT signers, will also forego nuclear arms. The International Atomic Energy Agency must assure all the signers that none of the signers are producing weapons from special nuclear materials diverted from peaceful atomic energy programs.

Accountability is an important part of nuclear safeguards. Accountability is that part of safeguards and materials management which encompasses the measurement system, records and reports to account for source and special nuclear material.[2] To meet accountability requirements, such as Part 70, Title 10 Code of Federal Regulations, IAEA standards, and for their own economic reasons, users and processors of source and special nuclear materials rely on the various assay methods discussed in Chapter II to evaluate their inventories of nuclear materials and the quantities of these materials transferred between different processing stages or different companies. The ability of a nuclear material handler to account for his inventories and control transfers of materials depends upon the accuracy of the assay methods available to him and on the applicability of these methods to each situation. The most precise methods are destructive to the sample assayed and take a relatively long time to accomplish. Care must be taken, when using a destructive method of analysis, to obtain samples that are representative of the entire quantity of material to which the results of the assay are applied. Non-destructive assay (NDA) methods are generally not as precise as destructive methods for a single sample; however, results are sometimes more accurate because sampling problems are often not as difficult. The statistical uncertainties

associated with most NDA methods decrease with increased sample size or number of samples and, since non-destructive methods leave the assayed material intact and reusable, larger sample bases are available. Whenever results are required on a short time scale, for instance in process control decisions, NDA methods are generally faster. In some cases, such as assembled fuel rods, NDA is the only acceptable method of analysis.

Special nuclear materials, materials containing more than the natural abundance of uranium-235 or containing uranium-233 or plutonium-239, and source materials, materials containing more than 0.05 percent uranium or thorium, differ in their values per unit weight, the risk of diversions, and their assay requirements at different stages in the nuclear fuel cycle. In the mining and milling operations uranium and thorium-containing materials have relatively low specific dollar value, and risk of theft is fairly low. Uranium ore contains uranium in concentrations of only a few kilograms per metric tonne. After the ore is concentrated by physical and chemical means to yellow cake, i.e., $Na_2U_2O_7$, it has a content of elemental uranium of up to about 85 percent by weight, of which uranium-235 is present as about 0.71 atomic percent of the elemental uranium. Yellow cake is converted to uranium hexafluoride for enrichment in the isotope uranium-235 or as a convenient starting material for producing uranium metal or UO_2. Assays for uranium are used at these stages for determining ore value, for process control, etc.

In the enrichment process, isotopic assay for uranium-235 uranium-238 ratios at various stages of the process is important for predicting and controlling plant operation. Currently no enrichment plant operation is

subject to IAEA safeguards because the existing plants are owned and operated by countries that already have nuclear weapons.[5] In the future with increasing commercial use of nuclear materials, international safeguards as well as domestic safeguards and process control will require assay of all material in enrichment plants. The character of the enrichment process makes accurate inventory-taking difficult. The process equipment used in diffusion plants has large surfaces exposed to corrosive UF_6. Pumps and other rotating machinery with moving metal surfaces and gas seals are used to maintain gas pressure and flow through a diffusion plant or to supply the separative force in a centrifugal process. The UF_6 can react with metal surfaces to produce solid corrosion products rich in uranium. Leakage of UF_6 through seals can allow significant amounts of uranium to escape from inventory. The uranium lost from measurable inventory is recoverable, to some extent, only when a process component or stage is removed from service and cleaned. Engineering data necessary for making a good estimate of process inventory are not available in a new plant until routine equipment replacement and cleaning has begun. New plants require many months to reach operational equilibrium. Uranium takes about two months to traverse a diffusion plant and is contained in many operational diffusion stages. Temperature, pressure, and the isotopic character of the UF_6 must be determined simultaneously at all parts of the operating system before a meaningful inventory can be taken.[5]

At the fuel fabrication facility uranium hexafluoride is converted to uranium oxide and pressed into pellets to be loaded into fuel rods. The materials presently handled in fuel fabrication plants for commercial

water-cooled reactors are low-enrichment uranium and natural uranium. Only small quantities of highly enriched uranium and plutonium are currently being processed. However, this situation may be changing. Plutonium-bearing fuels will probably be recycled for use in light water reactors and large quantities of plutonium may be fabricated into fuel for breeder reactors. Substantial quantities of highly enriched uranium fuel will be needed for high temperature gas-cooled reactors. Fuel fabrication is an area of particular concern for safeguards considerations. At this stage the fuel is clean, containing no radioactivity other than its own, which is of low intensity, and it is usually in solid form and easily transportable. Preparation of metal creates refractory slags of uncertain composition and conversion of fluorides to oxides creates dilute liquid waste and powdered residues containing some actinides. These are difficult to measure accurately and precisely.[5] The oxides of uranium, or plutonium in the case of recycled fuel, are compacted and fired into briquettes and then sized by grinding before loading into fuel rods. The high quality standard of process control required for reactor fuel results in substantial quantities of reject material, scrap, and dust.[5]

At the reactor fissionable materials are handled as fresh fuel, fuel inside the reactor, spent fuel being stored, and cooled spent fuel being shipped to reprocessing. The reactor operator needs a non-destructive assay method to verify the fuel fabricator's statements about the contents of the fuel. Modern power reactors may use several values of enrichment at one time, even in a single fuel element.[5] During the life of a fuel element the burnup of uranium-235 and production of plutonium-239 are

determined by the neutron flux level and energy spectrum the fuel element receives and by the flux history as well as the starting isotopic composition of the fuel elements. In the reactor, physical control over the nuclear material is simple; it is in containers that can be labeled and counted. But estimation of the isotopic make-up of the material in the containers requires detailed knowledge of the history of the fuel element in the operating reactor. Measurement of the fissionable material in spent reactor fuel is complicated by the intense gamma-ray emissions from included fission products. Spent fuel from a light-water reactor fueled with low-enrichment uranium typically contains about 0.7 percent uranium-235 and one percent plutonium-239.[6]

Shipment of spent fuel from the user to the reprocessor is complicated by the large gamma-ray background generated by the fission products present. Safe transportation requires heavy gamma-ray shielding and usually requires a 60-90 day cooling-off period before shipping. The difficulties in handling spent fuel in locations other than specially designed facilities limit the risk of diversion of nuclear materials in transit between the user and reprocessor. Since the fuel elements are not accessible or modified in transit, accountability obligations may be met by ensuring that the fuel shipments which leave the user arrive at the reprocessor intact.

The fuel reprocessor will receive spent fuel assemblies from the reactor operator, cut them up, and chemically remove the uranium and plutonium. Plutonium may then be recycled to the fuel rod fabricator and uranium that has not been depleted below the level of natural uranium can

be returned in the form of UF_6 as feed to an enrichment plant. Fuel discharged from natural uranium-fueled reactors and some reactors fueled with low-enrichment uranium may be depleted in uranium-235 below 0.2 or 0.3 percent, the level of the tails from an enrichment plant, and would not be useful for enrichment.

There is a fiscal accounting link between the reactor operator and fuel reprocessor in addition to their legal accountability obligations. The operator knows that his spent fuel contains plutonium and, possibly, recoverable quantities of uranium-235. The reprocessor will pay him for it, but uncertainty in individual input measurements currently ranges from one to five percent.

Reprocessing is a difficult task. Oxide fuel is refractory and difficult to dissolve, and the presence of fission products requires that the entire process be done remotely. HTGR discharge fuel will be even more difficult to handle, it consists of small beads of uranium or thorium carbide, difficult to dissolve in itself, coated with silicon carbide and pyrolytic carbon. The material will be burned to remove the carbon and ground to burst the spheres before chemical dissolution is attempted. Chemical assay of spent HTGR fuel is difficult for the reasons reprocessing is difficult. Assay for total uranium and plutonium of a few cubic centimeters is costly and takes several days to get the results.[7]

After the spent fuel is cut up and dissolved, the process produces streams in which fissionable material is not easily measured. The streams are not readily sampled and destructive assaying is costly and results in dissipation of material. In the reprocessing plant, material unaccounted

for (MUF) often resides in the equipment as precipitates and corrosion products, complicating the task of meeting accountability requirements. Cleaning is difficult and it is often hard to be sure the reprocessing equipment is completely clean. An on-line assay method would be useful in reprocessing systems.

Throughout the nuclear fuel cycle there are applications for assay methods for uranium and plutonium. The ability of a nuclear materials handler to meet his accountability obligations without economic disruption of his operation depends directly upon the assay methods he chooses. Accuracy of an assay method is important because it establishes a limit of error in the material unaccounted for (LEMUF), but factors other than accuracy may determine the applicability of a given assay method. There are applications which require a non-destructive method to prevent dissemination of materials or the destruction of fabricated elements, to measure a large fraction of material flow to circumvent sampling problems, or to assay materials in places where access is difficult. Some applications require an assay in the presence of a large gamma ray background or the assay of materials for isotopic content of fissionable materials. In this thesis a non-destructive assay method, applicable to several stages in the fuel cycle, is developed, and its feasibility is explored for use in safeguards situation requiring a non-destructive, isotopic assay relatively resistant to the presence of gamma radiation.

CHAPTER II

CURRENT METHODS OF ANALYSIS OF NUCLEAR MATERIALS

To meet current safeguard requirements and for economic reasons, the composition of nuclear materials must be monitored at various stages of the nuclear fuel cycle. Accuracies required by NRC and IAEA regulations for nuclear materials accountability are 0.5 to 1.0 percent of the total materials balance at the 1 σ (65% confidence) level.[8,9] (Accuracy is used throughout this paper to refer to probable deviation from the true value; precision is used to describe consistency and repeatability of data.) LEMUF, limit of error of the material unaccounted for, requirements differ at various stages of the nuclear fuel cycle according to the risk of diversion and strategic (bomb potential) value of the material at any particular stage. NRC requirements are also based on currently obtainable accuracies and are updated as measurement capability improves.[10]

The methods used to assay special nuclear material should incorporate several characteristics.[11] Ideally, an assay should be fast and accurate. Time is essential in process control situations, and quick detection of a diversion is necessary for credible safeguards. Unfortunately, speed and accuracy are sometimes mutually incompatible parameters. For methods where accuracy is dependent on counting statistics, longer counts usually mean better accuracy per sample but may mean that fewer samples can be taken of a given process or shipment. Insensitivity to self-shielding effects is important when nuclear materials may be

hidden by the finite thickness of the sample. In some applications, such as spent fuel elements, the assay system must tolerate intense gamma ray fields. Some situations, such as analysis of fresh fuel elements, require a non-destructive assay method if a substantial part of the throughput is to be measured. Non-destructive analysis is often desirable, to decrease sampling problems by allowing a larger fraction of the material flow to be assayed.

The accuracy with which material flow can be measured is limited in many instances by sampling biases. Solids often are found to be not homogeneous in isotopic makeup or particle size, and liquids, particularly solutions of plutonium, contain suspended or settled out solids or sludge.[12] Methods that infer the compositions of large volumes of materials from small samples suffer the most from sampling problems. Some materials, such as pellets inside assembled fuel elements, cannot be sampled in practice.

In a closed materials balance for safeguards accountability, all materials moving into and out of each step in the nuclear fuel cycle must be measured. For a closed materials balance, the following equation must hold.

(Input + Beginning Inventory) - (Output + Ending Inventory + Waste) = 0

Typically it does not, and the discrepancy, MUF, represents material lost (or gained) by unknown channels, or material that may have been diverted.[12] The assay method discussed in subsequent chapters is a candidate for use in a closed materials balance where more than one fissionable isotope is present, such as plutonium recycle fuel, light-water reactor

discharge fuel, HTGR fuel where uranium-233 and uranium-235 may be found together, fuel refabrication, and reprocessing waste. It may also be used in conjunction with another method, such as calorimetry, where precise knowledge of the ratio of two fissile isotopes can improve the accuracy of another measurement.

In plutonium recycle, PuO_2 may be mixed with UO_2 in the fuel, or the fuel element may contain plutonium as the only fissile isotope. In either case the fissile isotopes will be in concentrations of < 5 atom percent in uranium-238. Light water reactor-spent fuel will contain uranium-235 and plutonium-239 in about equal concentrations, typically 0.5 to 1.5 atom percents,[6] together with fission products that are intense gamma ray emitters. In reprocessing and fuel fabrication waste, uranium-235 and plutonium may occur in almost any concentration in solid or liquid form. The uranium will not normally be more than five percent enriched in uranium-235 if only commercial light-water reactor fuel is processed. Plutonium in the LWR fuel cycle typically contains 10 to 20 percent plutonium-240 and about five percent plutonium-241.[13] HTGR fuels will be highly enriched in uranium-233. As fast breeder fuel cycles are established, highly enriched uranium will be used in the fuel, but when the cycle is stabilized only one fissile isotope, plutonium-239, will be used. Plutonium and highly enriched uranium will probably not be used in the same fuel elements.

The analysis method described in Chapter III can compete with a number of analytical methods now in use or being developed for applications requiring fissile isotope identification; among them are wet chemistry, mass spectrometry, lead slowing-down spectrometer, coincidence

counting, and delayed neutron analysis.

Wet Chemistry

Wet chemical analysis generally requires a sample to be removed from the material flow and dissolved, if not already in solution. After removal of interfering ions the uranium or plutonium content of the sample is determined by precipitation or titration. Potentiometric titration, where oxidation or reduction potential is compared to a standard half-cell to detect the titration end point for determination of uranium, can easily obtain precisions of 0.2 to 0.5 percent.[14]

Plutonium is not stable in solution under some pH conditions, forming stable polymers with water that are not easily redissolved.[15] In addition uranium, which is often more abundant in the sample than plutonium, is an interfering ion that cannot be completely removed. In cases where there is a large uranium component, such as LWR discharge fuel, use of amperometric or coulometric methods to determine titration end points limits the interference of uranium. In amperometric titration, a current is passed through, and the element of interest is plated out. The current remains constant until the end point is reached; then it begins to change linearly with time.[15] Coulometric titration is the integral of amperometric titration.[15] Precisions of better than 0.2 percent are available for samples containing 10 mg plutonium.

Accuracies reported for wet chemical methods are generally better than 1.0 percent. Discrepancies between different laboratories are probably due to one or more interfering ions and the slightly different techniques used.[15] Sampling may be a problem also, since the composition of large volumes of materials must often be inferred from small samples.

Mass Spectrometry

In a mass spectrometer a very small sample, a few micrograms, is vaporized. The atoms or molecules of the sample are then accelerated in an electric field and directed through a magnetic field to a charge collector or photographic plate. The paths taken by the constituents of the sample in the magnetic field, and their impact positions on the target, are functions of the charge to mass ratio. Double-focusing mass spectrometers are precise to parts per million, but the equipment is expensive and obtaining small samples that are representative of the sampled material is difficult. The mass spectrometer is widely used for determining isotopic mass ratios, particularly in enrichment plants. Equipment available today can determine uranium-235 concentration to an accuracy of 0.15 percent.[12] Isotopic dilution techniques, where the sample or parent batch is spiked with an isotope not normally present, such as uranium-233 and plutonium-242 in LWR discharge fuel, yield precisions of one percent for plutonium concentration.[14]

Radiography

X- or gamma-ray radiography is of little use in distinguishing between the heavy elements and isotopes since the electron densities of heavy elements vary little from element to element, and not at all among isotopes of the same element. Neutron cross sections, however, vary considerably among the heavy elements and their isotopes. Neutron radiography, therefore, can be a useful tool in safeguards applications.

In neutron radiography a shadow image is made of the sample, which is placed in a neutron beam with little divergence for sharpness. The degree of shadowing is proportional to the neutron capture cross sections.

Both high energy neutron generators and reactor beams have been used as sources. Direct and indirect imaging techniques have been used. Recently, a new imaging technique has been developed that shows some promise; a "fission plate" is placed over a glass or plastic sheet and the fission tracks are etched out of the glass or plastic after exposure. This method has excellent gamma rejection and good definition due to the short range of fission fragments.[16]

Resonance self-indication analysis is a radiographic method of analysis using the energy-dependence cross sections. For this type of analysis a beam of epithermal neutrons with some arbitrary energy distribution is obtained by passing a reactor neutron beam through a thin sheet of cadmium. The beam is then tested, with and without the sample, with fission chambers, i.e., proportional counters lined with plutonium-239 or uranium-235. The sample is then interposed between the neutron source and the detectors. If the sample contains uranium-235 the beam will be deficient in neutrons of energies that correspond to the resonance peaks of uranium-235, and the uranium-235 fission chamber will show a decrease in beam intensity, whereas, the plutonium-239 fission chamber, which has different resonances, will be relatively unchanged. The effect is similar to using color filters in photography.[17]

Neutron radiographs of the SEFOR fuel showed dramatically that about half of the pellets in the fuel rods were deficient in plutonium and that the bad pellets were randomly distributed. If a radiograph had been made upon receipt of the rods, the failure of the first fuel loading could have been avoided.

Because variations in geometry (e.g., due to sample thickness) produce effects similar to fissile isotope loading, quantitative analysis with neutron radiography can be difficult. However, neutron radiography provides a good indication of fissile isotope distribution. Pellets 10 percent deficient in plutonium-239 were easily detected in SEFOR fuel.

Gamma-Ray Spectrometry

Passive gamma counting can be done on new fuel material to see the characteristic gamma photopeaks of the uranium and plutonium isotopes. On irradiated materials, some fission products gamma-rays can be used to determine burnup and fuel composition.

A 184 keV gamma-ray is emitted by uranium-235 as a natural-decay gamma-ray and it can be counted with a NaI(Tl) scintillator detector for an indication of the amount of uranium-235 present. The 184 keV gamma-ray is of such low energy that it is easily stopped by relatively thin layers of heavy materials. The attenuation from six mm of uranium is more than 99 percent. Counting of the 184 keV gamma-ray should include attenuation correction factors for assay if the equivalent heavy metal thickness of the sample exceeds about 0.4 mm.[18]

The gamma-rays of interest in plutonium analysis are bunched into a band around 400 keV. High-resolution Ge(Li) detectors are generally used for plutonium assay, rather than the high efficiency, lower resolution NaI(Tl) detectors used in assay for uranium-235. Solutions of plutonium nitrate in long, thin bottles have been assayed using gamma-ray spectrometry with accuracies of five percent.[19] This method is not practical for the analysis of spent fuel because of the probability of radiation damage

to the semiconductor detector in the intense fission-product gamma-ray field.

Fission product gamma-rays can be used in a normal neutron activation analysis manner to measure fissile isotope content and to determine the ratio of fissioning isotopes. Gamma-ray scanning of spent fuel for fission product gamma-ray peaks for determination of burnup is a somewhat extreme example of neutron activation analysis. Fission products useful in activation analysis of fissile materials have high energy gamma-ray peaks, providing good penetration of high-Z materials and low interference from Compton scattering from other peaks, high yield from fission, and a significant difference in yield between the fissioning nuclides that participate in the assay. To be useful in gamma-ray scanning of spent fuel for burnup measurements, fission products should have a relatively long half-life and low neutron cross section, to minimize saturation effects, and a low propensity to diffuse out of a fuel element.[20] Analysis for uranium-235 to plutonium-239 may be done by estimating total fissions from determinations of a single fission product, such as cesium-138, that has nearly equal yield for uranium-235 and plutonium-239 fissions, then determining the uranium-235 to plutonium-239 ratio from a fission product that has a greater yield for one fissile nuclide than the such as ruthenium-106 which has a yield from plutonium-239 fission that is 5.5 times as great as the yield for uranium-235 fission.

Total burnup measurements of spent fuel by gamma-ray scanning have been reported with accuracies of 5.0 percent.[21] Fissile contents have been found with precisions of 2.0 percent using two or more fission products in the analysis.[22]

Lead Slowing-Down Spectrometer

When high-energy neutrons are introduced into a large mass of lead they diffuse through it and lose energy by a large number of elastic collisions. The great difference between the mass of lead nuclei and that of the neutrons requires that the neutrons have a large number of elastic encounters before reaching thermal energies and, therefore, spend a long time, relative to a hydrogenous medium, in slowing down. If the pile of lead is pulsed with monoenergetic neutrons, all of the neutrons in the pile will have about the same energy at a given time after the pulse because each neutron will have had about the same large number of elastic collisions and lost, on the average, the same percentage of energy in each collision. The number of neutrons reacting with a sample in the pile at a given time after the initiation pulse is an indication of the cross section of the sample at the neutron energy corresponding to that time.[23] The source pulse length must be short compared to the neutron slowing down time, around 200 μs to reach a few eV, for good resolution, and must be intense enough to overcome high leakage, 96 percent in 10 μs for a 1.33 meter block of lead.[24]

Cross section can be measured as a function of energy by recording neutron transmission of the sample, capture gamma-rays, emissions from fission, etc. as a function of time after the pulse of neutrons injected into the lead pile. Repeated pulses are used to build up statistics and sample response counts are stored in a multichannel analyzer, each channel representing a certain time interval after a neutron pulse. Response is not dependent on pulse frequency as long as all the neutrons

from a pulse thermalize or diffuse out before the next cycle.

Isotopic composition of a sample can be determined by the resonant absorption peaks in the energy-dependent neutron cross sections of the different types of nuclides present in the sample. An assay is normally made by comparing energy dependent neutron cross-section data from a sample to data collected, using the same sample geometry, from a standard of known composition.[24]

Assay procedures of fuel materials using a lead slowing-down time spectrometer are currently being developed at Karlsruhe and the University of Michigan. The lead slowing-down time spectrometer may find use in spent fuel assays, where detection of neutron cross sections will allow use of neutron detectors and provide some discrimination against fission product gamma-rays.

Prompt Neutron Analysis

When a uranium or plutonium nucleus fissions, several gamma-rays and neutrons accompany the fission. These prompt emissions can be used to analyze a sample for fissionable material with coincident counting techniques to discriminate against fission-causing neutrons and (α,n) reactions. The sample to be assayed is surrounded by a number of detectors and is exposed to a source of neutrons. The source must generate neutrons that are not correlated to each other in time so that source neutrons do not activate coincidence circuitry in the detector system; (γ,n) sources, such as ^{124}Sb-Be, are used. Accumulation of counts indicating a fission in the sample requires coincident detection of neutrons in two or more of the detectors around the sample.[25] This method is good for total assay

of fissile material, but, because differences between neutrons-per-fission values are small for the different fissile nuclides this method is not useful for isotopic assay of fuel material.

Analysis by Delayed Neutrons

After a fission event, some neutrons will be emitted during the decay of a number of fission products. These delayed neutrons are emitted immediately following a beta decay in a fission product or an isobar in the fission product decay chain. The process is described more thoroughly in Chapter III. Differences in the abundance and half lives of these delayed neutron emitters for different fissile nuclides arise from the distribution of fission products for various nuclides, as explained in Chapter III.

Ten years ago delayed neutrons were used to look for uranium trapped in leached fuel element hulls in reprocessing operations.[26,27] Actually, analysis of uranium by delayed neutrons goes back much farther.[28] Delayed neutron analysis methods almost always use pulse techniques to distinguish the delayed neutrons from prompt neutrons and from any neutrons used in the interrogation pulse. Only delayed neutrons appear after termination of the interrogation pulse. Three general classes of analysis by delayed neutrons have been reported.[17] First, the sample may be moved past a neutron source and the delayed neutrons are then counted after the sample has been moved away from the source. Since delayed neutrons occur after less than one percent of all fissions, such a single interrogation pulse technique yields poor sensitivity. Secondly, the sample may be pulsed repeatedly and counted between interrogation pulses. If the time between interrogation pulses is shorter than about 0.1 second, corresponding to

the shortest half life of a delayed neutron group (see Chapter III), the delayed neutron response will not be a function of interrogation pulse rate,[29] and the data obtained are a function of the total delayed neutron activity. This technique has been used to measure total fissile content in samples of known isotopic composition, such as containers of UF_6, to within one percent.[30]

When the time between interrogation pulses is long compared to the longest half life of a delayed neutron group, the delayed neutron activity falls off between pulses as the sum of a number of exponential decays, each corresponding to the decay of a delayed neutron precursor. This decay curve is different for each fissile nuclide because different delayed neutron abundances and half lives are involved.[31]

Two versions of this type of delayed neutron analysis have been developed at Los Alamos by Keepin's group over the past several years; total delayed neutron counting and isotopic analysis by "time fiducial" techniques.[31] The first method, total delayed neutron counting, is straightforward. The sample was pulsed with a square-wave neutron beam with a duty cycle of about 50 percent and a period shorter than the period of the shortest delayed neutron group, typically 50 to 100 ms.[30] Delayed neutrons were counted during the 50 percent of the time that the sample was not in the interrogation flux. For this mode of irradiation, the measured delayed neutron count rate is proportional to the time-integrated delayed neutron yield and, in turn, to the amount of fissionable material present.[30] Variations in the pulse rate make little difference in the delayed-neutron activity as long as the pulse period remains short compared

to the shortest delayed neutron period.[29] No attempt has been made to correlate delayed neutron activity with pulse period.[17] By comparison with a standard of known mass and composition, a fuel element of known isotopic composition may be assayed to an accuracy of several percent, depending on composition.[31]

In the "time fiducial" method the analysis is performed by pulsing a sample with neutrons and observing the decay of the delayed neutron response after the pulse.[32] The ratio of the number of delayed neutrons counted before some fixed time after the end of the interrogating pulse to the number of delayed neutrons counted after that fixed time (time fiducial) can be used to determine the fissile nuclide. The ratio of counts before to that after the time fiducial is determined by the ratio of abundances of short-half-life delayed neutrons to long-half-life delayed neutrons, which varies between the fissile nuclide, as discussed in Chapter III. Pulse widths were shorter than the shortest half life delayed neutron group, 100 μs or less, and the time fiducial was chosen to give the best discrimination between the fissile nuclides. Pulses were repeated to build up statistics, but the delayed neutron response of the sample was allowed to die away between incident neutron pulses. The interrogation pulses were produced with a 14 MeV neutron generator. The ratio $^{235}U/^{239}Pu$ has been measured in spent LWR fuel with a burnup of 1000 MWd/T with precisions of 10 percent and in fresh fuel with accuracies of around five percent.[21] Delayed neutrons have been used by the Los Alamos group more recently to locate plutonium in containers of contaminated waste. Delayed neutron response to repetitive pulses of varying frequency

and duration were not investigated.[31]

Mass spectrometry and wet chemical analysis offer assay precisions that are better than the non-destructive analysis methods, but generate sampling problems and are difficult to use in some situations. Of the non-destructive analysis (NDA) methods available, none are applicable to all safeguards situations. Gamma ray spectrometry, delayed neutron analysis, and coincident neutron counting are NDA methods that are able to distinguish between different nuclides in nuclear fuel. Neutron detecting methods are useful in the assay of spent fuel materials because neutron detectors can be made to discriminate, somewhat, against the fission product gamma-rays that accompany spent fuel. The assay method described in the following chapters offers promise for good accuracy and immunity to gamma-ray interference. It is a non-destructive method which can differentiate between fissile nuclides by observing delayed neutrons after a pulse of interrogating neutrons induces fissions in the sample. This method, an extension of a technique to measure half-lives of activated indium developed for a special problems course in 1969,[29] differs from the work done at Los Alamos by H. O. Menlove, R. H. Auguston, G. N. Henry, and others in that the fissile nuclide composition of a sample is inferred from the frequency-dependent delayed neutron response of the sample to interrogating pulses rather than the time-dependent response. The frequency-dependent method allows more interrogation neutrons to be administered to the sample per unit time, and, therefore, more rapid accumulation of counting statistics and higher accuracy per gram of sample for a given assay time.

CHAPTER III

BACKGROUND AND THEORY

Methods of fissile isotope analysis that utilize delayed neutrons have characteristics that recommend their use in nuclear fuel cycle and safeguards applications. These methods are non-destructive; they can be used with any geometry sample and damage to or depletion of the sample is negligible. Fission parameters and delayed neutron precursor half-lives are completely insensitive to the intense gamma radiation fields associated with spent reactor fuel, and neutron detectors discriminate, somewhat, against gamma rays; so the method is useful for both fresh and irradiated fuel. Nuclear material is easily penetrated by fast interrogation neutrons. In fact, it may prove possible to measure axial concentration of fissionable nuclides by interrogation with neutrons of two or more distinctly different energies.

Delayed Neutrons

Methods that attempt fissile nuclide assay of nuclear material by delayed neutrons rely on the differences in intensities of the six observable delayed neutron groups generated by different fissioning species. The process by which these differences arise is straightforward and will be explored in the following paragraphs.

In the same year that neutron-induced nuclear fission was discovered, Roberts, Meyer and Wang[33] observed that some of the neutrons born of fission appeared at time intervals after the actual scission. The importance

of this discovery was not lost on Enrico Fermi and others who built the first fission chain reactors with only slight apprehension of the disaster that would have resulted from a reaction propagated by prompt neutrons alone. Delayed neutrons are so necessary to the control of fission reactions that, since 1939, a great number of studies have been launched to find and refine half-life, energy and abundance information about them. The delayed neutrons are assumed, both for theoretical reasons to be discussed later and for empirical reasons, to die away as a linear superposition of exponential decays. If a least-squares fitting to delayed neutron data is used, it is seen that six exponential periods generate a good fit for fissioning materials. If five or fewer groups are used, satisfactory convergence is not obtained and indicated errors are large. If seven or more groups are used, the weighted variance, defined as

$$S^2 = \frac{1}{n - k} \sum_{i=1}^{n} W_i \left(Y_{i\ obs} - Y_{i\ calc}\right)^2 \qquad (3\text{-}1)$$

is larger, indicating a poorer fit, than is obtained for six-group fitted parameters.[34] A typical set of half-life and abundance parameters is given for fast and thermal fission in Tables 2 and 3, taken from Keepin.[35]

It is apparent from Tables 2 and 3 that variations in group yields are much greater than the variations among group periods for the isotopes listed. Also, the total delayed neutron yield increases with neutron-proton difference for a given fissioning nuclide due, primarily, to short half-life groups; and the total delayed neutron yield generally decreases with atomic number.[11] It is these variations that are the basis of this

Table 2. Delayed-Neutron Half-Lives, Decay Constants, and Yields from Fast Fission (ref. (35))

Group index, i	Half-life (sec)	Decay constant (sec^{-1})	Relative abundance	Absolute group yield, %
		U-235 (99.9% 235)		
1	54.51 ± 0.94	0.0127 ± 0.0002	0.038 ± 0.003	0.063 ± 0.005
2	21.84 ± 0.54	0.0317 ± 0.0008	0.213 ± 0.005	0.351 ± 0.011
3	6.00 ± 0.17	0.115 ± 0.003	0.188 ± 0.016	0.310 ± 0.028
4	2.23 ± 0.06	0.311 ± 0.008	0.407 ± 0.007	0.672 ± 0.023
5	0.496 ± 0.029	1.40 ± 0.081	0.128 ± 0.008	0.211 ± 0.015
6	0.179 ± 0.017	3.87 ± 0.369	0.026 ± 0.003	0.043 ± 0.005
		U-238 (99.98% 238)		
1	52.38 ± 1.29	0.0132 ± 0.0003	0.013 ± 0.001	0.054 ± 0.005
2	21.58 ± 0.39	0.0321 ± 0.0006	0.137 ± 0.002	0.564 ± 0.025
3	5.00 ± 0.19	0.139 ± 0.005	0.162 ± 0.020	0.667 ± 0.087
4	1.93 ± 0.07	0.358 ± 0.014	0.388 ± 0.012	1.599 ± 0.081
5	0.490 ± 0.023	1.41 ± 0.067	0.225 ± 0.013	0.927 ± 0.060
6	0.172 ± 0.009	4.02 ± 0.214	0.075 ± 0.005	0.309 ± 0.024
		U-233 (100% 233)		
1	55.11 ± 1.86	0.0126 ± 0.0004	0.086 ± 0.003	0.060 ± 0.003
2	20.74 ± 0.86	0.0334 ± 0.0014	0.274 ± 0.005	0.192 ± 0.009
3	5.30 ± 0.19	0.131 ± 0.005	0.227 ± 0.035	0.159 ± 0.025
4	2.29 ± 0.18	0.302 ± 0.024	0.317 ± 0.011	0.222 ± 0.012
5	0.546 ± 0.108	1.27 ± 0.266	0.073 ± 0.014	0.051 ± 0.010
6	0.221 ± 0.042	3.13 ± 0.675	0.023 ± 0.007	0.016 ± 0.005

Table 3. Delayed-Neutron Half-Lives, Decay Constants, and Yields from Thermal Fission (ref. (35))

Group index, i	Half-life (sec)	Decay constant (sec^{-1})	Relative abundance	Absolute group yield, %
		U-235 (99.9% 235)		
1	55.72 ± 1.28	0.0124 ± 0.0003	0.033 ± 0.003	0.052 ± 0.005
2	22.72 ± 0.71	0.0305 ± 0.0010	0.219 ± 0.009	0.346 ± 0.018
3	6.22 ± 0.23	0.111 ± 0.004	0.196 ± 0.022	0.310 ± 0.036
4	2.30 ± 0.09	0.301 ± 0.011	0.395 ± 0.011	0.624 ± 0.026
5	0.610 ± 0.083	1.14 ± 0.15	0.115 ± 0.009	0.182 ± 0.015
6	0.230 ± 0.025	3.01 ± 0.29	0.042 ± 0.008	0.066 ± 0.008
		Pu-239 (99.8% 239)		
1	54.28 ± 2.34	0.0128 ± 0.0005	0.035 ± 0.009	0.021 ± 0.006
2	23.04 ± 1.67	0.0301 ± 0.0022	0.298 ± 0.035	0.182 ± 0.023
3	5.60 ± 0.40	0.124 ± 0.009	0.211 ± 0.048	0.129 ± 0.030
4	2.13 ± 0.24	0.325 ± 0.036	0.326 ± 0.033	0.199 ± 0.022
5	0.618 ± 0.213	1.12 ± 0.39	0.086 ± 0.029	0.052 ± 0.018
6	0.257 ± 0.045	2.69 ± 0.48	0.044 ± 0.016	0.027 ± 0.010
		U-233 (100% 233)		
1	55.00 ± 0.54	0.0126 ± 0.0003	0.086 ± 0.003	0.057 ± 0.003
2	20.57 ± 0.38	0.0337 ± 0.0006	0.299 ± 0.004	0.197 ± 0.009
3	5.00 ± 0.21	0.139 ± 0.006	0.252 ± 0.040	0.166 ± 0.027
4	2.13 ± 0.20	0.325 ± 0.030	0.278 ± 0.020	0.184 ± 0.016
5	0.615 ± 0.242	1.13 ± 0.40	0.051 ± 0.024	0.034 ± 0.016
6	0.277 ± 0.047	2.50 ± 0.42	0.034 ± 0.014	0.022 ± 0.009

particular method of nondestructive analysis by delayed neutrons.

Delayed neutrons are produced when a member of a fission product decay chain decays to an energy level for a nuclide whose excitation energy is greater than the binding energy of a neutron, E_n. This process is indicated in Figure 1. When a nuclide finds itself in such a situation it generally disposes of its excess energy in one of three processes: beta decay, gamma decay, or delayed neutron emission. Beta and gamma decay are, of course, the normal means of decay when the excitation energy is not sufficient to eject a neutron. When a neutron can be ejected, decay paths n_1 and n_2, neutron emission usually competes favorably with beta or gamma decay, which are somewhat hindered; whereas, neutron emission is highly favored for nuclides with sufficient excitation energy. The probability that a neutron will be emitted varies from zero for a neutron energy (in excess of neutron binding energy) of zero to unity for neutron energy greater than about 50 keV.

The probability that a given nucleus resulting from fission will decay by neutron emission is defined as P_n. Theoretical P_n values can be estimated using the original Bohr-Wheeler mechanism of delayed neutron emission.

$$P_n = \frac{\int_{B_n}^{Q_B} f(z+1,\ Q_8 - E)\ (E)\ [\Gamma_n/\Gamma_\gamma + \Gamma_\beta)dE}{\int_0^{Q_B} f(z+1,\ Q_B - E)\ (E)dE} \qquad (3\text{-}2)$$

$$(E) = \begin{cases} A & 0 < E < E_c \\ Ae^{b(E-E_c)^{\frac{1}{2}}} & E_c < E < Q_B \end{cases}$$

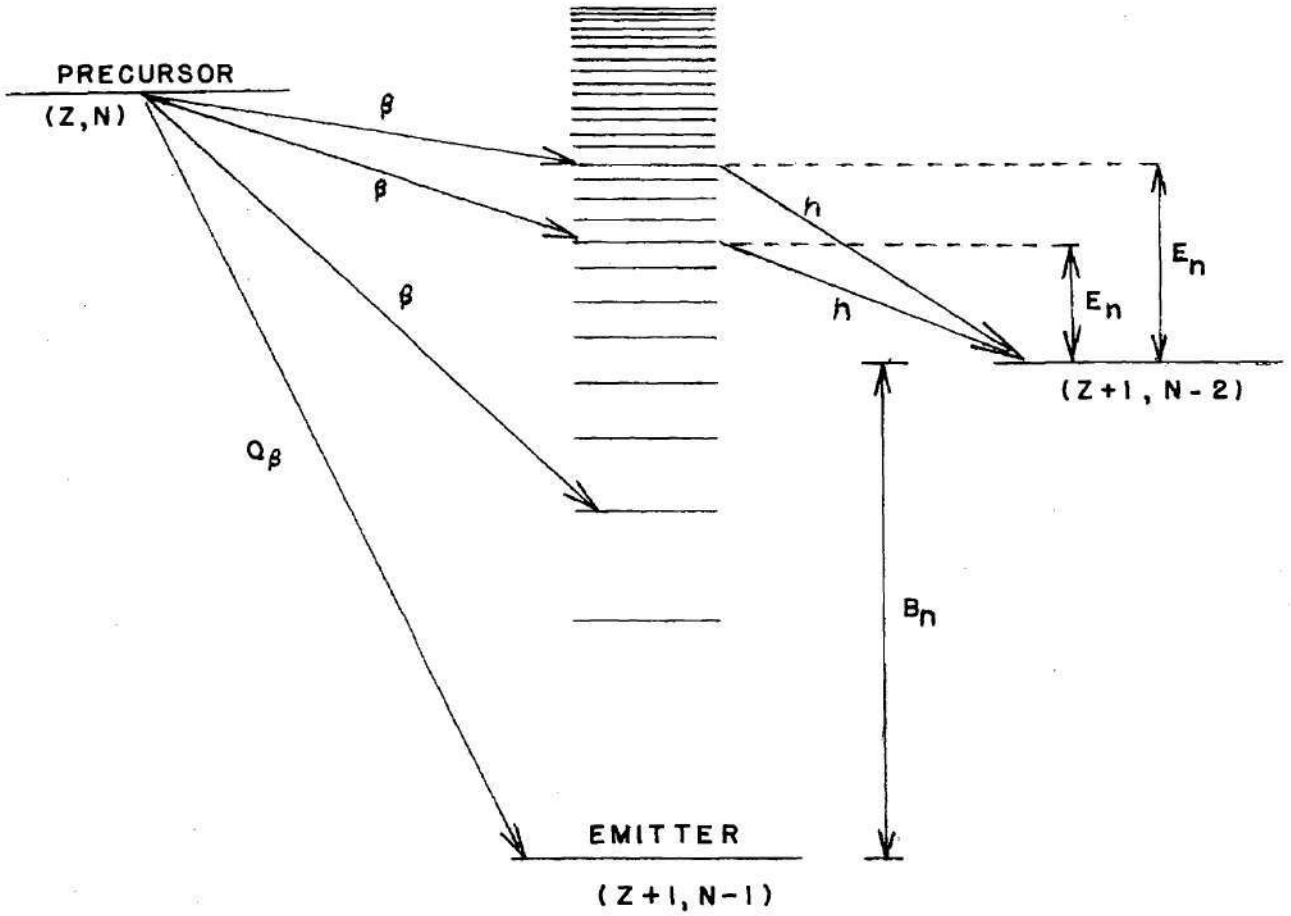

Figure 1. Energy Levels in Delayed Neutron Emission

A is the mass number, z is charge, and Γ_n, Γ_β, and Γ_γ are the partial widths for neutron, beta, and gamma-ray decay. E_c is the critical energy for pairing effects. Q_β and B_n are shell sensitive parameters and can be expressed as functions of charge displacement, $Z_N - Z$, where Z_N is the "most stable" Z for a given number of neutrons, N.[36] P_n is essentially constant for a given nuclide regardless of the fissioning nuclide. Equation 3-2 breaks down and consistency of P_n is lost in the presence of isomerism among delayed neutron precursors; i.e., a variation of relative population of isomeric and ground states with the type of fission would imply a dependence of P_n on Z and A of the fissioning nuclide.[35] However, current experimental evidence and shell theory interpretations indicate that conditions for isomerism and for delayed neutron emission are mutually exclusive.[36] Figure 2 shows the region of most probable delayed neutron precursors from calculations of P_n, shown by shaded boundaries[26] in a nuclide chart. These regions do not include nucleons with magic numbers of protons or neutrons.

It is evident that the probability of delayed neutron emission and the half-life of a delayed neutron precursor are independent of the fissioning nuclide. Differences in delayed neutron abundances and group half-lives must, then, come from differences in total fission yields of the various precursors for different fissioning nuclides.

Each fissioning nuclide is characterized by a mass distribution curve and, for each mass, A, on the mass distribution curve, a charge distribution curve characterized by a most probable primary nuclear charge, Z_p, and a distribution of primary nuclear charges around Z_p. Typical mass

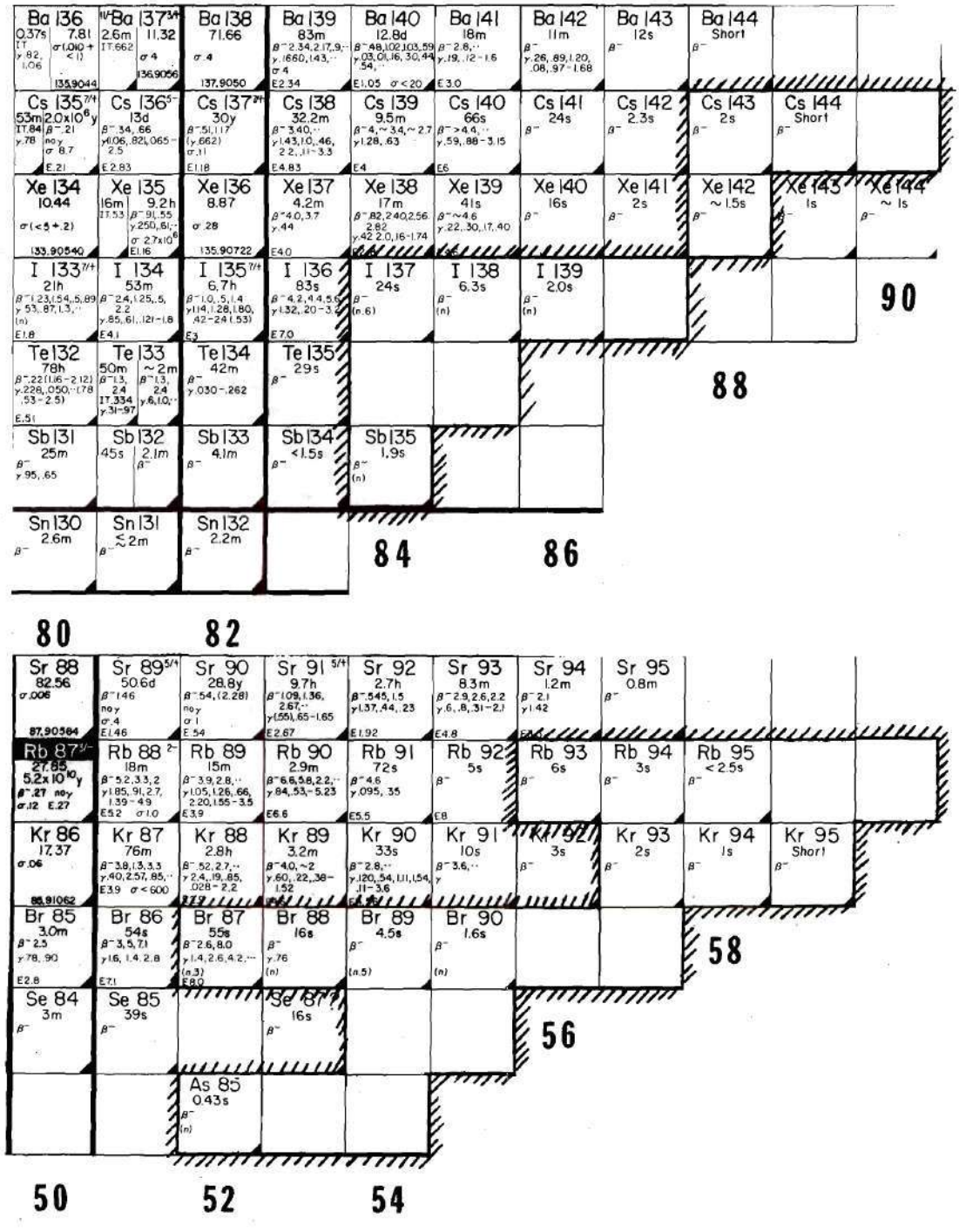

Figure 2. Chart of the Nuclides with Regions Expected to Contain Delayed Neutron Precursors Outlined with Hash Marks

and charge distribution curves are shown in Figure 3. The locus of Z_p values for a given fissioning nuclide is a line parallel to the line of most stable nuclear charges Z_A. The average fission chain length, $Z_A - Z_p$, varies from 3.6 for uranium-233 to 4.5 for uranium-238, with fissioning nuclides of higher (N - Z) values having longer fission chain lengths. A given delayed neutron precursor may lie well within the fission fragment charge distribution curve for uranium-238 and be only on the tail of the uranium-233 fission fragment charge distribution curve. The relative abundance for such a delayed neutron precursor would be much greater for uranium-238 fission than for uranium-233 fission due both to the larger primary yield and to the larger yield of lower Z nuclides that feed the delayed neutron precursor in their decay chain. This effect is greater for increased distance from the line of most stable charge. Since beta half-lives are shorter for greater distances from the charge stability line, the effect is noted primarily with short-period delayed neutrons. Differences in the fission fragment mass yield distributions have a similar, but less pronounced, effect.

Differences in delayed neutron group periods among the fissionable nuclides also arise from differences in fission chain lengths. When longer decay chains lead to a delayed neutron precursor, the precursor activity (and corresponding delayed neutron activity) exhibits a growth-decay behavior with time and the apparent delayed neutron period is lengthened. The degree of lengthening is dependent on the beta periods involved.[35]

Even though the delayed neutron precursors are exactly the same isotopes for each fissioning nuclide, differences in the fission product mass distributions produce differences in absolute and relative delayed

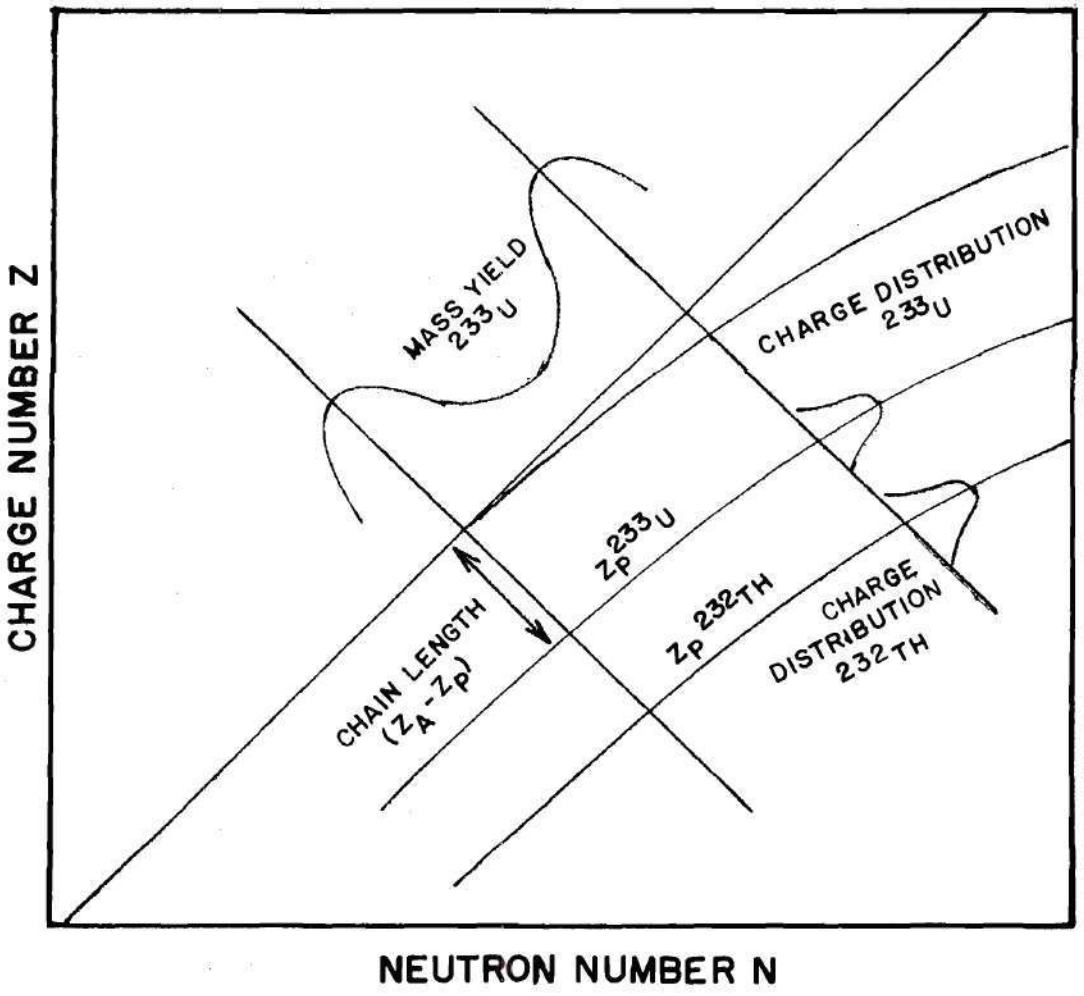

Figure 3. Mass and Charge Distribution of Fission Fragments Leading to Differences in Abundances and Half-Lives of Delayed Neutrons

neutron group yields; and differences in the average chain lengths (charge distributions) produce differences in both yields and periods of delayed neutron groups. Because each fissioning nuclide has characteristic fission product mass and charge distributions, there is a unique set of delayed neutron group yields and periods for each fissioning nuclide by which it may be identified

Cyclic Activation

For their delayed neutron analysis the Los Alamos group pulsed their sample repeatedly to accumulate good statistics, but they allowed delayed neutrons to die away after each interrogation pulse or did not allow sufficient time between pulses for any significant decay of delayed neutron activity. No attempt was made to correlate intermediate frequencies of cyclic activation to delayed neutron activity.[37] In the remainder of this chapter the relationships between the parameters of an activation-wait-count-wait cycle and the delayed neutron activity observed in the "count" part of the cycle are investigated. Results derived are applied to specific fissile nuclide analysis in later chapter, but the equations will be useful in a large number of cyclic activation applications.

The differential equations that describe the activity of a cyclicly activated sample are well known in form; but solutions to these equations can be somewhat difficult when attempted in the time domain. Nonetheless, some useful solutions have been found with time domain math by Campbell and Givens.[37,38] (The work of Givens et al. is, however, flawed by an incorrect summation, but, in most cases, the error causes little error in the agreement between our experimental results and Givens' equations.) In this section a solution for steady state activity under cyclic

activation will be produced using Laplace transform techniques.

The activity of a sample exposed to neutron radiation of a time independent nature and of known energy distribution is described by the differential equation:

$$\frac{dN}{dt} = \phi\sigma N_o - \lambda N \qquad (3\text{-}3)$$

where:

ϕ is the neutron flux

σ is the activation cross section

N_o is the parent atom population

λ is the decay constant of the daughter

N is the population of activated daughter nuclides of interest

Some of these parameters can be functions of time or other variables. The activation cross section and decay constant are known to be generally independent of time. The parent atom population will be assumed to remain constant during irradiation; this assumption should be valid as long as there is no significant burnup of the sample. The time dependence of activity of the sample, related directly to daughter population, is the quantity of interest. The total activity is, of course, the sum of the activities of all the activation products. Each activation product can be considered separately and the activities of the products, from Equation (3-3), summed for the total activity.

The neutron flux is a quantity in Equation (3-3) that can be varied in a time-dependent fashion, and, by observing the activation behavior,

some parameters of the activation equation can be deduced. Any modulation of the neutron flux that can be described by a mathematical function, such as a sine wave or exponential, is suitable for Laplace transform analysis; one of the simplest to achieve is square wave modulation, shown in Figure 4, along with detector gate timing and induced activity expected in a sample.

For square wave modulation the flux can be considered as an infinite sum of unit steps; one to turn the flux on, one at a later stage to turn it off, and so on.

The neutron flux as a function of time is seen to be:

$$\emptyset(t) = \emptyset_m[U(t) - U(t - b) + U(t - a) - U(t - b - a) \ . \ . \ .] \qquad (3\text{-}4)$$

where:

$\emptyset_m$ is the maximum flux

a is the time at which the flux turns on

b is the time at which the flux turns off

U(t) designates a unit step beginning at time (t)

The time dependent flux is easily Laplace-transformed as a repetitive function as follows:

$$\emptyset(s) = [\emptyset(t)] = \frac{\emptyset_m(1 - e^{-as})}{s(1 - e^{-bs})} \qquad (3\text{-}5)$$

Transforming the decay equation, Equation (3-3), into the Laplace domain produces:

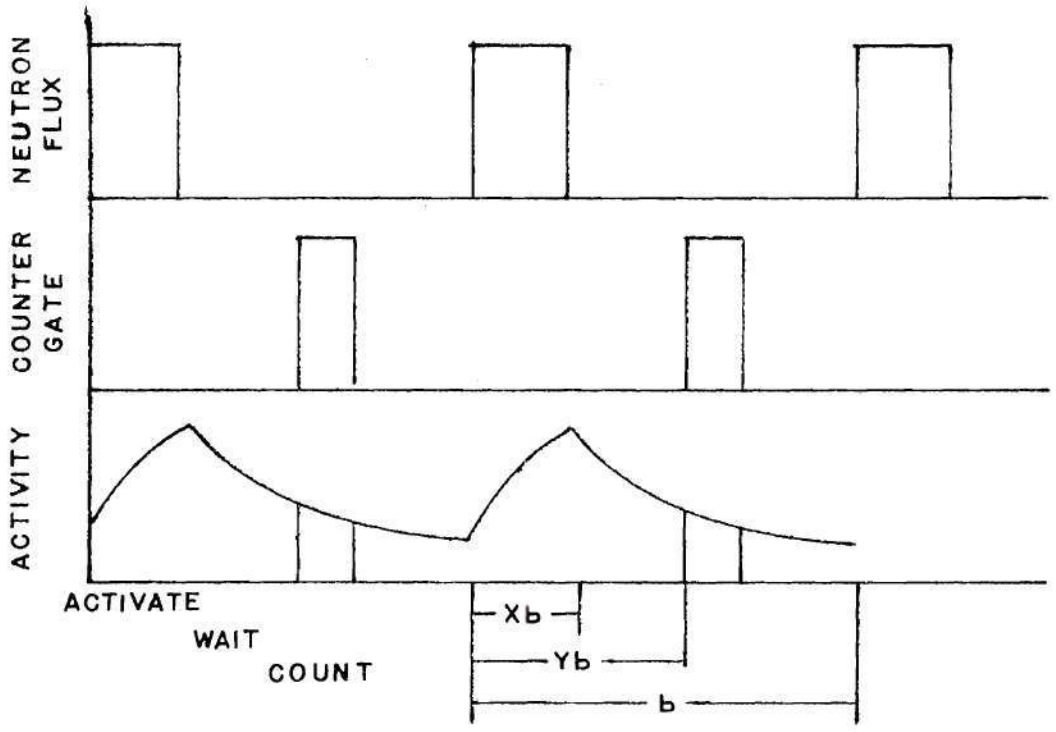

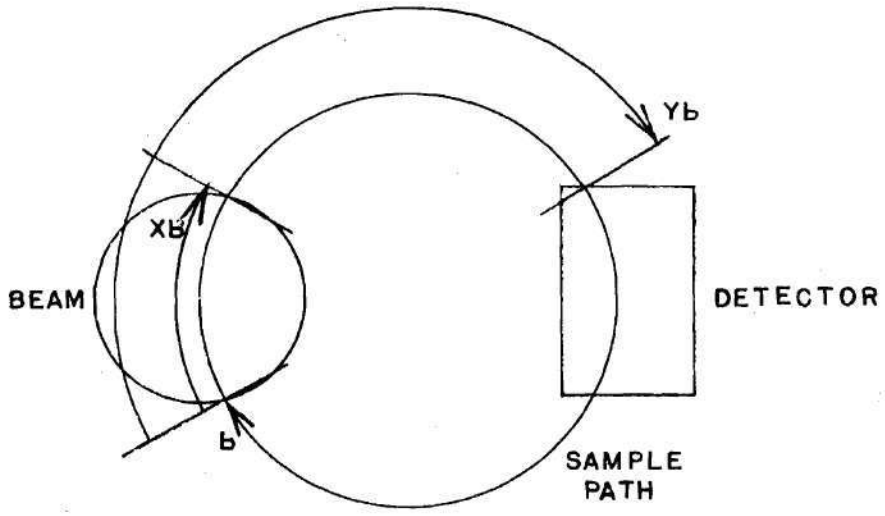

Figure 4. Timing Diagrams for the Activation Cycle Used to Derive Equation (3-28)

$$sN(s) = \sigma N_o \emptyset(s) - \lambda N(s) \tag{3-6}$$

Using the Laplace transform of the square wave modulated flux, Equation (3-5), and substituting for the constant-term, $\sigma N_o \emptyset_m$, the simpler A, produces the equation:

$$sN(s) = \frac{A}{s}\left[\frac{1 - e^{-as}}{1 - e^{-bs}}\right] - \lambda N(s) \tag{3-7}$$

Solving for N(s) produces:

$$N(s) = \frac{A}{s(s + \lambda)}\left[\frac{1 - e^{-as}}{1 - e^{-bs}}\right] \tag{3-8}$$

To transform Equation (3-8) into the time domain the exponential term in the denominator can be expanded as an infinite series:

$$N(s) = \frac{A}{s(s + \lambda)}(1 - e^{-as})(1 + e^{-bs} + e^{-2bs} + e^{-3bs} + \ldots) \tag{3-9}$$

Then by use of partial fractions and by multiplying out the exponential terms the following is obtained:

$$N(s) = \frac{A}{\lambda}\left[\frac{1}{s} - \frac{1}{s + \lambda}\right](1 + e^{-bs} + e^{-2bs} + e^{-3bs} \ldots - e^{-(a+b)s} - e^{-(a+2b)s} \ldots) \tag{3-10}$$

Equation (3-10) can be transformed into the time domain:

$$N(s) = \frac{A}{\lambda}\left[U(t)(1 - e^{-\lambda t}) + U(t - b)(1 - e^{-\lambda(t-b)}) + \ldots\right. \tag{3-11}$$

$$\left. - U(t - a)(1 - e^{-\lambda(t-a)}) - U(t - (a + b))(1 - e^{-\lambda(t-(a+b))}) \right.$$

$$\left. \ldots \right]$$

After an infinite number of cycles the number of daughter atoms is given by Equation (3-11). After a finite number of cycles, n, the number of daughter atoms can be found by summing the series of unit steps in Equation (3-11) only to that point in time where:

$$(n - 1) < t < (n + 1)b + a \tag{3-12}$$

This time corresponds to the activation portion of the n^{th} cycle. All of the step terms cancel except $U(t - (n - 1)b)$, leaving:

$$N(t) = \frac{A}{\lambda}\left[1 - e^{-\lambda t}(1 + e^{\lambda b} + e^{2\lambda b} + \ldots + e^{(n-1)\lambda b}) \right. \tag{3-13}$$

$$\left. + e^{-\lambda(t-a)}\ (1 + e^{\lambda b} + e^{2\lambda b} + \ldots e^{(n-2)\lambda b})\right]$$

Each of the finite exponential series in Equation (3-13) has a simple sum. Summing the series and multiplying through by λ/A produces:

$$\frac{\lambda N(t)}{A} = 1 - e^{\lambda t}\left[\frac{1 - e^{nb\lambda}}{1 - e^{\lambda b}}\right] + e^{-\lambda(t-a)}\left[\frac{1 - e^{(n-1)\lambda b}}{1 - e^{\lambda b}}\right] \tag{3-14}$$

For the decay portion of the cycle, i.e.,

$$(n - 1)b + a < t < nb \tag{3-15}$$

the number of step terms in Equation (3-5) is again finite. When the series of step terms is summed all of the terms again cancel except the last, $U(t - (n - 1)b + a)$ producing the equation:

$$N(t) = \frac{A}{\lambda}\left[- e^{-\lambda t}(1 + e^{\lambda b} + e^{2\lambda b} + \ldots e^{(n-1)\lambda b}) + e^{-\lambda(t-a)}(1 + e^{\lambda b} + e^{2\lambda b} \ldots e^{(n-1)\lambda b})\right] \tag{3-16}$$

Summing the exponential series and multiplying through by λ/A produces:

$$\frac{\lambda N(t)}{A} = - e^{-\lambda t}\left[\frac{1 - e^{n\lambda b}}{1 - e^{\lambda b}}\right] + e^{-\lambda(t-a)}\left[\frac{1 - e^{n\lambda b}}{1 - e^{\lambda b}}\right] \tag{3-17}$$

Equations (3-14) and (3-17) constitute a complete solution for $N(t)$ in the interval $(n - 1)b < t < nb$. The $e^{-\lambda t}$ and $e^{-\lambda(t-a)}$ terms are independent of the number of cycles experienced and, therefore, represent decreasing transients. If sufficient time is allowed for the transients to die out, the steady state solutions are found to be:

for $(n - 1)b < t < (n - 1)b + a$

$$\frac{\lambda N_{ss}}{A} = 1 + \frac{e^{n\lambda b - \lambda t} - e^{(n-1)\lambda b - \lambda(t-a)}}{1 - e^{\lambda b}} \tag{3-18}$$

and for $(n - 1)b + a < t < nb$

$$\frac{\lambda N_{ss}}{A} = \frac{e^{n\lambda b-\lambda t} - e^{n\lambda b-\lambda (t-a)}}{1 - e^{\lambda b}} \tag{3-19}$$

For simplicity time can be normalized to the start of a cycle; then $t = t' - (n - 1)b$ where t' is real time. The steady state equations become:

for $0 < t < a$

$$\frac{\lambda N_{ss}}{A} = 1 + \frac{e^{-(t-b)\lambda} - e^{-(t-a)\lambda}}{1 - e^{\lambda b}} \tag{3-20}$$

and for $a < t < b$

$$\frac{\lambda N_{ss}}{A} = \frac{e^{-\lambda (t-b)} - e^{-\lambda (t-(a+b))}}{1 - e^{\lambda b}} \tag{3-21}$$

To limit the background problem in this application, no data will be taken during the activation part of the cycle; i.e., while $t = 0 \rightarrow a$; therefore, knowledge of the steady state activity during the activation part of a cycle equation (3-20) is of no particular interest and attention will be focused on Equation (3-21) which describes the steady state activity for that part of the cycle during which no further activation occurs, $t = a \rightarrow b$ in Figure 4. By expressing a as a fraction, x, of the cycle time and observing the activity at some other fraction, y, of a cycle time, b, the following is obtained from Equation (3-21):

$$a = xb$$

$$t = yb$$

$$1 > y > x$$

$$\frac{\lambda N_{ss}}{A} = \frac{e^{-\lambda b(y-1)} - e^{-\lambda b(y-x-1)}}{1 - e^{\lambda b}} \tag{3-22}$$

Grouping terms in Equation (3-11) yields:

$$\frac{\lambda N_{ss}}{A} = \frac{e^{-\lambda b(y-1)}}{1 - e^{\lambda b}} \left[1 - e^{\lambda bx}\right] \tag{3-23}$$

Equation (3-23) describes the steady state activity for the non-activation portion of the cycle and has some interesting properties. If the cycle time is short, i.e., the frequency is high, the steady state activity can be shown to be independent of frequency. Taking the limit of the steady state activity as the cycle time approaches zero, using L'Hospital's rule and grouping terms has the following result:

$$\lim_{b\to 0} \frac{\lambda N_{ss}}{A} = \lim_{b\to 0} \frac{\frac{d}{db}\left[e^{-\lambda b(y-1)} - e^{-\lambda b(y-x-1)}\right]}{\frac{d}{db}\left[1 - e^{\lambda b}\right]} \tag{3-24}$$

$$\lim_{b\to 0} \frac{\lambda N_{ss}}{A} = \lim_{b\to 0} \frac{\lambda(y-1)e^{-\lambda b(y-1)} - \lambda(y-x-1)e^{-\lambda b(y-x-1)}}{-\lambda e^{\lambda b}}$$

$$\lim_{b\to 0} \frac{\lambda N_{ss}}{A} = (y-1) - (y-x-1)$$

$$\lim_{b\to 0} \frac{\lambda N_{ss}}{A} = x$$

Equation (3-24) is no surprise; if the frequency of activation is very high, the level of activity reached will be proportional to the fraction of time spent in the neutron field. When the cycle time is long, i.e., the frequency is low, the steady state activity decreases exponentially with cycle time, which can be shown as follows:

$$\lim_{b\to\infty} \frac{\lambda N_{ss}}{A} = \lim_{b\to\infty} \frac{e^{-\lambda b(y-1)}}{1 - e^{\lambda b}} \left[1 - e^{\lambda bx} \right] \qquad (3\text{-}25)$$

$$\lim_{b\to\infty} \frac{\lambda N_{ss}}{A} = \frac{e^{-\lambda b(y-1)}}{} \left[- e^{\lambda bx} \right]$$

$$\lim_{b\to\infty} \frac{\lambda N_{ss}}{A} = e^{-\lambda b(y-x)}$$

Equation (3-23) describes the steady state activity at some time, yb, in the cooling portion of the cycle. In the experiment, data acquisition was not limited to a single discrete time; delayed neutron counts were collected over a finite portion of the cycle. The activity observed from the sample as it passes through this counting portion of the cycle is the integral of Equation (3-23) over that part of the cycle.

$$A' = \int_{w}^{w+c} \left[\frac{1 - e^{-\lambda bx}}{1 - e^{\lambda b}} \right] e^{-\lambda b(y-1)} \, dy \qquad (3\text{-}26)$$

where:

A' is the activity observed

w is the portion of the period between activation and counting

c is the portion of the period spent counting

$$A' = \frac{1 - e^{-\lambda bx}}{1 - e^{\lambda b}} \int_{w}^{w+c} e^{\lambda b} e^{-\lambda by} dy \qquad (3\text{-}27)$$

$$= \left[\frac{1 - e^{-\lambda bx}}{1 - e^{\lambda b}}\right] e^{\lambda b} \frac{e^{-\lambda by}}{-\lambda b} \Big|_{w}^{w+c}$$

$$= \frac{1 - e^{-\lambda bx}}{(e^{-\lambda b} - 1)(-\lambda b)} \left[e^{-\lambda b(w+x)} - e^{-\lambda bw}\right]$$

$$= \frac{(1 - e^{-\lambda bx})}{b\lambda(1 - e^{-\lambda b})} (1 - e^{-\lambda bw})(e^{-\lambda bc} - 1)$$

Equation (3-27) is the response expected for the case of only one decay constant. The total delayed neutron response as a function of cycle time is as follows:

$$A' = \sum_{i=1}^{n} \frac{(1 - e^{-\lambda_i bx})(e^{-\lambda_i bw})(e^{-\lambda_i bc} - 1)}{\lambda_i b(1 - e^{-\lambda_i b})} \qquad (3\text{-}28)$$

where:

λ_i is the i^{th} delayed neutron decay constant

n is the total number of delayed neutron decay constants

If the logarithm of the activity, A' in Equation (3-27), is plotted as a function of the cycle time, b, the resulting curve looks like Figure 5. Any activation product will generate a characteristic curve when activity is plotted against cycle time, as in Figure 5, where the amplitude, break-point, and slope of the long cycle time part of the curve are determined by the abundance and decay constant of the activation product.

The single activation product response, described as a function of cycle time, b, for short cycle times by Equation (3-24) and for long cycle

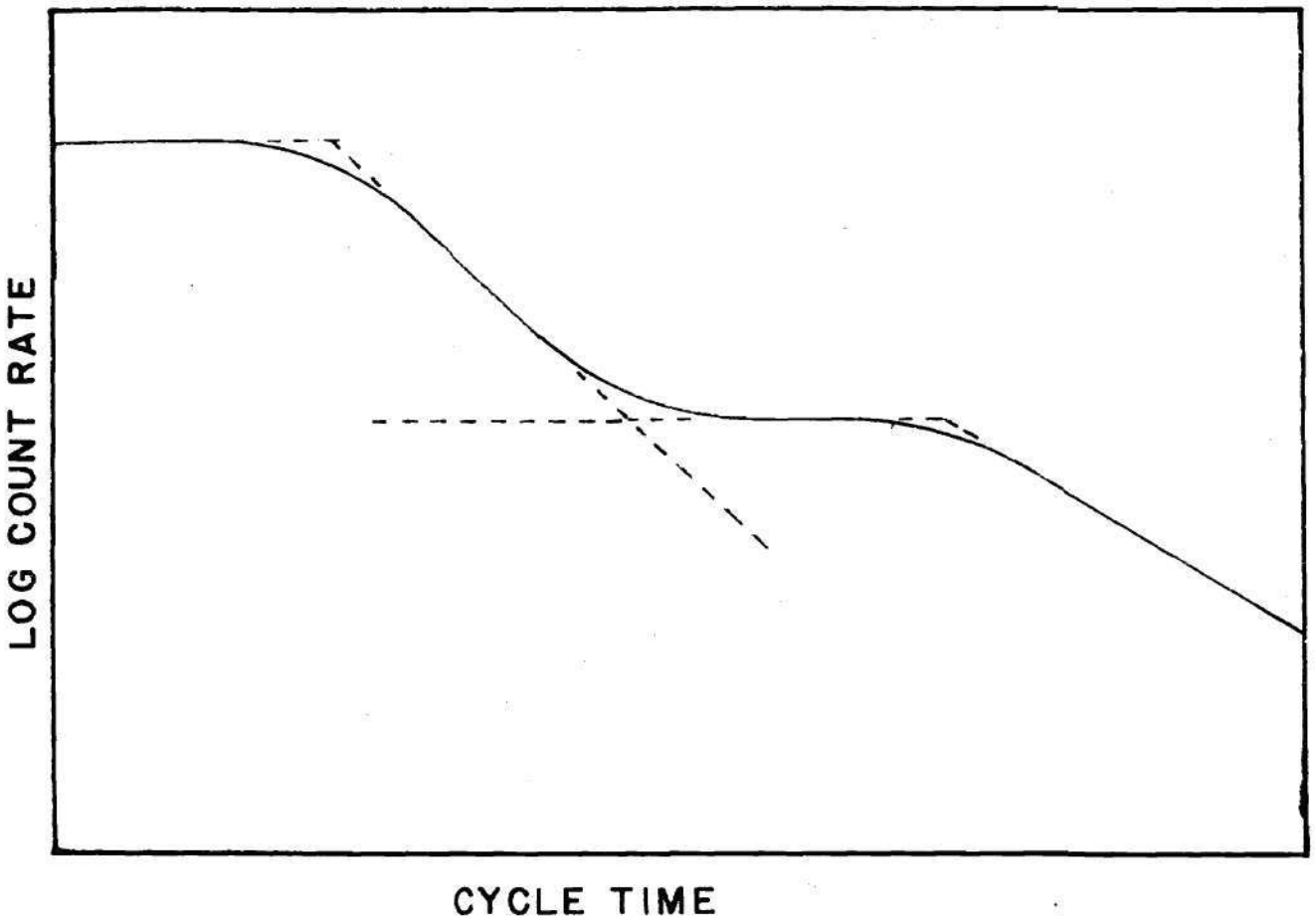

Figure 5. Log Count Rate as a Function of Cycle Time (inverse frequency) Curve (The solid line results from the superposition of the count rates from two activation products having different half lives.)

times by Equation (3-25), begins to decrease with increasing cycle time at the break point described by setting equations (3-24) and (3-25) equal and solving for the cycle time,

$$b_c = \frac{- \ln x}{(y - x)\lambda} \tag{3-29}$$

The break point is a function of counting cycle parameters, x and y, and activation product decay constant, λ. The activation fraction of a cycle, x, appears in the short cycle time response, Equation (3-24), as a constant in the level of response obtainable and in the long cycle time response, Equation (3-26), as part of an exponential term. If x is small, the delayed neutron response is also small; and as x approaches 100 percent, the dependency of the delayed neutron response on cycle time disappears. The length of the activation fraction of the cycle is, to some extent, a trade-off between ease of construction of equipment and precision of data analysis. In these experiments a wide beam of neutrons was chosen to retain a reasonable fraction of a cycle for activation while locating the neutron detectors away from the beam to decrease background.

In the presence of six or more decay constants, the decay constants are not easily inferred from changes in the slopes in Equation (3-28). Furthermore, the situation is complicated by the various lengths of decay chains leading to the delayed neutron precursors, which, by growth and decay of precursors, produce changes in slopes. However, the delayed neutron activity vs cycle time plot is unique for each fissioning nuclide, and by comparison of these plots, the nuclides can be identified without computing delayed neutron abundances and half lives from the "signatures."

For cycle times that are short compared to the short-half-life delayed neutrons, the delayed neutron response is independent of cycle time, as seen in Equation (3-24).

Because little decay occurs between subsequent reactivations, at short cycle times the delayed neutron response is independent of cycle time and contains contributions from all of the delayed neutron groups. This response is, therefore, an indication of the total number of delayed neutrons being produced. However, this information does not indicate the total amount of fissionable material present without knowledge of the isotopic makeup of the material. At longer cycle times, of the order of several seconds, the delayed neutron response reflects the abundances of only the longer half-life delayed neutron groups. In this region of cycle times, the responses of uranium-235 and plutonium-239 are different because the abundances and decay constants of the various delayed neutron groups are different for these two fissioning isotopes. When cycle times become long, 100 seconds or more, differences in delayed neutron responses between uranium-235 and plutonium-239 decrease because only the longest delayed neutron groups contribute to the response, and the activities decrease exponentially with cycle time, as seen in Equation (3-25). The ratio of the main fissile nuclides present, uranium-235 and plutonium-239, can, then, be inferred from the ratio of the short cycle time delayed neutron response to the delayed neutron at some intermediate cycle time. Plutonium-239 has a smaller delayed neutron response at all intermediate frequencies than uranium-235 because fission of plutonium-239 is less likely to produce delayed neutron precursors with long half-lives or long decay chains.

The theory of this chapter describes a response to periodic activation. Periodic activation can be accomplished by moving the sample into and out of a neutron beam, as was done in these experiments, or by pulsing the interrogation flux, as with a neutron chopper or neutron generator. If the interrogation flux is pulsed, the mathematical model developed here holds only if the pulse widths, wait times, and count times all remain fixed fractions of the entire cycle for all cycle times, a situation that is automatic with the moving sample technique used in these experiments.

CHAPTER IV

EQUIPMENT AND PROCEDURES

The mathematical model predicting different delayed neutron responses as a function of an activation-decay cycle for uranium-235 and plutonium-239, developed in Chapter III, was tested with experiments intended also to evaluate the usefulness of an assay for different fissile nuclides based on this model for safeguards applications. The experiment was designed for the exposure of small specimens to a fluctuating neutron beam by mounting them on a rotating arm that moved them steadily from the exposure site to a counter system and back again. The instrumentation needed to conduct these experiments did not have to be extremely sophisticated; yet, to amass statistics on delayed neutrons, care had to be taken to adequately shield the neutron detectors from interrogating neutrons and prompt neutrons. Accuracies of the assays done in these experiments were dependent on counting statistics, precision of cycle time measurements, sample geometry, neutron flux and detector sensitivity, and background. Cycle time measurements were made by counting pulses generated by the sample arm rotating mechanism, described later. The precision of these measurements was easily controlled, and was not a controlling factor in the accuracy to which assays could be obtained. The samples available for these experiments were limited to flat foils, unlike the material found in most safeguards situations. With such small foils, it was easier to move the samples into and out of a continuous

neutron beam rather than pulsing the beam. On the other hand, for the bulkier samples encountered in many safeguard applications, such as fuel rods, cyclic movement through a steady neutron beam would be awkward, and a neutron generator or beam chopper could be used to accomplish the cyclic activation better in that case.

Figure 6 is a diagram of the experiment set-up. In these experiments the neutron beam was not chopped, hence the delayed neutron detectors had to be shielded from this potential source of background radiation. The detectors were removed from the direct beam by rotating the samples on a circle, the axis of which was parallel to the beam. Distance between the detectors and the beam was limited by the beam diameter; large beam diameter allowed more distance between the beam and detector while retaining a reasonable percentage of the cycle for activation.

Assay accuracy was found to be limited by counting statistics, as shown later. Counting statistics are controlled by the sensitivity of the detectors, the available neutron interrogation flux, and the background count rate. Beam port H-1 of the GTRR was chosen for high neutron flux as well as for beam diameter to allow greater separation of the beam and the detector assembly.

Samples of pure metallic uranium and plutonium were activated in a thermal neutron beam, moved to an epithermal, delayed-neutron detector and counted, then moved back to the beam for reactivation. Each step, activation, move, count, move, was a fixed percentage of the total cycle time for varying cycle times. Uranium and plutonium each generate a characteristic decay time spectrum, or signature, of delayed neutrons counted as a function of the period of activation; the composition of a

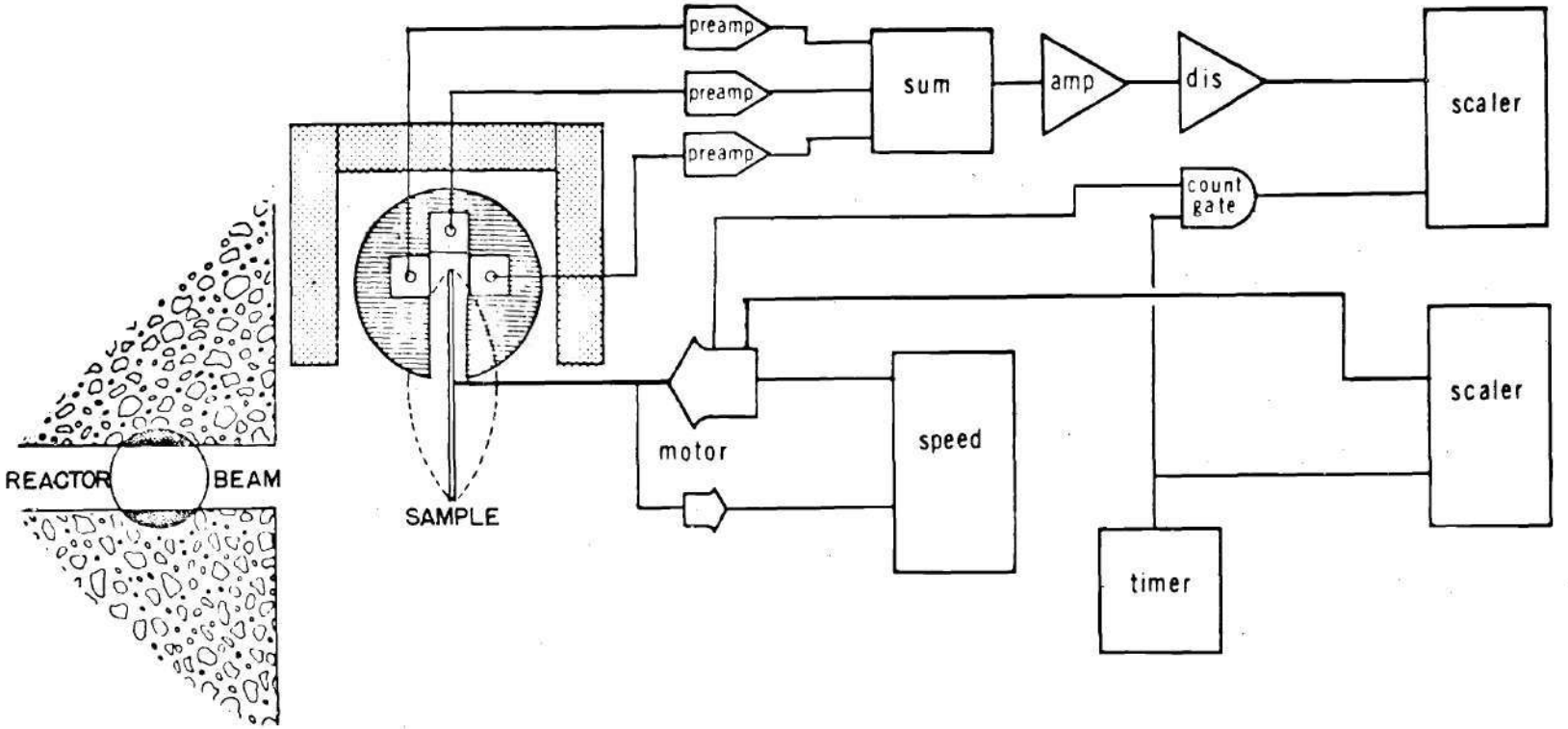

Figure 6. Schematic of Experiment Setup at Beam Port H-1

mixed sample can be inferred from its delayed neutron activity as a function of cycle frequency, as described in Chapter III.

The equipment and instrumentation necessary to perform this type of assay can conveniently be considered in the following four categories:

1. the neutron source
2. the cycle generator
3. the delayed neutron detector
4. signal processing and count accumulation electronic equipment.

Figure 6 shows the overall arrangement of the equipment and instrumentation used in the execution of this experiment. Thermal neutrons, produced in the Georgia Tech Research Reactor, streamed from the reactor at horizontal port, H-1, through the region where interrogation of the samples took place, and into a beam catcher. The sample to be assayed, consisting of small disks in this experiment, was mounted on the end of a bar 410 mm in length. The bar, driven by a motor in the cycle generator, moved the sample in a circular path, first through the neutron beam and then into the detector assembly where the exothermal delayed neutrons, arising from fission events that took place while the sample was in the neutron beam, were moderated, and detected in BF_3 detectors. In addition to the moderating material and the BF_3 tubes the detector assembly included adequate shielding to reduce the fast and thermal neutron background that existed near H-1 to an acceptable level. Delayed neutron count pulses, generated by the BF_3 tubes, were amplified in a preamplifier near the detector assembly. Three BF_3 tubes were used at various angles around the sample. Delayed neutron pulses from the three preamplifiers were added together, further amplified, routed through a discrimina-

tor to remove gamma pulses and background noise, and accumulated in a scaler. The scaler was gated on by a timer pulse and a signal from the period generator that indicated that the sample was in the detector. Thereby, an accumulation of background counts was avoided while the sample was being interrogated or was in transit from the neutron beam to the detector and back. The same timer that was used to gate the delayed neutron count scaler also gated a second "time free" scaler that collected pulses generated by the cycle generator. Two hundred and sixty pulses were generated by the cycle generator during every revolution of the sample bar; by using a known timer output, the period of sample revolution could be computed from these counts.

The Neutron Source

The choice of a neutron source for a fuel assay system is subject to several parameters. For quantitative assay of samples thicker than a millimeter or so, or for qualitative assay of inhomogeneous, thick samples, fast neutrons are necessary for sufficient penetration so that the entire sample volume participates in the assay. For samples that are neutronically thin or for qualitative assay of samples where homogeneity is assured, a thermal neutron source offers some advantages. Neutrons in a thermal flux are below the fission threshold of fertile materials, such as uranium-238 and plutonium-240. Flux tailoring devices, moderators, filters and reflectors, needed with fast neutron sources to prevent fertile materials from participating in the assay, are not necessary when using thermal neutrons. The high cross sections for thermal neutrons responsible for self-shielding problems produce, as an advantage, also

better statistics, hence better accuracies, for a given interrogating flux. One of the best sources of thermal neutrons for interrogation, a nuclear reactor, is not portable, but it may often be found at a site where nuclear materials are assayed. Compared to other sources of neutrons, reactors produce high neutron fluxes and are inexpensive when the neutrons produced by the reactor are a by-product of some other primary function, such as the production of electrical power.

Development of the mathematical model in Chapter III did not presume a specific source of interrogating neutrons. Any source that could be pulsed would suffice except that, in a fast neutron assay, fertile material would participate, if it were present in the sample. In the experiments, thermal neutrons were chosen for the interrogating beam because relatively high fluxes were readily available from the Georgia Tech Research Reactor (GTRR).

The Georgia Tech Research Reactor

The GTRR is a CP-5 type heavy-water-moderated-and-cooled reactor. Fuel loading is approximately 2125 kilograms of uranium, 93 percent enriched uranium-235, in the form of uranium-aluminum alloy plates. Up to nineteen assemblies of these plates arranged in a hexagonal array, comprise the cylindrical core, which is roughly 60 centimeters in diameter and 60 centimeters high. The core is surrounded radially by a 60 centimeter thick D_2O moderator, a 60 centimeter graphite reflector, and about a meter and a quarter of high density concrete and lead for biological shielding. When this experiment was performed the reactor power level was 1000 kilowatts thermal and it produced a peak thermal neutron flux in the moderator in excess of 10^{13} $n/cm^2/sec$.[39] Figure 7 shows a hori-

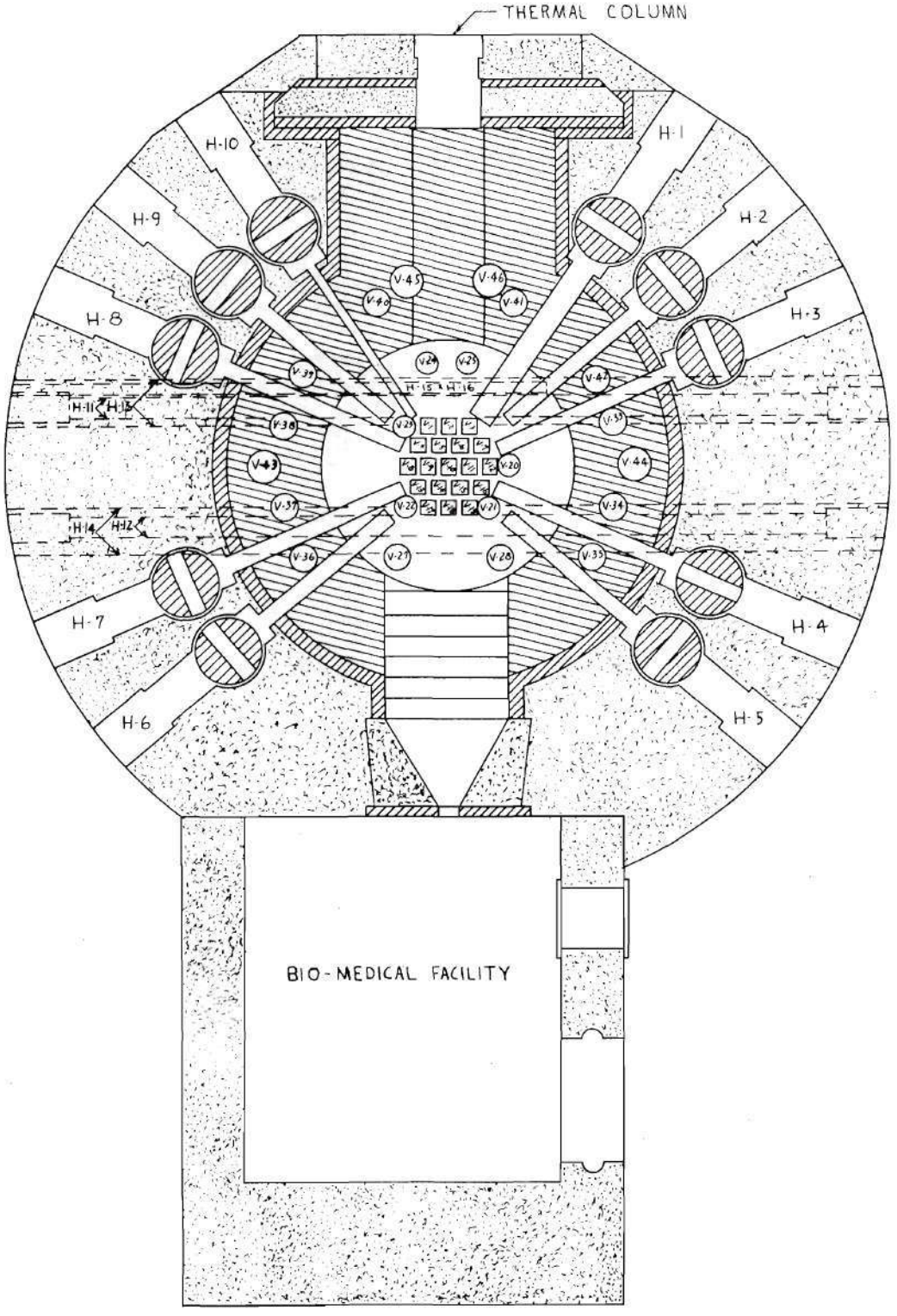

Figure 7. Mid-plane Section of the Georgia Tech Research Reactor

zontal section of the GTRR.

The Beam Port

For background considerations it was desirable to locate the detector as far from the beam port as possible. However, the percentage of a cycle that the sample spends in the interrogation flux is controlled by beam diameter, as shown in Figure 4. Efficiency for detecting delayed neutrons is, in turn, affected by the fraction of a cycle spent in activation. These two considerations suggest that the beam port chosen as a source of interrogation neutrons has a large diameter. In order to compile data rapidly it is also desirable to have a high thermal flux. Beam port H-1 meets these qualifications; and since H-1 was available for use when the experiment was initiated, it was chosen as the source of interrogation neutrons.

Beam port H-1 is circular with a diameter of six inches. As shown in Figure 7, H-1 originates in a high flux region of the GTRR near a fuel element. A thermal flux or more than 10^{13} $n/cm^2/sec$ had been measured at the reactor end of H-1[39] and a fast neutron flux component can be expected from the proximity of a fuel element. Between the reactor end of H-1 and the H-1 shutter, graphite stringers moderate the fast component of the flux, provide some gamma shielding, and decrease the thermal flux by scattering.

A beam plug was designed for beam port H-1 to allow a well defined beam of neutrons to exit the reactor while preventing excess neutrons and gamma rays from entering the experiment area and raising the counting background. Details of the plug are shown in Figure 8. The plug has a structural casing of carbon steel, and is filled with layers of lead,

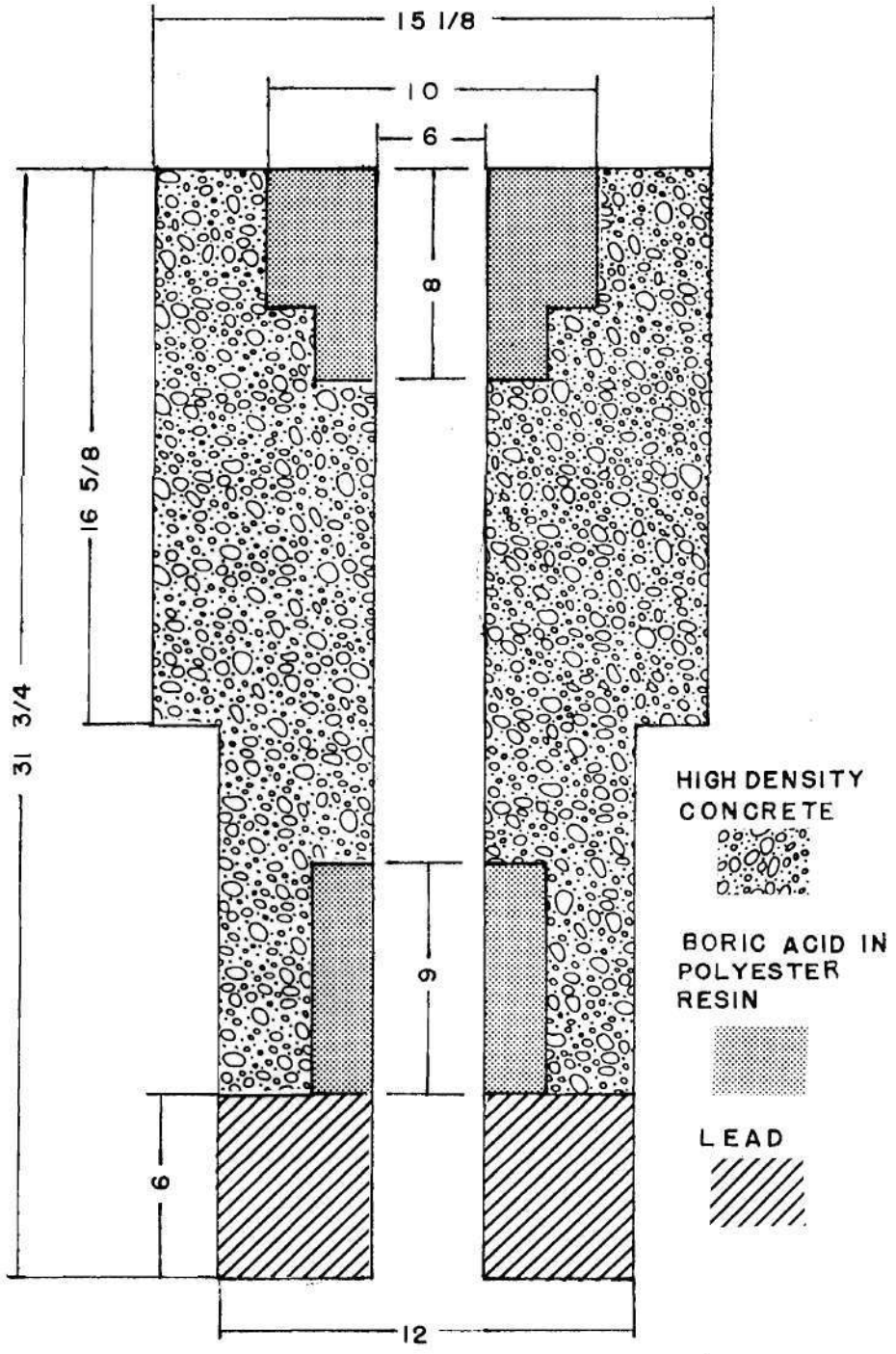

Figure 8. Beam Plug Made for Beam Port H-1
(Dimensions in inches.)

high density concrete, and boric acid in a matrix of polyester resin. A collimator of boric acid and polyester resin was inserted to produce a sharply defined neutron beam with a diameter of six inches (15 cm). Even though a well-defined neutron beam is needed to predict the delayed neutron response after interrogation, sharp definition of the beam is not as important in the actual experiment because assay of unknown samples is accomplished by comparison with reference delayed neutron signatures of uranium-235 and plutonium-239 obtained with the same experimental set-up. Step construction was utilized in the plug to reduce streaming of unwanted gamma and neutron radiation outside the beam. Center beam thermal neutron flux was measured by indium foil activation to be about 5×10^8 $n/cm^2/sec$ at the reactor face and the beam center.

Defects in the reactor shielding in the vicinity of H-1 resulted in some fast neutron leaks of moderate intensity. Shielding provided around the BF_3 detectors in the experiment was not sufficient to eliminate the contribution of these leaks to the background count, so some additional shielding of paraffin slabs and cadmium sheets was added next to the reactor biological shielding wherever fast neutron leaks were found. The most serious leak of fast neutrons came from a crescent-shaped void in the biological shield directly below H-1. When paraffin and cadmium shielding were applied in this area, background was reduced substantially.

After passing through the experimental system, the neutron and gamma radiation beam from H-1 terminated in a beam catcher. The beam catcher was constructed by G. H. Weaver and D. S. Bridges; it consisted of a 55 gallon steel drum filled with a mixture of paraffin, boric acid, and lead shot.

The Cycle Generator

In this experiment an intermittent activation-count cycle was produced by physically moving the sample through a neutron beam, then into the detector, back through the beam, et cetera. The collection of foils comprising the sample rode the sample arm as it was rotated by an electric motor and gear train. This arrangement is depicted in Figure 9, a photograph of the system as it was operated.

Because the cycle time is a crucial parameter in the final analysis of data, it is important that the rotation period be very stable and reproducible. A linear servo-amplifier with negative feedback was used in the motor speed control used in this experiment. The speed control drives a 24 V, series-wound, DC motor and incorporates a tachometer feedback from the gear train to eliminate cycle time inaccuracies that could result from minor variations in load, such as bearing aging or thermal expansion of the gears. Silicon-controlled rectifier devices were avoided to exclude the possibility that the pulses they produce and the high frequency noise generated by the switching transients of SCR's would disrupt some other electronic equipment in the system. In order to optimize stability of the cycle time over the wide range needed, front panel controls for feedback, open loop gain, and threshold were provided. Long and short term stability over the range of periods of interest, 0.1 to 150.0 sec, was found to be better than ± 0.2 percent.

The sample arm was driven by the speed controlled motor through a train of speed reducing gears with an overall ratio of 30/254 or about 1 to 39.8. The gear ratio between the tachometer and motor was 17/20 or about 1 to 1.178. A photograph of the gear train is shown in Figure 10.

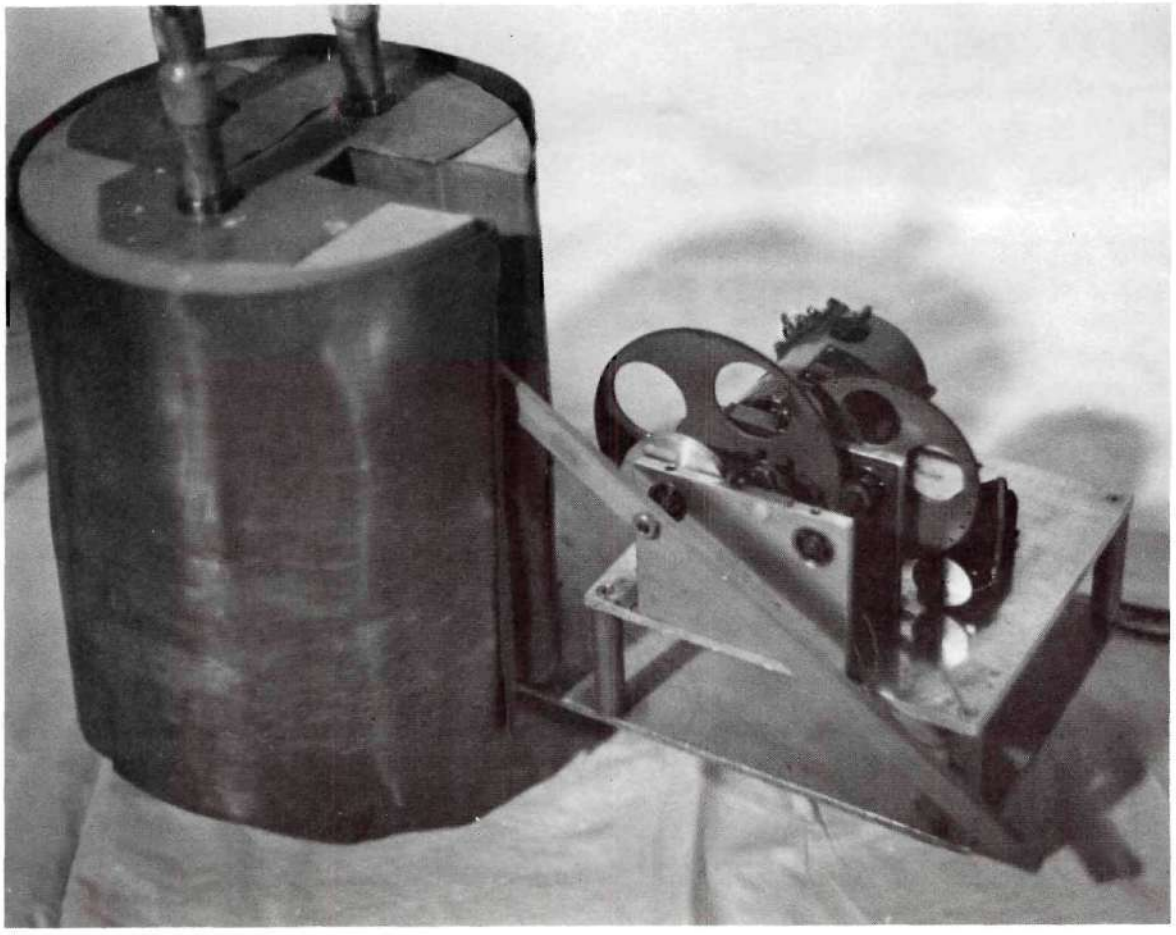

Figure 9. Photograph of Assembled Detector, Motor, and Gear Train

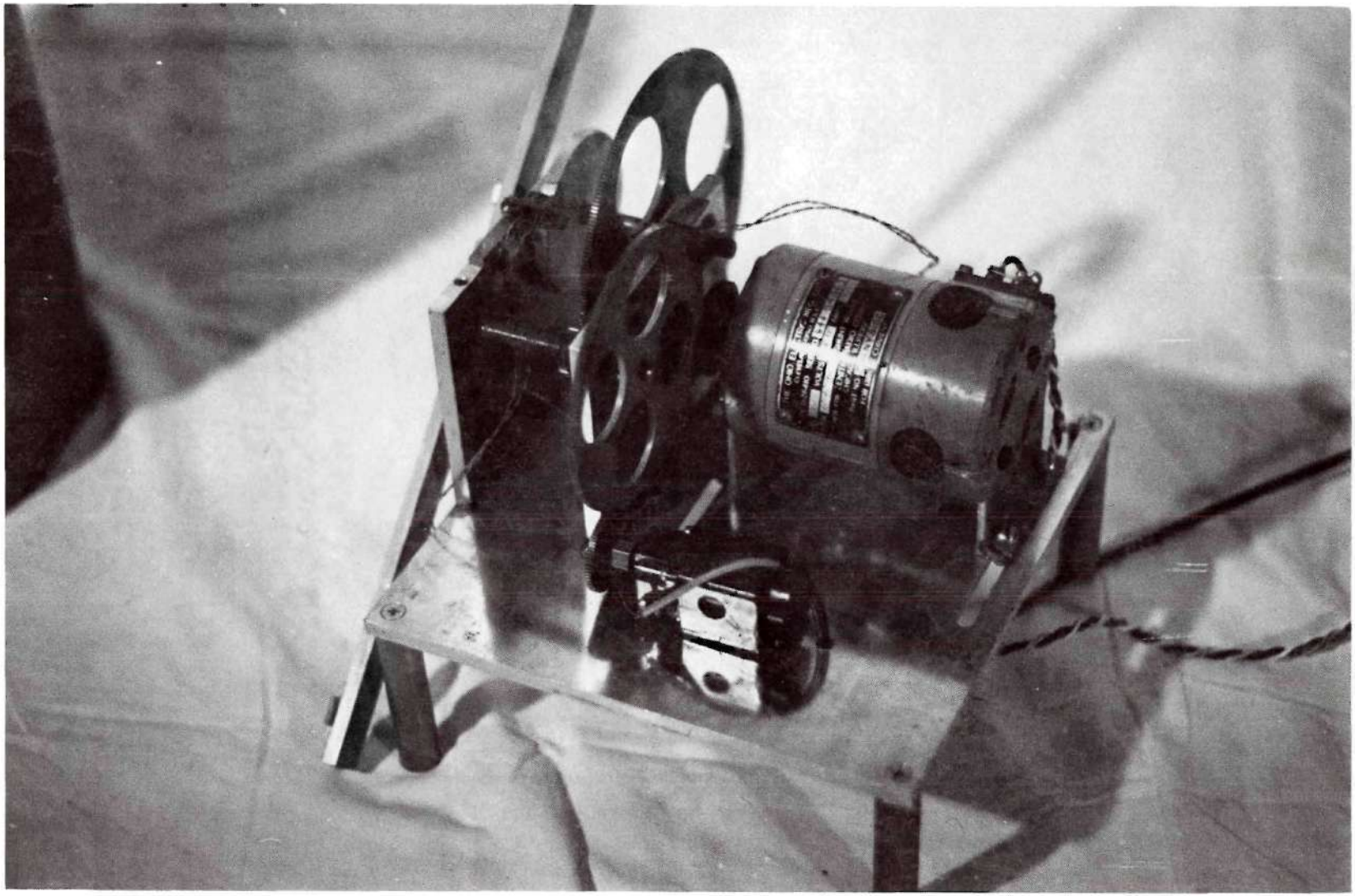

Figure 10. Photograph Showing Motor and Gear Train Used to Drive the Sample Arm

Rather than take the analog output of the tachometer as an indication of instantaneous time, a more direct method of counting the number of revolutions in a given time was used to eliminate the necessity of developing a linear amplifier for the output of the tachometer, which, itself, is of dubious linearity (in this speed control, monotonicity, rather than linearity, is the important quality); it also allowed digital accumulation of data indicative of period time. To this end thirty small holes were drilled near the perimeter of a gear that turns with a ratio of 26/3 with the sample arm. The passage of these holes was detected with a General Electric H-11B interruptable light-coupled device, consisting of a light sensitive transistor and an infrared light emitting diode coupled through a small air gap. A scaler, gated by a timer, accumulated the pulses generated by the passage of holes through the light-coupled device. In one revolution of the sample arm 260 pulses were detected, so the number of revolutions (cycles) in a given time, controlled by the timer, could be determined with a maximum error of 0.0039 revolution.

A fiberboard target attached to the shaft holding the sample arm interrupted the light beam in a second H-11B whenever the sample was not in the detector. The output of this device was coupled through an "AND" gate with the timer output and used to gate the scaler that accumulated delayed neutron pulses from the BF_3 tubes. This method of gating prevented the unnecessary accumulation of prompt neutrons as background while the sample was out of the detector and in the neutron beam.

The sample arm was a flat piece of 3/16 inch by 3/8 inch aluminum stock drilled and tapped in the center and threaded onto the output shaft

of the gear train. Doublesided tape, applied to one end of the sample arm, was used to hold the sample during the experiment.

Neutron Detector

The neutron detector in this experiment needed to have as large an efficiency for detecting epithermal delayed neutrons as possible and to be somewhat insensitive to the thermal neutron and gamma ray background. BF_3 detectors were chosen for their efficiency and availability. Paraffin was added to moderate the delayed neutron spectrum somewhat to increase the sensitivity of the BF_3 detectors, and the moderator was surrounded by cadmium to eliminate thermal neutrons while allowing delayed neutrons to penetrate.

Figure 11 is a photograph of the partially assembled delayed-neutron detectors and the shielding. A drawing of the detector-shield assembly is shown in Figure 12 for easier identification of the various shielding and moderating elements.

Detection of the delayed neutrons was accomplished with three independent boron trifluoride-filled detectors. One of these detectors was a Reuter-Stokes model RSN-7A and the other two were LND model 2025. These two types of detectors are functionally and mechanically equivalent. The detectors were 2.5 cm in diameter and had a length of about 30 cm, 20.64 cm of which comprised the active volume. The fill gas was BF_3, and the detectors were filled to a pressure of 400 torr. Factory information which accompanied the detectors is shown in Appendix A.

Count versus anode voltage plots was obtained for the LND detectors and these plots are included in Appendix A. The plateau found

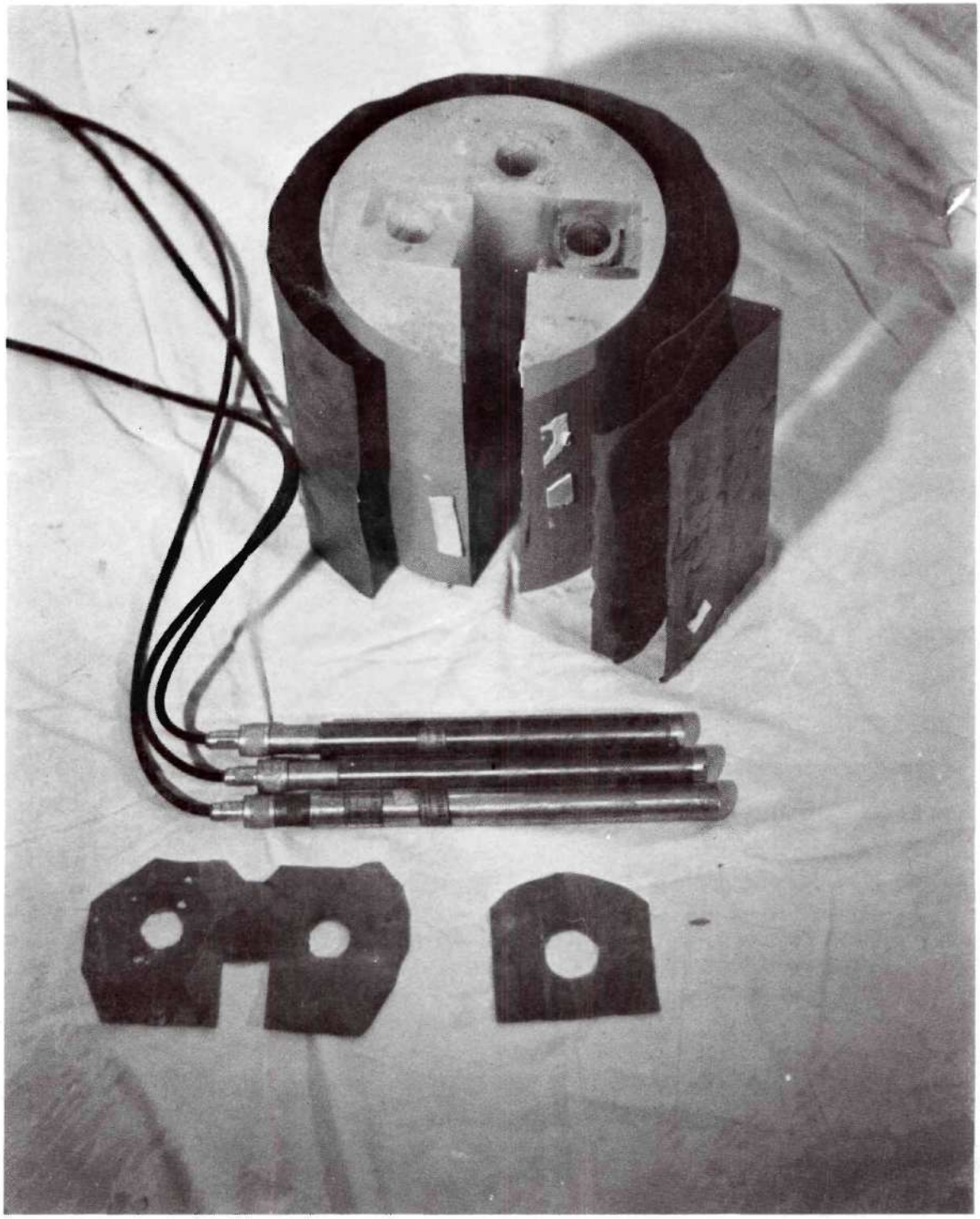

Figure 11. Photograph Showing the Construction of the Delayed Neutron Detector

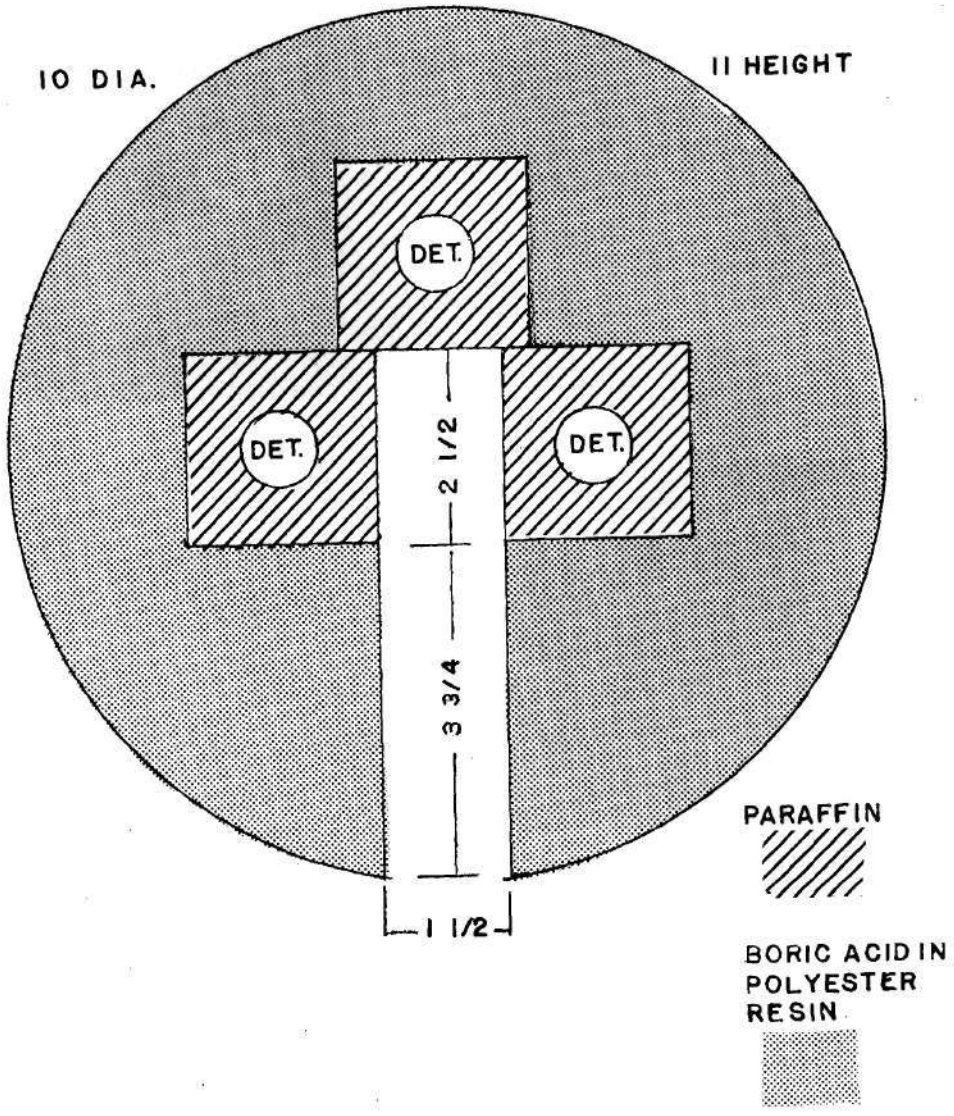

Figure 12. Drawing of Detectors, Moderator, and Shield (Entire assembly, including sample slot, was sheathed in cadmium. Dimensions in inches.)

for the LND detectors and the curve supplied by the factory for the Reuter-Stokes detector were used to select an operating voltage of 1275 volts. All three of the detectors showed flat plateaus from 1200 volts to 1350 volts.

The arrangement of the shield and moderator surrounding the detectors can be seen in Figures 11 and 12. Each detector was enclosed in a paraffin moderator to render the epithermal delayed neutrons more detectable by reducing their energy. The paraffin moderator was enclosed on three sides by a cast cylindrical block of boric acid in a matrix of polyester resin. The cylinder supplied support for the moderator-detector assemblies. And, because it was formed from a neutron moderator, polyester resin, and a neutron absorber, boric acid, the cylinder also shielded the detectors from any ambient background of thermal and epithermal neutrons. The reactor gamma ray background was not sufficiently intense to cause pile up and spurious counts in the BF_3 detectors. The four sides of the moderator blocks form the detection volume. This arrangement was chosen to give the counting chamber as near 4π geometry as possible with detectors that are long and thin. The counting chamber itself was lined with 0.5 mm of cadmium metal to shield against any thermal neutrons that might stream in through the slot for handling samples. Epithermal delayed neutrons easily penetrate the cadmium lining. Further shielding was provided by lining the sample handling slot with cadmium and covering the outer surface of the boric acid-polyester resin cylinder with 0.5 mm cadmium sheet.

BF_3 detectors discriminate well against gamma radiation such as that generated by the samples, relatively free of fission products, used

in this experiment. In assay situations involving spent fuel, very high gamma radiation fluxes may be encountered, and gamma pulse overlap in intense gamma fields may add significantly to the neutron count. When intense gamma fields are expected, the counting chamber may be shielded with a material, such as lead or bismuth, that is a good gamma shield, yet is relatively transparent to neutrons.[40] A later section on calibration describes an experiment to determine the gamma radiation sensitivity of the BF_3 detectors used in the experiment and to define the gamma radiation levels at which further lead shielding would have been necessary in this experiment.

Background radiation is a factor in counting statistics that was somewhat controllable. Boric acid in polyester resin and cadmium sheet shielding at the detectors and paraffin and cadmium shielding at leaky places in the reactor biological shielding reduced the background encountered in these experiments to a few counts per second. This was still a substantial contribution to the total counts at long cycle times, long delayed-neutron precursor half lives, but was not a significant effect at cycle times of three and ten seconds, where the differences in delayed neutron yields of uranium-235 and plutonium-239 are greatest. Further reductions in background are possible (Ralph Altman was able to achieve a background of one count per minute in a similar BF_3 detector at beam port H-9) but that would not have resulted in much improvement in assay accuracy.

Signal Processing and Count Accumulation

Figure 13 is a schematic of the signal processing equipment. This equipment had the function of recording both the delayed neutron pulses

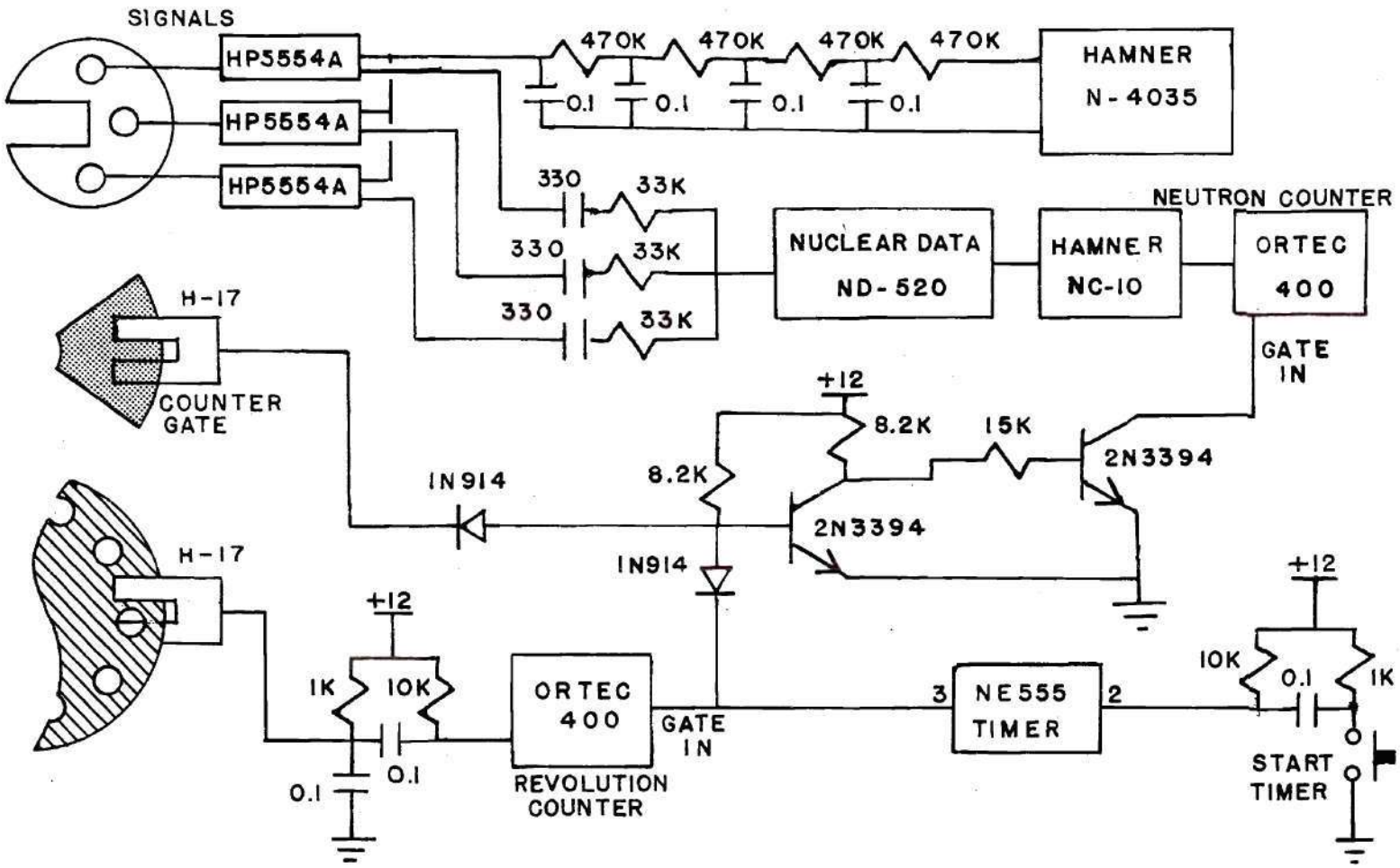

Figure 13. Schematic Diagram of the Signal Processing and Recording Equipment

generated by the BF_3 detectors per unit time and the period of the activation cycle.

The three BF_3 neutron detectors were supplied with high voltage by a Hamner model N-4035 high voltage power supply. The high voltage was filtered by an R-C ladder network, 470 kΩ resistors and 0.1 μF capacitors, before reaching the preamplifiers and detectors to prevent damage to the field effect transistors in the preamplifier inputs from a power-up or power-down transient.

Pulses produced by the three neutron detectors were amplified by Hewlett-Packard model HP-5554A preamplifiers, one preamplifier for each BF_3 detector. The internal bias resistor in each detector was 100 MΩ. Charge sensitivity was set at 300 μC/V and voltage gain was set at 8.

The signals from the preamplifiers were added by an RC network, shown in Figure 13, and the combined signal from the three outputs was fed into a Nuclear Data model ND-520 pad. Coarse voltage gain of the pad was set at 4 and the fine voltage gain was set to about mid-scale.

Discrimination against noise and signals, other than those that resulted from $B^{10}(n,\alpha)Li^7$ reactions in the BF_3 detectors, was accomplished by a Hamner discriminator, model NC-10.

The output of the discriminator was applied to an Ortec Model 400 scaler to accumulate a count from the (n,α) events that occurred in the detectors. The scaler was set up to count positive-going pulses of about five volts in amplitude. The slave switch was set to "normal" and the gate was set "on."

Light pulses from the optical cycle time hole detectors were applied through a resistor-capacitor network shown in Figure 13 to another

Ortec Model 400 scaler. This scaler was set up to record negative-going pulses of about three volts amplitude. The slave switch was set on "normal" and the gate switch set to ON.

Both scalers were gated by a timer built around a Signetics NE555V integrated circuit, also, as shown in Figure 13. The timer could be initiated by either a front panel push button or a remote push button located on top of the reactor near the H-1 shutter control. A front panel switch allowed time constants of 1, 10, 100, 1000, and 2000 seconds to be selected.

The scaler used for accumulation of cycle time data (passage of holes) was gated directly by the timer but, in order to prevent accumulation of background and prompt neutron pulses while the sample was out of the detector assembly, the count accumulation scaler was gated by the outputs of the timer and the optical coupler that indicated the sample was in position to count delayed neutrons. The output of the optical coupler was about 10 volts when the sample was in the detector and zero volts while the sample was out of the detector. Two transistors and two diodes configured in a DTL AND gate, shown in Figure 13, were used to gate the count accumulation scaler from the timer and optocoupler outputs.

Calibration

Timer

Since the timer was constructed from integrated circuits using formulas given in the Signetics Data Book to set up the resistor-capacitor timing networks, both accuracy and precision had to be checked. Actually, it was not necessary to know the actual time resulting from each of the

five timer settings, but, rather, the ratio of the times to one another and the error between one time event and the next for each setting, because the data of interest were a series of time spectra, each taken using the same timer, rather than the absolute half lives of the various delayed neutron groups. The timer was used to time data collection and to determine the time required for one cycle. Activate, count, and transport portions of the cycle were mechanically held to fixed fractions of the total cycle time.

To calibrate the timer and test its timing interval error the circuit shown in Figure 14 was set up on a breadboard. The circuit consists of a 100 kHz crystal oscillator driving a Schmitt trigger for pulse shaping, followed by four TTL decade counters. An astable multivibrator can be driven by any one of the four counters to provide 10, 10^2, 10^3, or 10^4 pulses per second. The output of the multivibrator drove the signal input of one of the Ortec scalers used in the experiment while the timer to be calibrated was connected to the gate input. The multivibrator was connected to the proper decade counter to accumulate approximately 10^4 pulses in the time interval expected, based on the integrated circuit manufacturer's formulas.[41] For each timer setting, the scaler was cleared and the timer started a number of times to collect a series of timer interval data. From these data the mean time interval and the standard deviation in the series of time intervals were calculated for each setting. The results of this calibration are presented in Table 4. Rather than try to trim the time intervals exactly to 1, 10, 100, 1000, and 2000 seconds by varying circuit components, each experimental measurement was recorded with the timer setting used to generate it and the Univac 1108

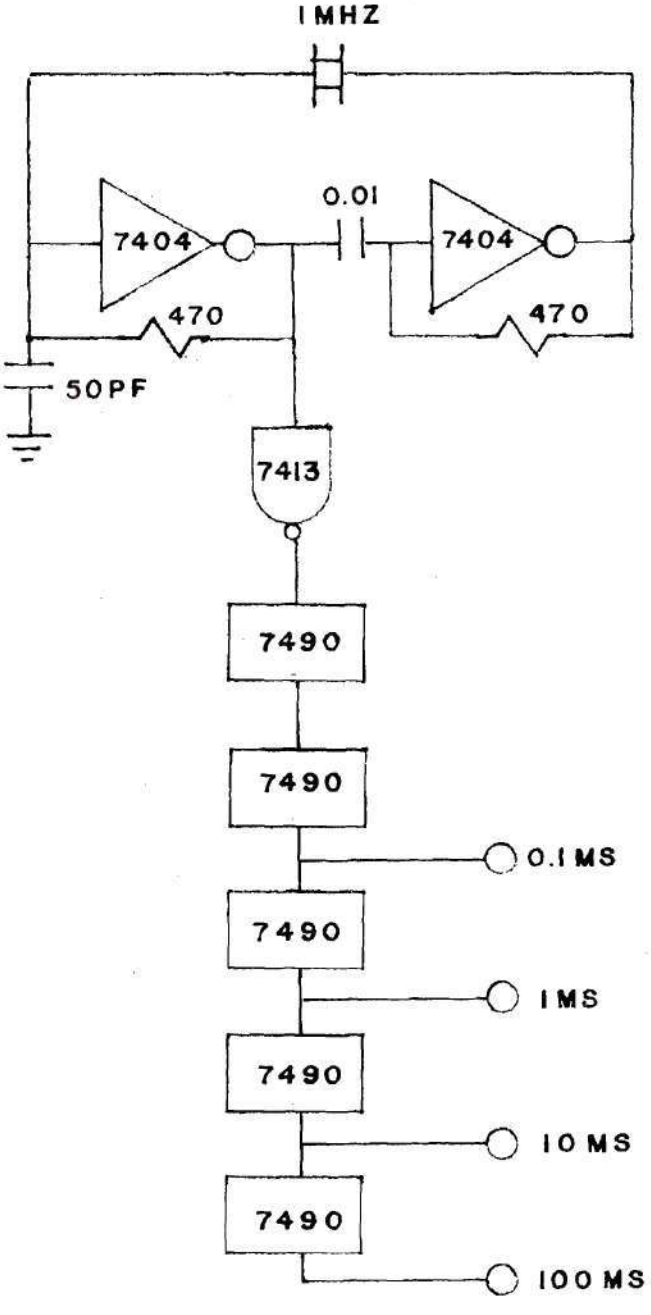

Figure 14. Schematic of the Circuit Used to Calibrate the Timer

calculated counts per unit time using the information in Table 4.

Table 4. Timer Settings and Accuracies

Timer Setting	Time Interval (sec)	Standard Deviation (%)
A	1.129	0.3
B	12.37	0.3
C	115.4	0.3
D	1031.0	0.2
E	2206.0	0.3

Motor Speed Control

The speed control was tested for stability using the crystal oscillator constructed to test the timer. Pulses from the optical coupler generated by holes in the perimeter of one of the drive gears (260 pulses per revolution) were applied to one scaler and the output of the crystal oscillator-counter circuit was applied to a second scaler. Both scalers were gated by the timer. Since the number of pulses per second from the oscillator-counter circuit was known very precisely and accurately, the actual revolution time could be determined independent of any error introduced by possible inaccuracies in the timer.

The accuracy of the speed control was tested at cycle times of approximately 1, 100, and 1000 seconds. The number of counts in the scaler connected to the crystal controlled oscillator was divided by the number of counts per second from the oscillator to determine the time, and the count from the scaler connected to the speed control was divided by 260 to determine the number of revolutions. Data were collected at

three time intervals to determine both the long term and short term stability of the speed control.

Table 5 shows some typical speed settings and the corresponding long term and short term stability from one time interval to the next. In every case the 1σ stability is better than one percent.

Table 5. Accuracy of the Motor Speed Control

Revolution Time (sec)	σ % (1 sec)	(100 sec)	(1000 sec)
0.1	0.3	0.4	
1.0	0.5	0.4	
10		0.4	0.6
100		0.6	0.9

It was found, however, that a 15 minute warm up was necessary before stable operation was achieved. The speed control demonstrated some fine "hunting" at very long periods. This causes noisy operation but had little effect on stability in time periods even as short as one second. Gain and threshold controls were added to the speed control circuitry to eliminate the hunting but little further improvement in stability was obtained, even when hunting was eliminated.

Neutron Beam Flux Determination

The neutron beam emerging from beam port H-1 with the shutter open and the reactor operating at one megawatt was measured with an indium foil with a mass of 79 mg and a diameter of 1 cm. The foil was irradiated in the H-1 beam at the reactor face and, after an hour cooling off time

to let the 2 and 14 second half-life activities die away, its 54.1 minute half-life beta activity was counted with a gas flow counter. Saturation activity was found with the formula[42]:

$$A_s = \frac{\lambda (C-B)}{F \epsilon (1-e^{-\lambda t_r})(e^{-\lambda t_1} - e^{-\lambda t_2})}$$

where

A_s is saturation activity

λ is the decay constant of ^{116m}In

ϵ is the overall detector efficiency for beta rays

$(C-B)$ is counts minus background

t_r is the irradiation time

t_1 is the time from the end of irradiation to the beginning of the count

t_2 is the time from the end of irradiation to the end of count

F is the fraction of neutrons absorbed that contributes to A_s

In a neutron beam the saturation activity is related to beam thermal neutron flux by:

$$A_s = a \varphi_{th} (1-e^{-\Sigma_{ath} d})$$

where

A_s is saturation activity

a is foil area

φ_{th} is the thermal neutron beam flux

d is foil thickness

Σ_{ath} is the macroscopic absorption cross section

The neutron flux from H-1 at one megawatt at the reactor face was found to be about 5×10^8 neutrons per cm^2 per second. In a similar experiment with cadmium covers it was determined that the cadmium ratio for indium foils was six.

Dead Time Determination

An attempt was made to determine the dead time of the BF_3 detectors used in the delayed neutron detector system, using a PuBe neutron source as a point source and assuming that the neutron flux in the air around the source decreased as the square of the distance from the source. It was established that the dead time was less than 50 μs, not enough to affect the low count rates encountered in the delayed neutron experiment.

Gamma Sensitivity

To be assured that counts resulting from gamma pileup in the BF_3 detectors were not influencing the results of this experiment the detectors were tested for gamma sensitivity with a 60 kilocurie cobalt source in the fuel storage pool. The counting equipment was set up at the edge of the pool, and gain and discriminator levels were set to the values used in the delayed neutron experiment. Thermoluminescent dosimeters were attached to a BF_3 detector and the detector was lowered on a glass fiber string down an aluminum pipe toward the cobalt source. The detector was stopped at a given level, the count rate recorded, and the detector was raised to retrieve the TLD. This process was repeated for several different levels down the pipe.

Figure 15 is a plot of the count rate induced in the BF_3 detectors as a function of radiation field from the cobalt-60 source. In the delayed neutron experiment the gamma radiation level encountered by the BF_3

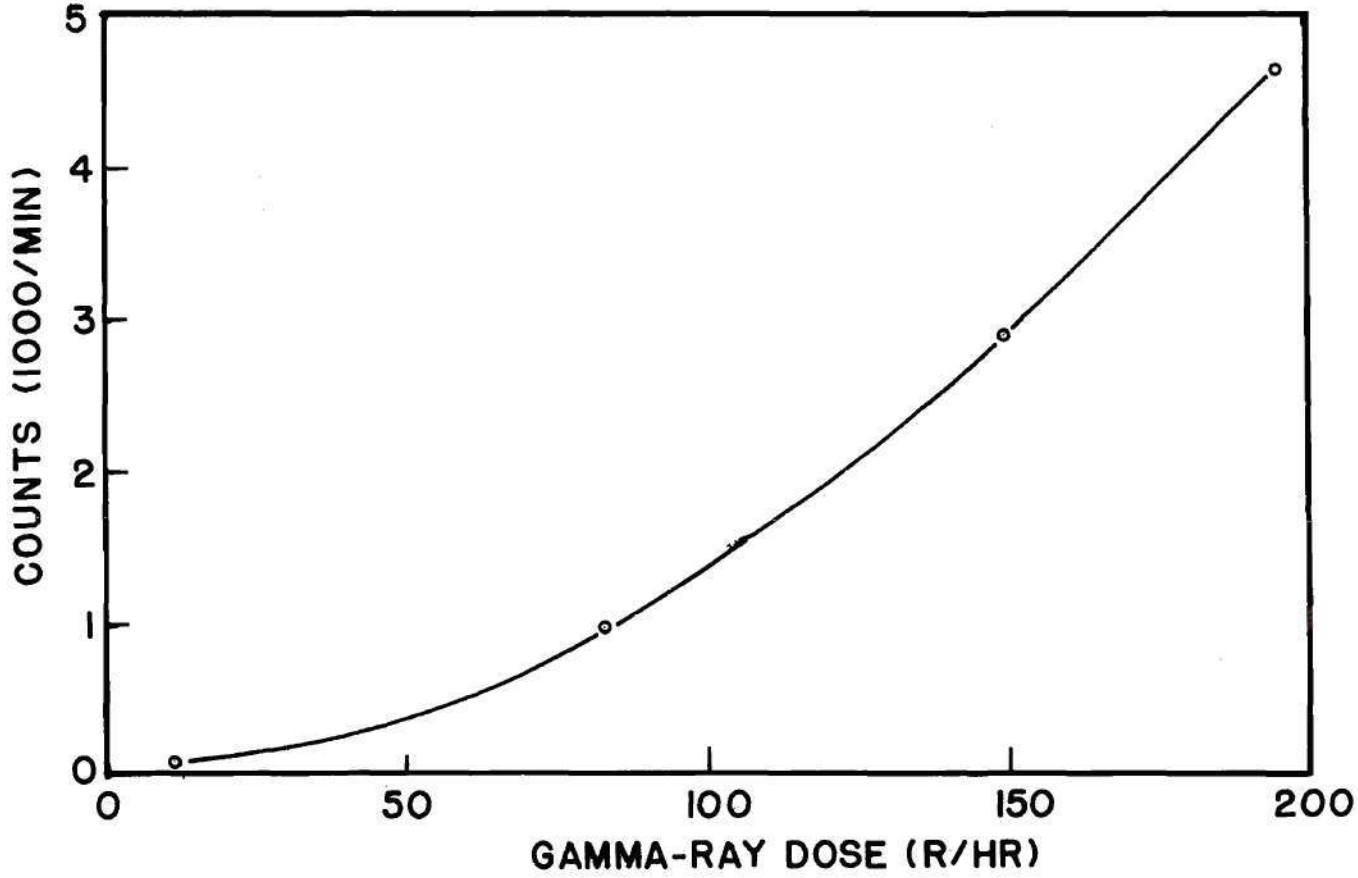

Figure 15. Sensitivity of BF_3 Neutron Detectors to Gamma-Ray Radiation from ^{60}Co

detectors, less than 100 mR per hour, was not sufficient to perturb the count rate. At 30 R per hour, gamma induced counts would have presented a serious background problem, and at 150 R per hour the count rate from gamma radiation would have approached the count rate from delayed neutrons. Had it been necessary to contend with gamma fields of this magnitude, from, for instance, spent fuel elements, a dense material with low neutron absorption cross section, such as bismuth or lead, would have been used to shield the detectors from gamma rays.[43]

Description of the Samples

For the present experiment the samples of fissionable material that were available consisted of a series of small uranium metal foils and five large, encapsulated plutonium foils. Sample size and shape will, of course, exert a considerable influence on the configuration of the assay experiment. Samples, for instance, that are massive or bulky would require fast, rather than thermal, neutrons to penetrate and assay more than just the outside few millimeters of material; and samples that are awkward to handle may require pulsing of the neutron source rather than physical movement of the sample.

The uranium foils were discs of uranium metal 1.27 cm in diameter and about 0.02 mm thick. Table 6 lists the uranium foils available for the experiment with the mass of each foil. These foils were oxidized on the surface, so, to prevent loss of mass and contamination by uranium oxide around the experiment area, the foils were encapsulated in small polyethylene bags and sealed. The bags were weighed before and after inserting the uranium foils and the differences between the masses deter-

Table 6. Fission Foils Used and Data Used to Determine Self-Shielding Factors for the Plutonium Foils

Uranium-235

Foil Number	Mass (grams)
1	0.1833
2	0.1904
3	0.1794
4	0.1885
5	0.1891

Plutonium-239

Foil Number	Pu Content (grams)	Test Time at 0.1 Sec Cycle Time (sec)	Counts	Self-shielding Factor Calculated (Eq. 5-1)
1 (P-296)	1.0	500	38,813	0.152
2 (P-297)	1.0	500	35,411	0.147
3 (P-298)	1.0	500	37,095	0.150
4 (P-299)	1.0	500	42,157	0.163

mined from the two weighings were used as the foil masses in these experiments. The contribution of oxygen to these measurements was assumed to be negligible. The total weight of the polyethylene in an encapsulating bag was found to be, typically, 0.06 gram. Wall thickness of the bags was 0.025 mm and the bag wall and foil were in contact in the experimental set up, so the polyethylene should not have detectably affected the fissions per unit time in the sample or changed the number or spectrum of delayed neutrons reaching the BF_3 detectors from the fission products in the sample.

The plutonium used in the experiment consisted of five plutonium foils on hand at Georgia Tech. The plutonium was in the form of plutonium metal which, because plutonium metal is toxic and chemically reactive, was encapsulated in a stainless steel can with a wall thickness of 0.254 mm. The samples used contained about 1.0 gram of 99 percent pure plutonium-239.

Fissionable Material Safety

In this experiment there were never more than five grams of fissile material, uranium-235 or plutonium-239, in use at any time. This amount of fissile material is not sufficient to form a critical mass in any physical configuration. The introduction of this much fissile material into the containment building is acceptable; the mass of fissile material, other than the material in the reactor core, is limited by the Georgia Tech Research Reactor (GTRR) operating specifications to five grams.

Even though five grams of fissile material are not sufficient to form a critical mass, care had to be taken to prevent any fissile material from accidentally entering the reactor core. Beam port H-1 was open during

the experiment but graphite stringers left between the shutter and the core would have prevented objects entering the face of the beam port from approaching the core. Samples were rotated around an axis perpendicular to the face of the reactor so, even if a fissionable sample had broken from the sample arm while being rotated, it could not have been thrown toward the reactor. Rotation speeds were not very great but calculations showed that at a maximum rotation rate of about 10 rps, a sample freed from the rotating arm at the proper time could have been thrown as high as the top of the biological shielding. It was considered unlikely that a sample of fissionable material thrown from the vertically moving arm would land on the top of the reactor rather than falling directly back down, or that the sample could penetrate the top shield plugs if it did find its way to the top of the reactor; but to prevent any possibility of such an occurrence the ends of the sample arm were drilled and taped for small set screws to prevent any radial movement of the sample on the arm.

Ionizing Radiation

Ionizing radiation encountered in this experiment arose from four sources: the inherent activity of the fissionable material, the fission products produced by neutron irradiation of the samples, the prompt fission activity encountered during the course of the experiment, and radiation from the reactor itself.

Sample Activity. Before the experiment the neutron exposure history of the samples was very limited. The plutonium had not been previously subjected to neutron irradiation and only a few of the uranium foils had received any neutron irradiation, and those had had considerable

elapsed time for the fission product activity to die away. Thus the samples were relatively free of any induced activity prior to the experiment. A calculation of the activity of the approximately one gram of uranium-235 that was on hand showed that it had an activity of considerably less than one mCi. A similar calculation for plutonium-239 yielded about 10 mCi for a one gram sample. Radiation levels of about five mR/hr for the uranium and 100 mR/hr for the plutonium were measured at contact. The fresh samples, then, did not present much of a hazard. Even so, the fresh samples were always handled with forceps and stored in a properly labeled lead pig.

Induced Activity. During a test as many as 10^{11} fissions may have been induced, resulting in a sizeable fission product activity. Since most fission products have short half lives and since the maximum fission rate in the samples was less than 10^{8} fissions per second, the fission product activity did not build up as rapidly or as high as the first order approximation from the total fissions induced might indicate.

The hazard of fission product radiation was evaluated experimentally to eliminate any calculational uncertainty. The experiment was set up and, with health physics in attendance, beam port H-1 was opened for about three seconds. After closing the shutter to H-1 the radiation level of the sample was monitored. This procedure was repeated leaving the shutter open for longer periods until irradiation times approximating the irradiation times to be encountered in the experiment were achieved. Because it was the most massive, the plutonium sample was the most active. It read 10 rad per hour at contact immediately after closing the shutter to H-1 after a 600 sec test period. The procedure during

the experiment was to allow the samples to cool in the experiment area for 30 to 60 minutes after a run of the experiment, then the irradiated sample was removed from the sample arm with forceps and stored in a lead pig. Several samples, particularly the plutonium, received many irradiations; therefore, fission product activity was monitored before and after a sample was used to be assured that the activity was not building up unacceptably.

Reactor Beam Hazard. The most intense source of radiation involved in the experiment was the reactor beam from H-1. The beam was stopped after traversing the experiment by the beam catcher. The two-foot path traversed by the beam between the face of the reactor and the beam catcher was roped off and labeled a high radiation area when the shutter was open. The experiment controls and data collection electronics were sufficiently remote from the beam to permit operation of the controls when the shutter was open, but, because no intervention was necessary while data were being collected, the shutter was usually closed before the area was approached to record data and make cycle time changes. A remote switch allowed initiation of a data run from the top of the reactor after the shutter was opened.

While the shutter was open, enough reactor and prompt fission radiation still by-passed the beam catcher to cause an alarm on the area monitor near the experiment. Health Physics ascertained that the radiation levels outside the roped off area were not excessive. However, the "Do Not Enter Light" on the air lock was lit and anyone entering the containment building was advised of the situation.

Prompt Fission. While a sample was in the neutron beam it was

experiencing as much as 10^8 fissions per second with a corresponding output of prompt gamma radiation. However, during the time that fissions were being produced in the sample, the sample was between the reactor biological shielding and the beam catcher, and, therefore, fairly well shielded from the floor of the containment vessel. Health Physics monitored radiation levels near the beam and the fissioning sample when the experiment was begun, and the steps taken to limit exposure from the reactor beam supplied protection from the prompt fission activity as well.

Toxic Materials

Plutonium is one of the most toxic substances and plutonium metal is very active chemically; consequently care had to be taken that the plutonium metal samples, though hermetically sealed in 0.0125 inch thick stainless steel cans, did not leak. Health Physics took smears from the plutonium samples and the lead pig in which they were stored to check for possible dispersal of plutonium. None was found.

The uranium metal foils used were oxidized on the surface and small flecks of the oxide could be removed mechanically. To prevent contamination by uranium oxide and to preserve the integrity of the foils, the uranium samples were sealed in small, thin polyethylene bags. The bags and the lead pig in which they were stored were tested by Health Physics to be assured that there was no dispersal of uranium.

CHAPTER V

DATA COLLECTION AND RESULTS OF THE EXPERIMENT

To analyze a sample for composition of uranium-235 and plutonium-239, the delayed neutron response of the sample as a function of activation cycle frequency was compared to similar responses from known standards with the aid of computer programs that will be described in Chapter VI. It was necessary to take a number of delayed neutron counts at various frequencies for each sample to construct a delayed neutron count rate function for each sample for comparison to the similar function from a known standard sample. Each analysis was done with a delayed neutron count rate function consisting of delayed neutron count rates taken at 25 to 50 different cycle periods, spaced approximately logarithmically between 0.1 second and 50 or 100 seconds. Various samples were constructed from the foils available to test the sensitivity and accuracy of this analysis method, and to test the ability of the method to distinguish between the fissile isotopes uranium-235 and plutonium-239.

Once the experiment was set up, collection of data was very straightforward. The electronic systems were turned on and high voltage was set to 1250 volts. The timer was set to a cycle time of one second (actually 1.129 sec) and the speed controls were set to get about 2935 counts in the revolution counting scaler. It was difficult to set the speed exactly, but on most data points is did not matter because the actual cycle period could be calculated from the counts in the revolution

counter. However, since the first point, 10 rps, was used as a normalization point in the analysis, pains were taken to get this period as close to nominal as possible even though the delayed neutron signatures are very flat in this region. The beam shutter was opened and several minutes were allowed for equilibrium response to be reached. The data collection timer was set to 100 sec and delayed neutron counts were collected in one scaler each time the sample passed through the neutron detector. In a second scaler pulses from the optical coupler in the gear train were collected to compute the cycle time (inverse of cycle frequency) for the data point. After the data in the two scalers had been recorded, the speed control was set for the next cycle time (calculated to give about 25 to 50 points logarithmically spaced on the resultant delayed neutron response as a function of cycle time curve) and the timer retriggered. By this time the short half-lived precursors had reached equilibrium and small changes in period would not affect the equilibrium response of the long half-lived delayed neutron precursors. This procedure was repeated until a period of about 100 seconds was reached. For longer periods a longer time was allowed between runs for transients to die away. The resulting set of delayed neutron count rates at various cycle periods described the cyclic activation response of the sample and was entered, along with the background count rate, into the Univac 1108 programs described in Chapter VI.

Data were collected in the manner described above for plutonium alone and for uranium alone for the analysis program for use as a reference. Then, a series of data runs was made for sample compositions of uranium-235 and plutonium-239 ratios varying from 10:90 to 60:40.

Because the plutonium foils available were about one gram in mass there was not sufficient uranium on hand to make up samples richer in uranium-235 than about 60 percent. In this experiment the thermal neutrons used for interrogation were not able to uniformly penetrate the samples, and significant self-shielding effects, described in Chapter VI, had to be corrected for in the relationships between delayed neutron response and the actual mass of fissionable isotope present. The thickness of the plutonium foils was not measurable because the foils were sealed in stainless steel capsules for safety reasons. Of the 1.5 mm thickness of the capsule, probably at least 1.0 mm was plutonium metal, equivalent to about five mean free path lengths for thermal neutrons. The thickness of the uranium foils was measured to be about 0.15 mm, a little less than 0.5 mean free path for thermal neutrons.

Determination of the relationship between delayed neutron response and sample mass did not affect this isotopic analysis significantly because the samples were constructed of uranium foils and plutonium foils having similar self-shielding factors (foils were not stacked) and the analysis was in terms of standards having the same self-shielding factors. It is of some interest, though, to assess the performance of this technique for thin or homogeneous samples, or for an interrogating source with greater penetrating ability than thermal neutrons, such as fast neutrons or high energy gamma rays. To assess the self-shielding effects of the thickness of the plutonium foils the short cycle time response (total delayed neutron response) of a 0.8665 gram foil of uranium-235 was measured and compared to each of the plutonium-239 foil short cycle time responses. Self-shielding factors were calculated for each plutonium

foil by the following equation:

$$F = \frac{n_P \, N_U \, \beta_U \, \sigma_{fU} \, \nu_U}{n_U \, N_P \, \beta_P \, \sigma_{fP} \, \nu_P} \qquad (5\text{-}1)$$

where

F is the self-shielding factor of a plutonium foil relative to a uranium foil

N is the number of atoms

β is the percentage of neutrons that is delayed

σ_f is the isotopic fission cross section

ν is the average number of prompt neutrons following fission

n is the delayed neutron short period count rate

P subscript is plutonium-239

U subscript is uranium-235

The factor so calculated is actually the ratio of self-shielding for the plutonium foil to the self-shielding factor for the uranium foil used for comparison. Since the foils were not stacked, using the uranium foil mass to normalize the uranium standard curve and the plutonium foil mass times this factor to normalize the plutonium standard curve should yield the same results as homogeneous mixtures of uranium-235 and plutonium-239. Table 6 lists the plutonium foils used and the self-shielding factors found for them.

To test the theory developed in Chapter III and to evaluate this assay method for safeguards applications, a series of runs was made under similar conditions (count time, number of data points, etc.) with varying quantities of fissionable material and isotopic ratios. Table 7 lists

Table 7. Samples Constructed with the Foils Available

Run No.	Sample Pu Foils	Make Up of U Foils	No. of Points	Counts at 0.1 Sec Cycle Time
1	1,2,3,4	1,2,3,4,5	50	66529
2	1,2,3	all	50	62798
3	1,2	all	48	60015
4	1	all	50	56954
5	all	1,2,3,4	49	55461
6	1,2,3	1,2,3,4	50	52166
7	1,2	1,2,3,4	50	48995
8	1	1,2,3,4	50	46010
9	all	1,2,3	50	44580
10	1,2,3	1,2,3	49	41223
11	1,2	1,2,3	50	38114
12	1	1,2,3	50	35067
13	all	1,2	50	34197
14	1,2,3	1,2	49	30839
15	1,2	1,2	49	27720
16	1	1,2	48	24684
17	all	1	49	23192
18	1,2,3	1	49	19834
19	1,2	1	48	16725
20	1	1	48	13678

Note: The number of data points taken was distributed approximately logarithmically between 0.1 sec and 100 sec cycle times. Count times for each point were 100 sec.

these runs. In addition, two standards runs were made, one with all of the uranium-235 foils in place and one with all the plutonium-239 foils in place. These two runs contained 50 points each. The counts taken at cycle times of 0.1 second, indicating total delayed neutron response, were 65502 and 18391, respectively.

Table 8 shows some longer run time data that were taken to test the error analysis developed in the next chapter. These runs consisted of 20 points each. Each point was counted for 500 seconds. No points were taken at cycle times longer than 50 seconds. The delayed neutrons

Table 8. Samples Analyzed with 20 Data Points between 0.1 Second and 50 Seconds Cycle Time

Run No.	Sample Pu Foils	Make Up of U Foils	No. of Points	Total Counts for 0.1 Sec Cycle Time
1	all	all	20	332751
2	1,2,3	all	20	313950
3	1,2	all	20	300793
4	1	all	20	284161

were counted at each of the 20 different cycle times for 500 seconds, giving a total counting time of about two hours and 45 minutes per sample.

To further test self-shielding of plutonium, two plutonium foils were stacked and delayed neutrons were counted at a cycle time of 0.1 sec. The count rate of two plutonium foils or of a plutonium foil covering a uranium foil was essentially the same as for one plutonium foil alone, indicating that few thermal neutrons could penetrate the entire plutonium foil.

CHAPTER VI

ANALYSIS OF DATA

Data collected in the delayed neutron experiments were loaded into Univac 1108 Fastran files and programs were written in Fortran IV to reduce these data and infer from them the concentration of plutonium-239 and uranium-235 in the samples used. Calculational methods, described later, were used to obtain the ratio of plutonium-239 to uranium-235 in the samples from comparison of the delayed neutron response as a function of activation period signature for the unknown samples with delayed neutron signature references obtained with samples containing only plutonium-239 or uranium-235. Once this ratio was known, the total mass of plutonium-239 and uranium-235 could be estimated from the total (short cycle time) delayed neutron response. Programs were also written to check the fit of the experimental data to predicted results, which were obtained by using the six group abundances and effective half-lives found by Keepin for uranium-235 and plutonium-239.

Data recorded during each experimental run were entered via a remote terminal to a Fastran file on the Univac 1108 computer. A Fortran program named NCERT was used to insert cycle period, data count, and data count time as a file element into the scratch file. NCERT calculated the cycle period from the position of the timer switch, entered as a number 1 to 5, and the number of photocell pulses recorded during that time interval. NCERT included as a data statement the timer intervals shown in

Table 4. A second program, CLTUR, then subtracted background and normalized the data to 1.0 for the period nearest to 0.103 second, stored the normalization factor as element 1, and the periods and corresponding normalized data as succeeding elements in the appropriate file. The data from each run occupied a separate file. The normalization period of 0.103 second was chosen because it was the shortest period at which data were taken in the runs with the standards, "uranium-235 only" and "plutonium-239 only." Figures 16 and 17 show that periods between 0.1 second and 0.2 second are in a region of saturated response. Small variations of period in this range would have no effect on the normalization factor; so no attempt was made to interpolate a function for a point at 0.103 second when none existed; a point nearest the 0.103 second period, always less than 0.2 second, was chosen for normalization.

Normalization of the delayed neutron data allows easy comparison of the shapes of curves from samples exhibiting different absolute levels of response. Higher long cycle time response implies a greater percentage of delayed neutrons have long half-lives.

The normalization factor is the total response of delayed neutrons contributed by all the delayed neutron-emitting groups with half lives greater than about 0.1 second and, therefore, can be used as a measure of the total mass of fissioning material contributing to the delayed neutron response.

Figures 18 and 19 are plots of normalized data as a function of cycle time for "uranium-235 only" and "plutonium-239 only" samples. Normalized data as a function of cycle time for a 50:50 mixture of uranium-235 and plutonium-239 are plotted in Figure 20. These three plots also

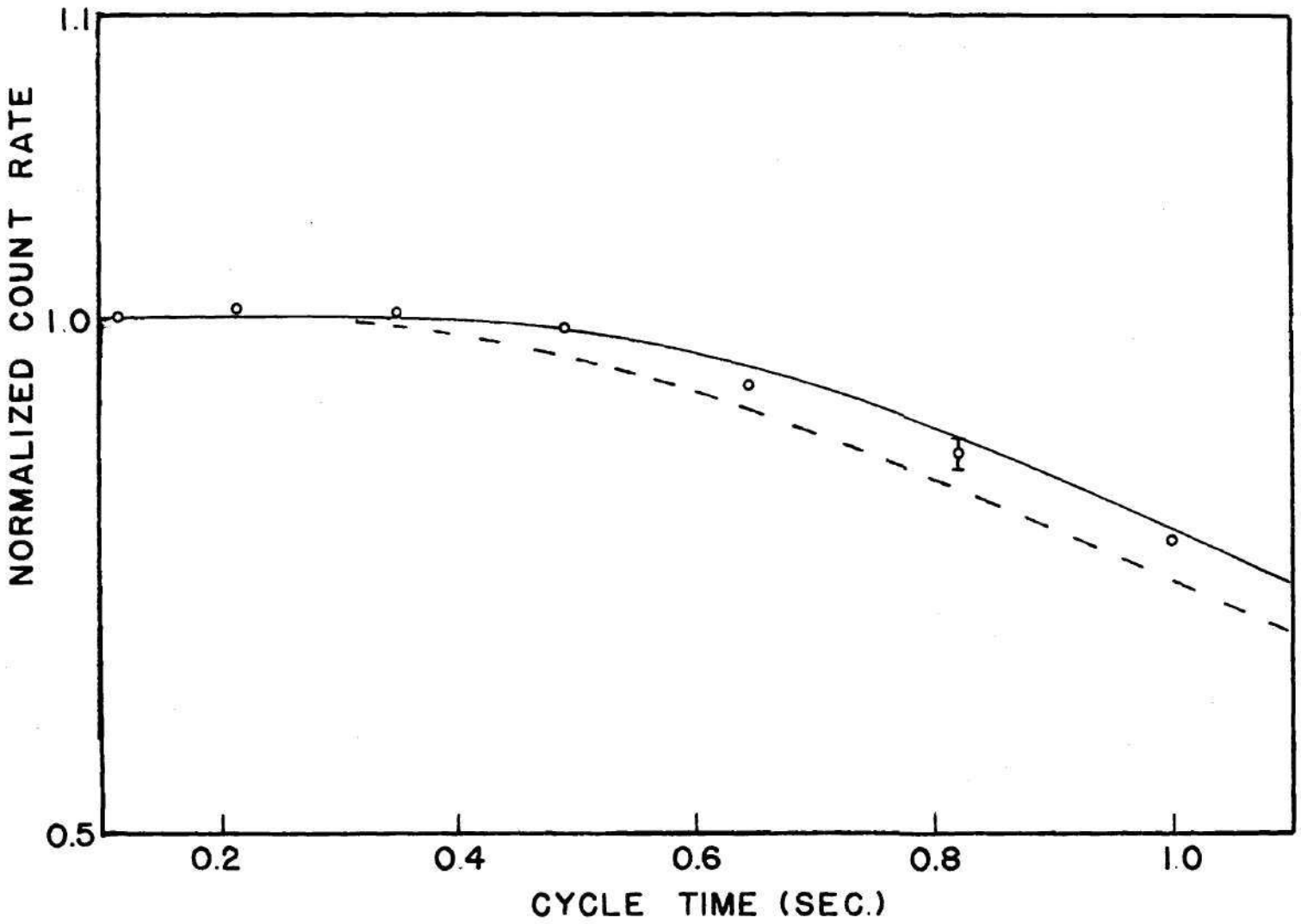

Figure 16. Short Cycle Time Delayed Neutron Count Rate vs Cycle Time for ^{235}U

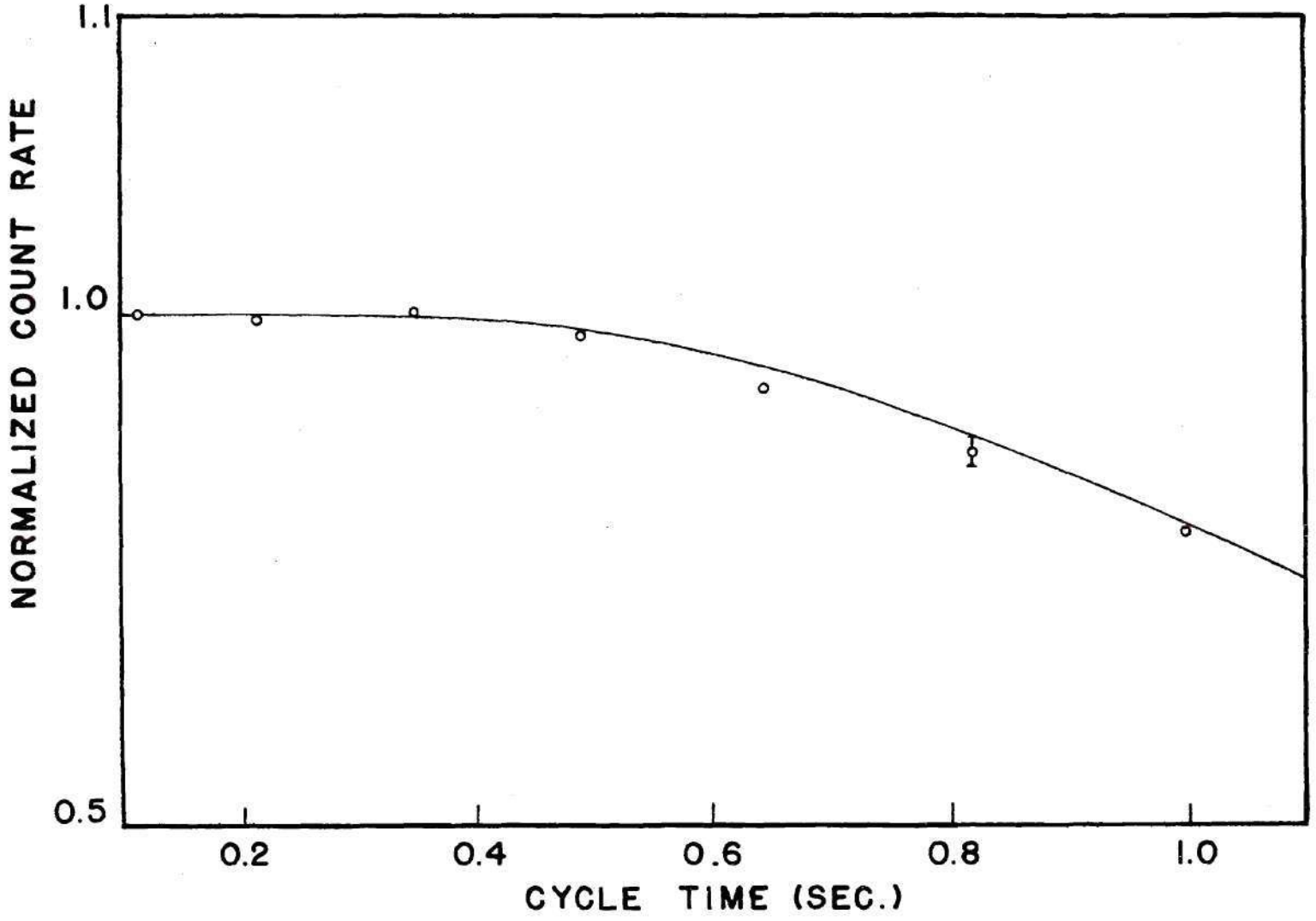

Figure 17. Short Cycle Time Delayed Neutron Count Rate vs Cycle Time for ^{239}Pu

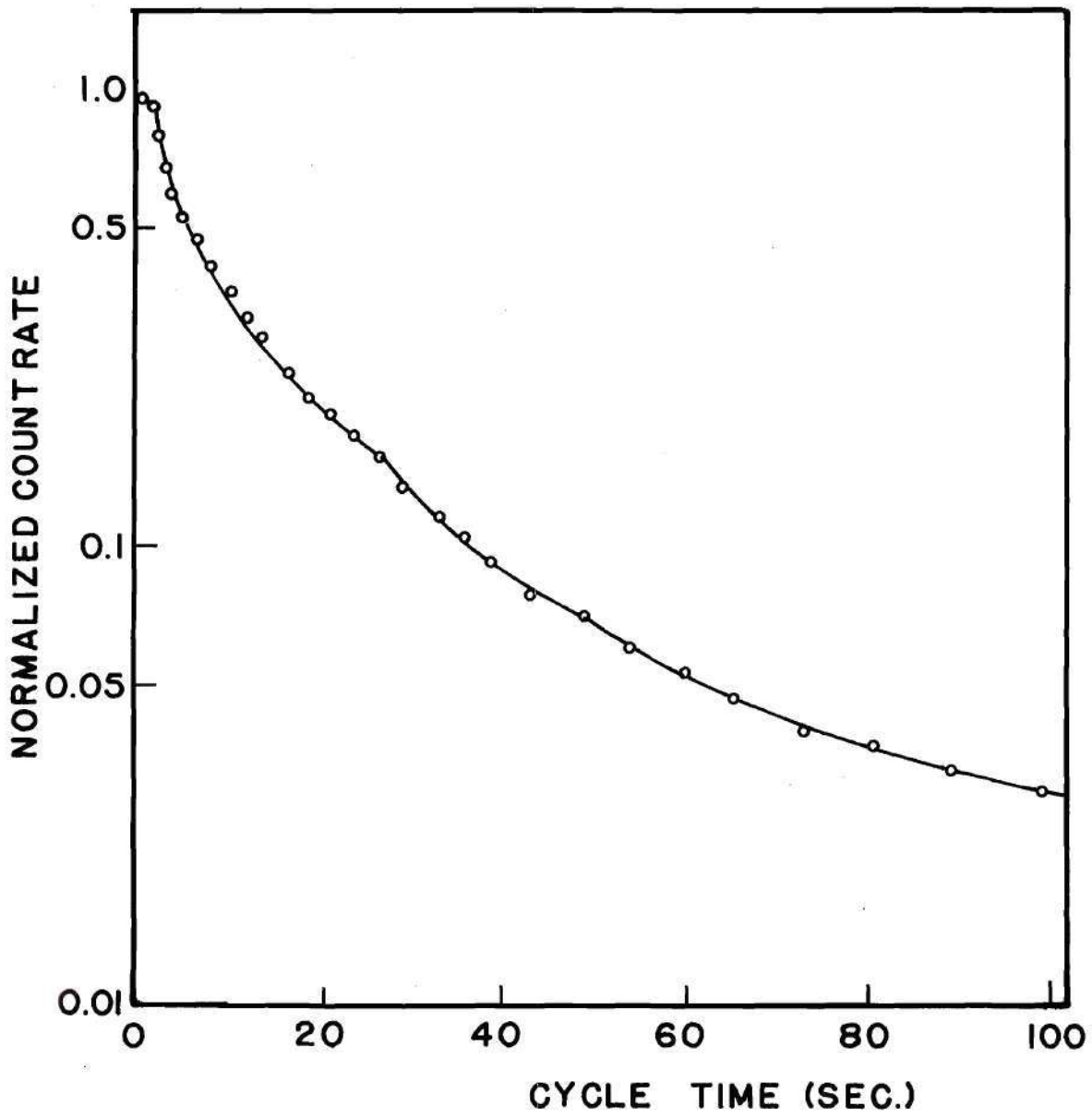

Figure 18. Normalized Delayed Neutron Count Rate vs Cycle Time for ^{235}U

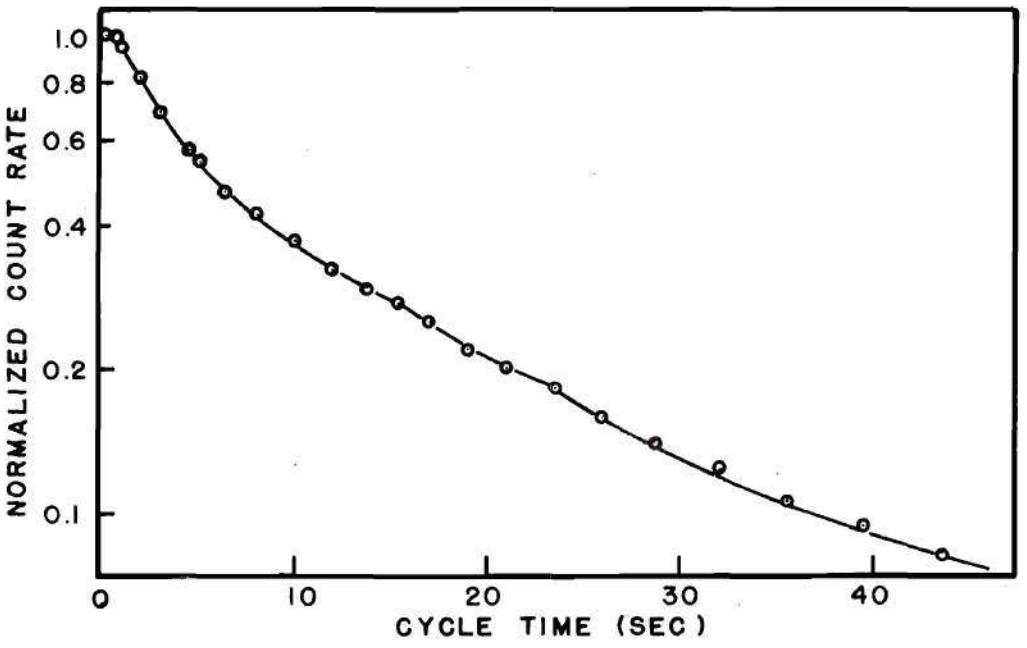

Figure 19. Normalized Delayed Neutron Count Rate vs Cycle Time for ^{239}Pu

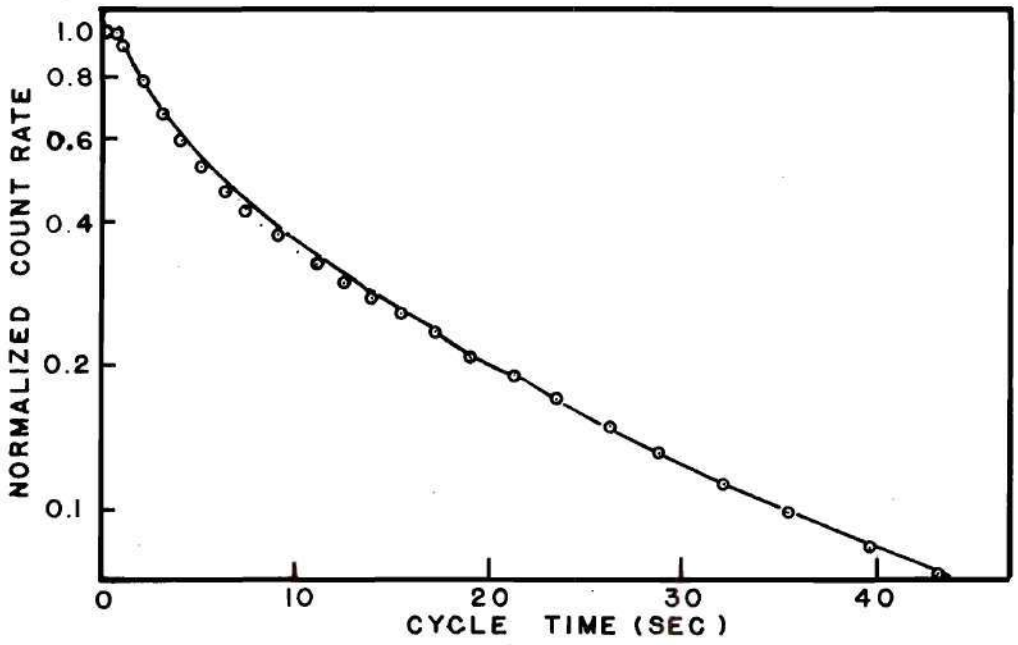

Figure 20. Normalized Delayed Neutron Count Rate vs Cycle Time for 50% ^{235}U, 50% ^{239}Pu

include, as a solid line, a curve generated with equation 3-28 using six delayed neutron precursors with the half-lives and abundances measured by Keepin.

Even though good agreement of the data with curves predicted using Keepin's six delayed neutron groups was obtained, as seen in Figures 18, 19, and 20, isotopic analysis of a sample was made using experimental standards rather than the theoretical curves. Use of a relative assay method using experimental standards run with the same experimental configuration as the unknown samples eliminated problems that could have arisen from imprecise definition of experimental parameters, such as beam width or active region of the detector, and avoided inaccuracies arising in any deviation of actual delayed neutron response from six group theory.

Figure 21 is a plot of the difference between a plutonium-239 delayed neutron signature with the short cycle time--saturation--response normalized to 1.0 and the similarly normalized response of uranium-235 only and of two samples containing both uranium-235 and plutonium-239. A similar plot is shown in Figure 22 for differences between normalized signatures of a uranium-235 standard and the signatures of plutonium-239 and of two samples of mixed composition. In Figure 5, two curves are shown which have similar short cycle time response but different half-lives generating the single break point. The activation product having the longer half-life will exhibit greater response at all cycle times except in the region of saturated response. Because plutonium-239 has a greater ratio of long to short half-life delayed neutrons than uranium-235, at periods between 0.1 second and 150 seconds, the normalized delayed neutron signatures of samples containing uranium-235 were, within statistical

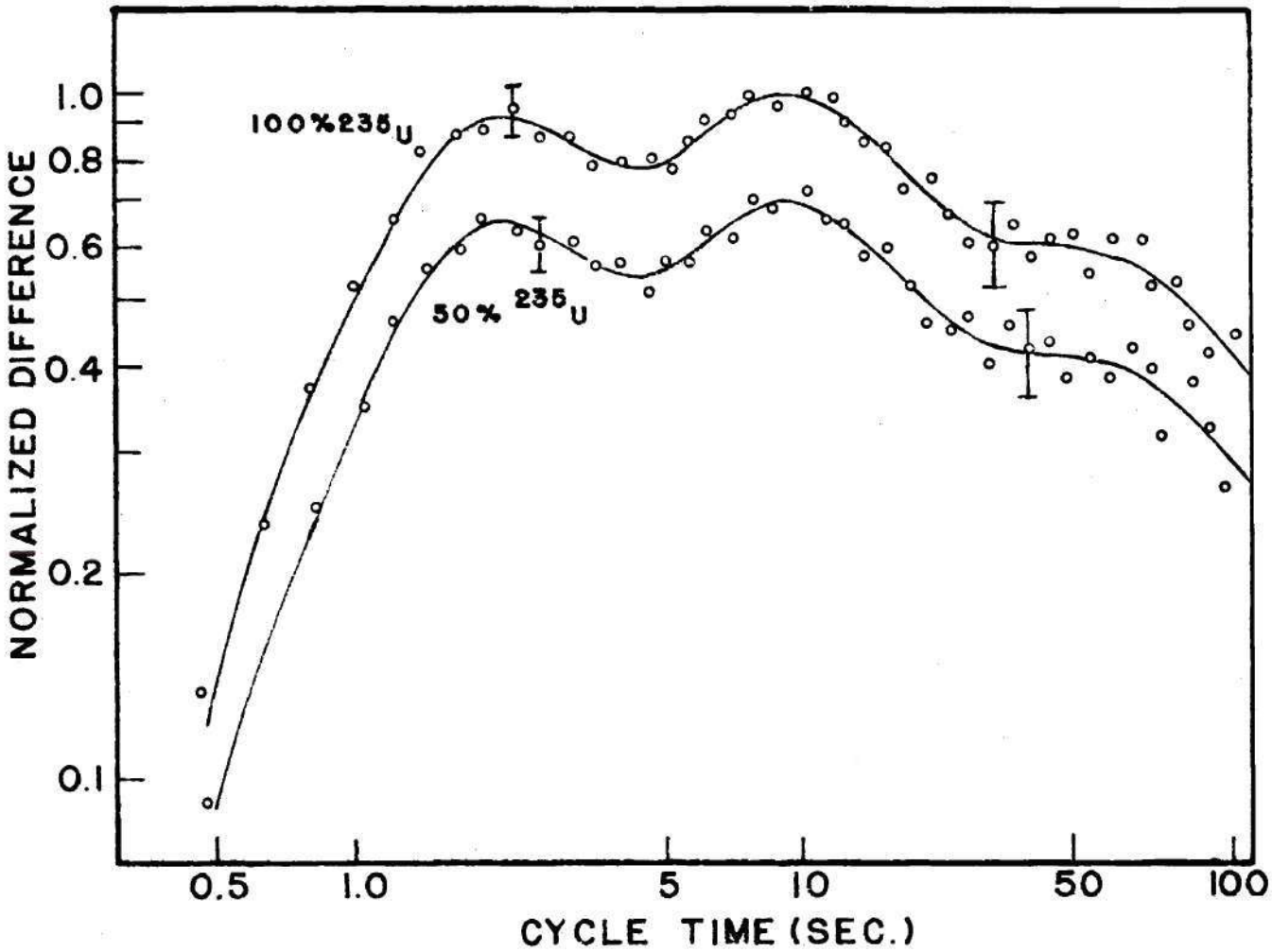

Figure 21. Difference in Delayed Neutron Count Rate of ^{239}Pu and Two Samples Containing ^{235}U as a Function of Cycle Time

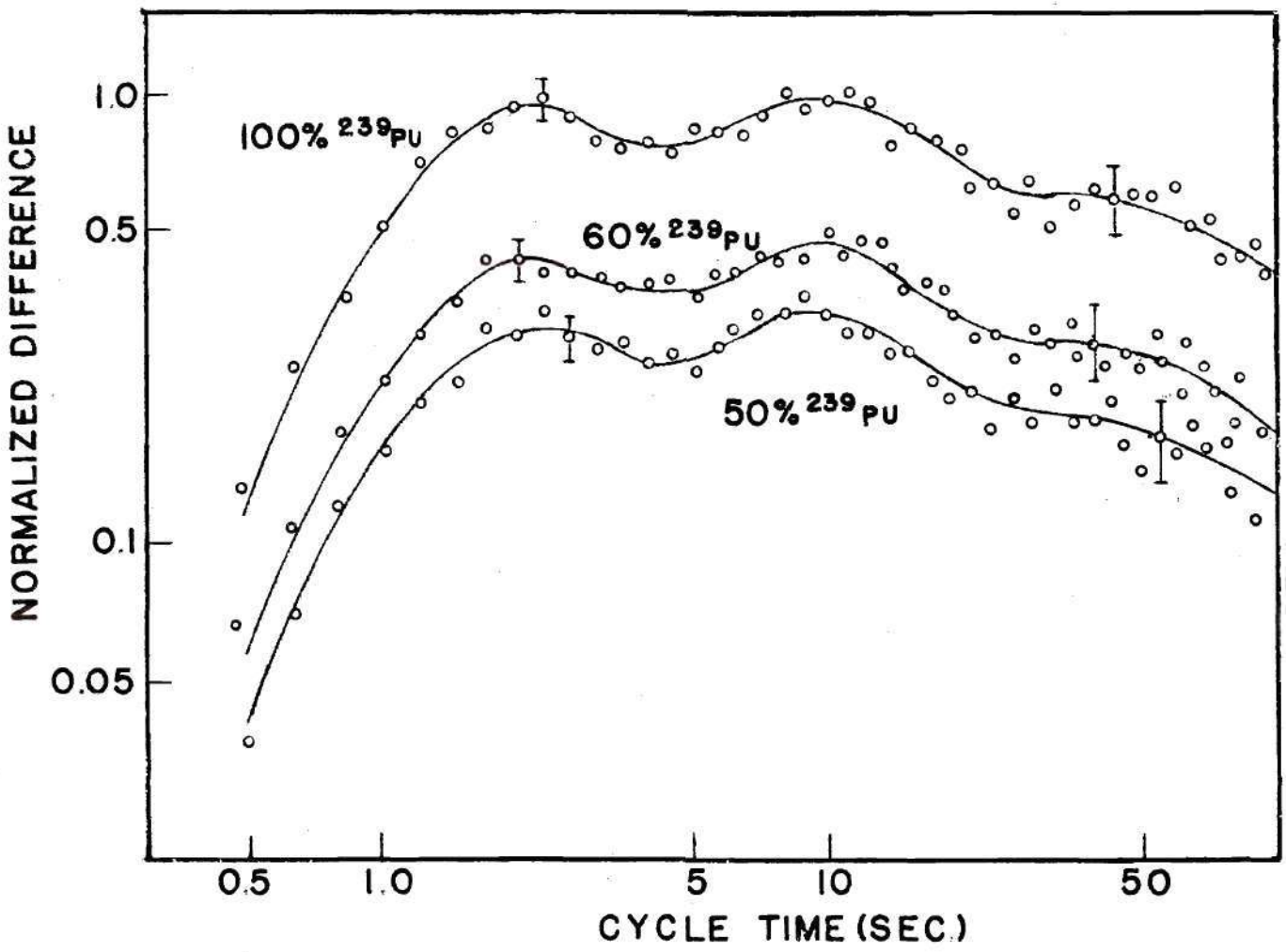

Figure 22. Difference in Delayed Neutron Count Rate of ^{235}U and Three Samples Containing ^{239}Pu as a Function of Cycle Time

deviations, less than or equal to the signature of plutonium-239 alone. Overlap of the curves occurs only at short periods, saturated response, and for long periods, where differences are lost in the statistics of small responses. Similarly, samples containing plutonium-239 always, in the range of periods of interest, yielded normalized curves that were greater than or equal to the normalized curve of uranium-235 alone. These differences should reflect the number of delayed neutrons contributed to the total delayed neutron response by each of the two fissioning nuclides in the sample and, through the normalization factors obtained by use of the standards, the mass of each fissioning isotope in the sample. Differences between normalized curves, Figures 21 and 22, as a function of cycle time are indicative of the ratio of abundances of delayed neutrons, in the samples, that contribute to break points at, or greater than, the cycle time on the ordinate of the plot.

A Fortran program named DELTAR was written to estimate the isotopic composition of a constructed sample by analyzing the differences between the sample's normalized delayed neutron signature and the signatures of the plutonium-239 and uranium-235 standards. A flow chart for DELTAR is depicted in Appendix B. The integrated area between the response vs log cycle time curves of the standards and samples is used by DELTAR as the difference between signatures. This area is generated by DELTAR as the sum of the areas of trapezoids bounded by measured points on the standard or sample signatures, and response values for the same period from the sample or standard curves, respectively. The ratio of the area thus obtained between the sample curve and the uranium-235 standard curve to the area between the plutonium-239 and uranium-235 standard curves themselves

is indicative of the ratio of the delayed neutrons contributed by plutonium-239 to the total number of delayed neutrons in the response. Likewise, the ratio of the area between the sample curve and the plutonium-239 curve to the area between the standard curves represents the portion of the total delayed neutron response contributed by uranium-235. Once an estimate is made of the percentage of the delayed neutrons contributed to the response by each of the two fissioning nuclides the quantitative response of plutonium-239 and uranium-235 is calculated by multiplying the delayed neutron percentage by the normalization factor for the sample. From the normalization factors of the standards, values of delayed neutrons per gram of fissioning material were determined. These values are compared to the quantitative delayed neutron response from the samples to determine the mass of plutonium-239 and of uranium-235 in the sample. Table 9 shows a list of samples, their composition, the composition of each sample as determined by its delayed neutron response using DELTAR, and the percentage discrepancies between the known and assayed composition values.

Error Analysis

Experimental bias can be introduced into this assay from several sources, but accuracy seems to be limited primarily by statistics. Geometry was unchanged for the duration of the experiment and the precision of the timer, on which count rate and frequency determination were based, was checked several times during the experiment. Any deviation in the power level of the reactor affected the delayed neutron count rate in the experiment. Data collected while the reactor power level was changed showed expected distortion and were discarded. All of the data used were

Table 9. Data Collected to Estimate Uranium and Plutonium Content of Samples Described in Table 7

Sample	Uranium (grams) (including self-shielding)	Plutonium (grams) (including self-shielding)	U/Pu Ratio	Derived Composition (grams)		Derived U/Pu Ratio	Probable σ(%)		Deviation of Derived Composition from Constructed Composition (%)	
				Uranium	Plutonium		Uranium	Plutonium	Uranium	Plutonium
1	0.8665	0.612	1.4	0.880	0.562	1.6	2.5	10.6	+1.5	- 8.1
2	0.8665	0.449	1.9	0.881	0.505	1.7	2.6	14	+1.7	+12.5
3	0.8665	0.297	2.9	0.880	0.350	2.5	2.0	18	+1.5	+18
4	0.8665	0.150	5.8	0.856	0.126	6.7	1.3	24	-1.2	-16
5	0.6904	0.612	1.1	0.704	0.567	1.2	2.9	9.7	+2.0	- 7.3
6	0.6904	0.449	1.5	0.673	0.411	1.6	2.9	13.2	-2.3	- 8.5
7	0.6904	0.297	2.3	0.677	0.338	2.0	2.8	20	-2.0	+14
8	0.6904	0.150	4.6	0.702	0.192	3.7	2.7	35	+1.7	+28
9	0.5149	0.612	0.84	0.499	0.645	0.78	3.4	8.7	-3.0	+ 5.4
10	0.5149	0.449	1.1	0.528	0.386	1.4	3.3	11	+2.5	-14
11	0.5149	0.297	1.7	0.525	0.261	2.0	3.0	17	+1.9	-12
12	0.5149	0.150	3.4	0.499	0.192	2.6	3.1	31	-3.0	+28
13	0.3478	0.612	0.57	0.363	0.640	0.57	4.2	7.2	+4.3	+ 4.6
14	0.3478	0.449	0.77	0.342	0.411	0.83	4.2	9.8	-1.8	- 8.5
15	0.3478	0.297	1.2	0.337	0.263	1.3	4.1	14	-3.0	-11.5
16	0.3478	0.150	2.3	0.337	0.199	1.7	3.9	28	-3.0	+33
17	0.1707	0.612	0.28	0.183	0.587	0.31	6.8	5.8	+7.2	- 4.0
18	0.1707	0.449	0.38	0.178	0.468	0.38	6.5	7.5	+4.3	+ 4.2
19	0.1707	0.297	0.57	0.162	0.326	0.50	5.9	10.5	-5.2	+ 9.8
20	0.1707	0.150	1.1	0.172	0.183	0.94	5.8	20	+1.4	+22

collected with the reactor operating at 1000 kW and with the power level under automatic control. Variations in power level resulting from reactor regulator rod action do not seem to have caused inaccuracies that are significant in comparison to the statistical precision obtainable.

Dead time measurements were described in the calibration section. At the count rates encountered in this experiment, around 10,000 cps maximum, dead time effects in the detectors were small. Dead time of the detectors dominated the system dead time.

Steady-state gamma-induced background was very small, limited both by the BF_3 detector's inherent discrimination against gamma rays and by the neutron shielding around the detectors. Steady-state neutron background was, potentially, a much larger problem, and was controlled at a few cpm by keeping the detectors as far as possible from the beam of interrogation neutrons, keeping the beam as short as possible, and by shielding the detectors with paraffin, cadmium, and boric acid in a polyester matrix. The neutron background was somewhat dependent on the activity of nearby experiments. Background measurements were made any time there was reason to believe the background level might have changed. Background was also reduced by counting only when the samples were in the active region of the detector assembly.

As seen in the section on calibration, the gamma activity of the samples was not great enough to introduce error or bias in the results of the experiment. Samples capable of exposing the detectors to a gamma dose rate of 30 R/hr would have disturbed the results; however, the samples used in this experiment caused a detector gamma dose of less than 100 mR/hr.

Counting statistics play the major role in the accuracy to which an assay can be made. All of the assays reported in Table 8 were made with the same count time per period, 100 seconds; and each sample was analyzed with the same number of periods, fifty, spaced approximately logarithmically from short to long periods. About 1.5 hours were needed to make each run. In the preceding analysis the isotopic percentage of uranium-235 or plutonium-239 was obtained as a normalization factor times ratio of the area between normalized count rate vs period curves and a standard curve. The area between the curves was estimated by summing the areas of trapezoids whose bases were terminated by the normalized count rates of the two curves, and whose heights were the differences between log periods at which observations were made.

$$A = 1/2[(a-b) + (c-d)]\Delta P \qquad (6\text{-}1)$$

where

A is area

a and c are count rates on one curve

b and d are count rates on the other curve

ΔP is the difference in log periods at which counts are made

Some of the count rates, a, b, c and d, were interpolated. However, the interpolated points were on a slowly varying function between points that were not very different, so the standard deviation in the interpolated points was similar to the points from which it was generated, approximately the square root of the count rate. The standard deviation of the average of the bases of a trapezoid can be found using the formula

$$\sigma_x^2 = \left(\frac{\partial x}{\partial u}\right)^2 \sigma_u^2 + \left(\frac{\partial x}{\partial v}\right)^2 \sigma_v^2 + \cdots \tag{6-2}$$

to be

$$\sigma_L^2 = \frac{1}{4}\left(\sigma_a^2 + \sigma_b^2 + \sigma_c^2 + \sigma_d^2\right) \tag{6-3}$$

Similarly the standard deviation of the area of a trapezoid is

$$\sigma_A^2 = P^2\sigma_L^2 + L^2\sigma_P^2 \tag{6-4}$$

or

$$\frac{\sigma_A^2}{A^2} = \frac{\sigma_L^2}{L^2} + \frac{\sigma_P^2}{P^2} \tag{6-5}$$

$\frac{\sigma_P^2}{P}$ is small by several orders of magnitude compared to $\frac{\sigma_L^2}{L}$ and can be disregarded. The total area between curves is the sum of the areas of all the trapezoids, and the square of the standard deviation of the total area is the sum of the squares of the standard deviations of the areas of the trapezoids.

$$\sigma_{area}^2 = \Sigma\ \sigma_A^2 = \Sigma\ P^2\sigma_L^2 \tag{6-6}$$

The quantity of fissioning isotope is found from a constant times the ratio of the area between the normalized curve and a standard curve and the area between the standard curves for uranium-235 and plutonium-239. The precision to which this quantity can be determined is

$$\frac{\sigma_q^2}{q^2} = \frac{\sigma_{\text{area 1}}^2}{(\text{area 1})^2} + \frac{\sigma_{\text{area 2}}^2}{(\text{area 2})^2}$$

Table 9 includes a column which indicates the precision expected in each assay.

Figure 23 shows the assay accuracy in percent, at the 67 percent confidence level, against the percentage make-up of about one gram of material. Data for this plot were taken from Table 8. Figures 24 and 25 show the accuracy of the analysis of uranium in the presence of 0.15 gram plutonium and 0.618 gram plutonium, respectively. Figures 26 and 27, similarly, show the plutonium analysis in the presence of 0.1707 gram and 0.8665 gram uranium. Data points in these figures are taken from Table 9. The solid lines have a one to one slope, indicating perfect correspondence between measured value and the actual components of the sample. Agreement between the data points and solid line indicates the good linearity of the method. Scatter of the points shows decreased accuracy for smaller samples and for increased percentages of interfering fissioning isotopes, uranium-235 in the assay of plutonium-239 and plutonium-239 in the assay of uranium-235. As expected, errors tend to be proportional to the square root of the delayed neutron response.

Increased count rates or longer count times improve statistics. Sample 5 was counted for twice the time as the run listed in Table 9 with the result, after analysis with DELTAR, that the uranium assay was 1.3 percent over the expected value and the plutonium assay was 4.0 percent over. As expected from the error analysis, the errors were multiplied by a factor of about 0.7.

Very-Short-Half-Life Delayed Neutrons

Delayed neutrons following a fission with half-lives shorter than

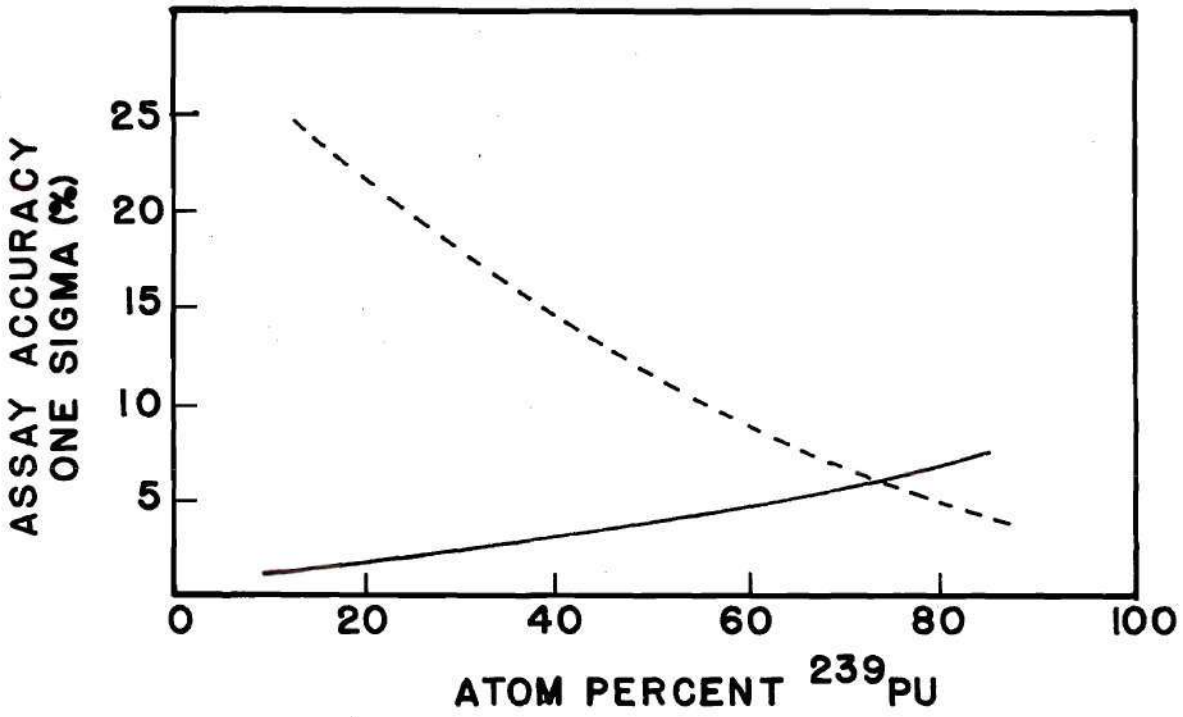

Figure 23. Accuracy Expected in the Assay of U and Pu ~ 1 Gram in Sample of Mixed ^{239}Pu and ^{235}U as a Function of Pu/U Ratio (Data are taken from Table 9. Dotted line is calculated for ^{239}Pu and the solid line is for ^{235}U, from data in Table 9.)

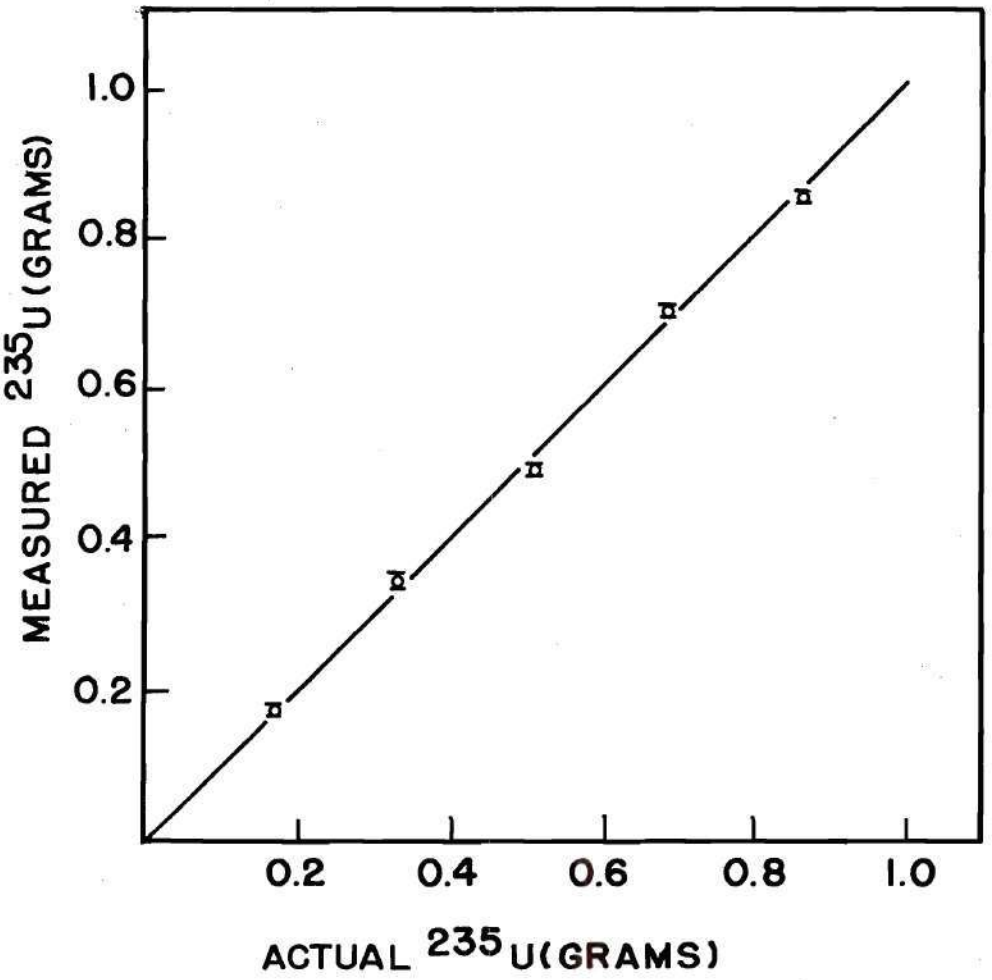

Figure 24. Analysis of ^{235}U in the Presence of 0.150 gm ^{239}Pu (Points are samples 20, 16, 12, 8, and 4 from Table 9.)

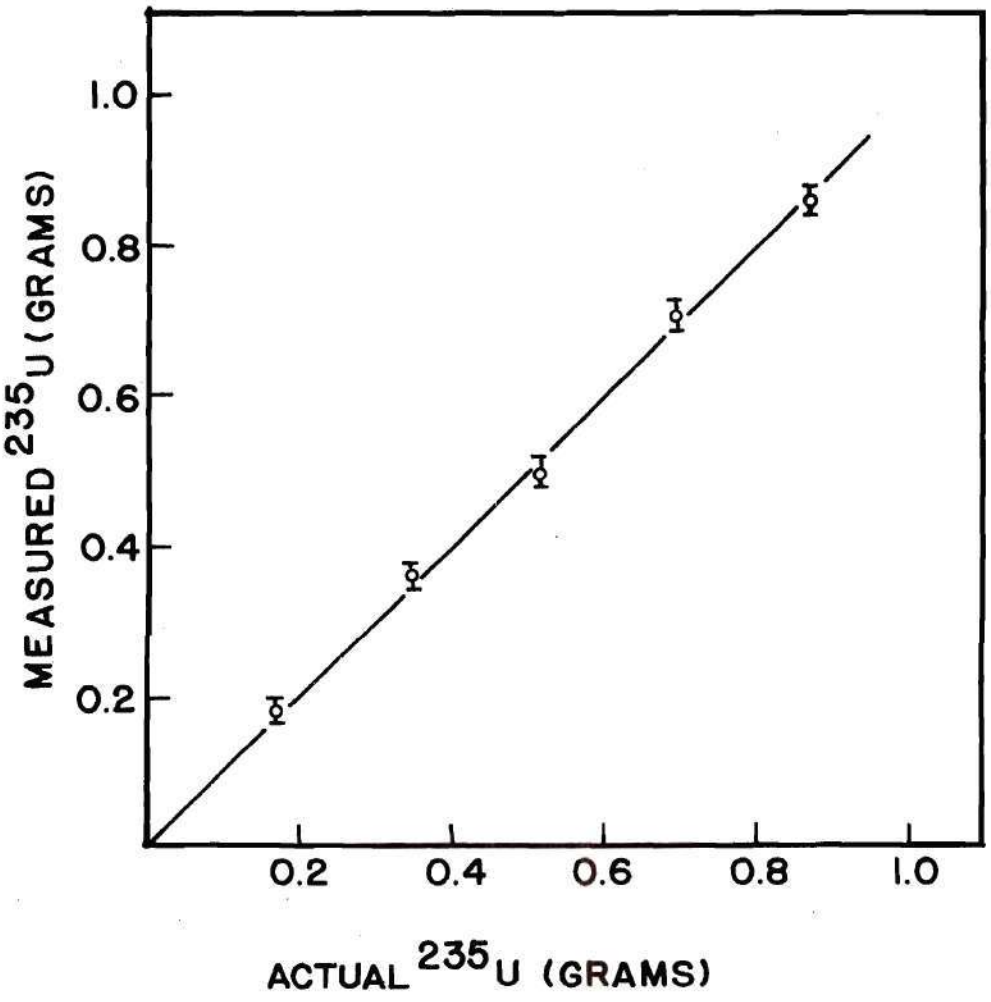

Figure 25. Analysis of ^{235}U in the Presence of 0.612 gm ^{239}Pu (Points are samples 17, 13, 9, 5, and 1 from Table 9.)

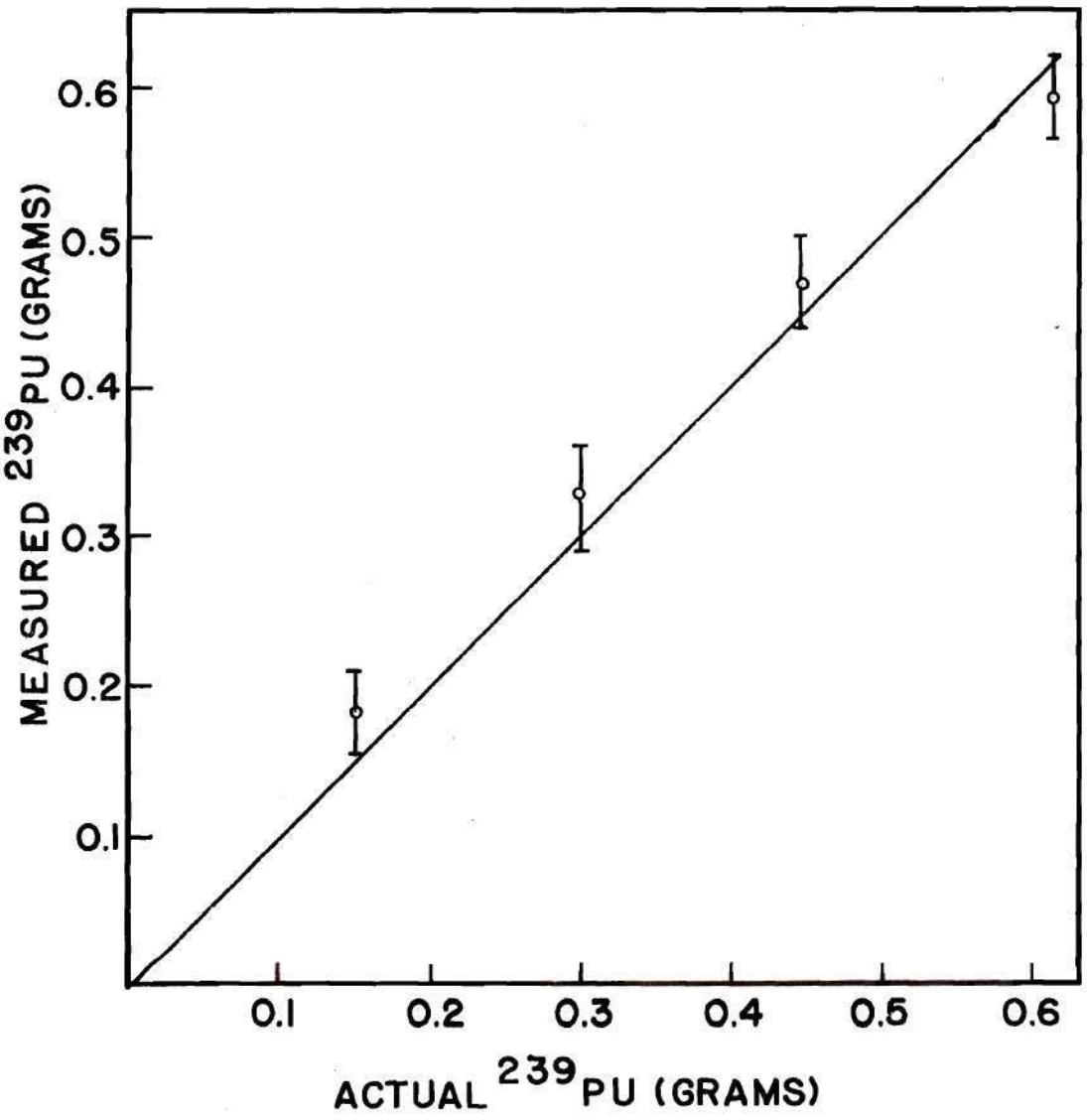

Figure 26. Analysis of ^{239}Pu in the Presence of 0.1707 gm ^{235}U (Points are samples 20, 19, 18, and 17 from Table 9.)

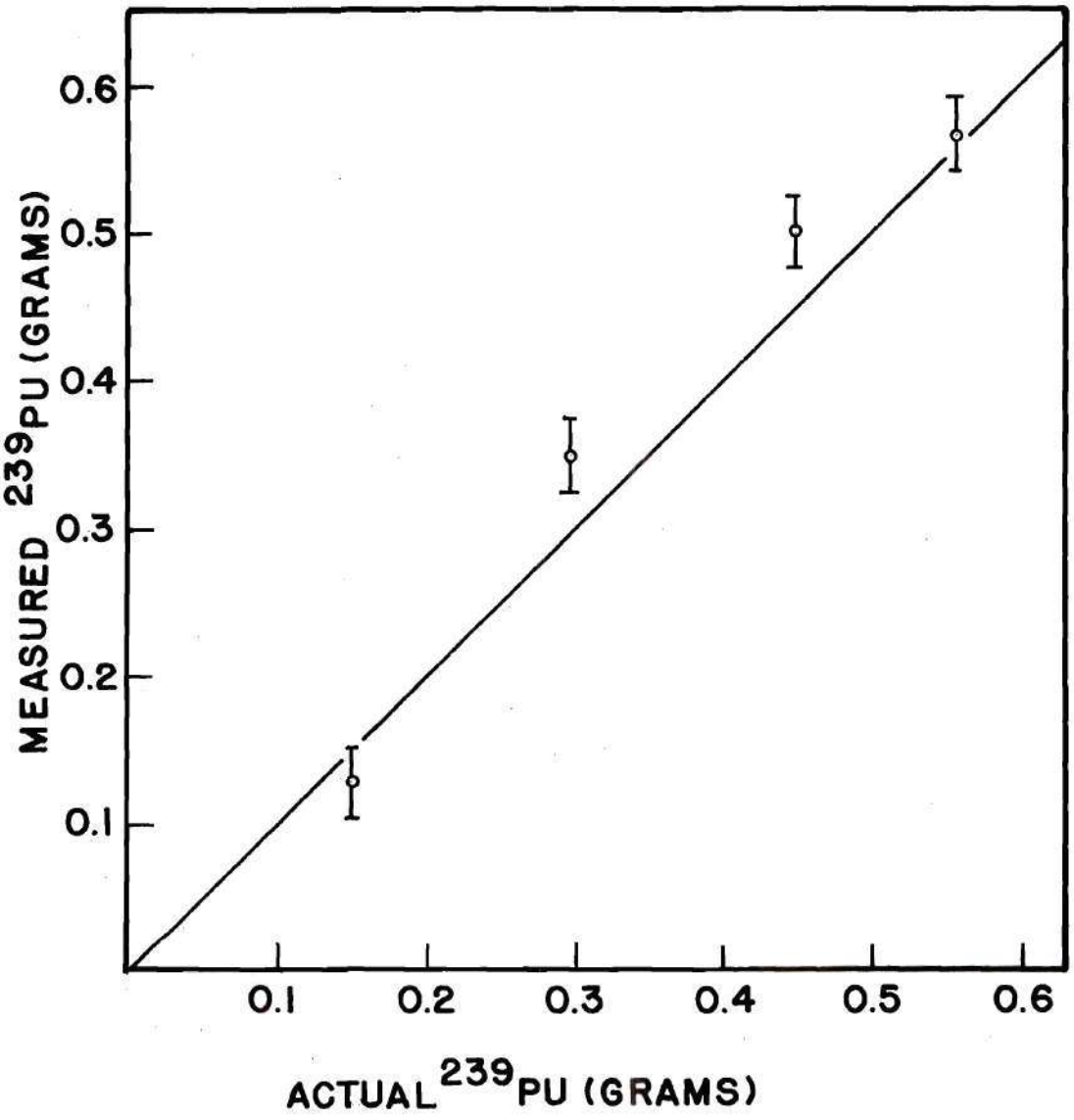

Figure 27. Analysis of ^{239}Pu in the Presence of 0.8665 gm ^{235}U (Points are samples 4, 3, 2, and 1 from Table 9.)

about 0.2 second have not been reported in the literature, nor are they expected on theoretical grounds. Beta transitions leading to a nuclide sufficiently excited to emit a neutron are hindered for half-lives shorter than about 0.2 second. Even though these short half-lived delayed neutrons were not expected, the ease with which some half-lives could be deduced from the available data prompted an analysis. The background counts associated with uranium-235 only and plutonium-239 only test runs were subtracted from the appropriate sets of data on Fastran files and the experimental data points for cycle times shorter than 1.0 second are plotted for uranium in Figure 16 and for plutonium in Figure 17. The theoretical delayed neutron curve, generated from equation 3-28 using Keepin's six delayed neutron abundances and half-lives is plotted as a solid line for uranium-235 and plutonium-239 in Figures 16 and 17, respectively. One standard deviation for the experimental points is less than 1.0 percent for both uranium and plutonium.

For the beam width, wait times, and detector aperture used, the 0.2 second half-life delayed neutron group was responsible for a break from the level saturation curve near 0.5 second period, in Figures 16 and 17, as predicted by theory. Delayed neutrons with half-lives shorter than the 0.2 second half life group would shift the break in the direction of shorter periods. If there were any delayed neutron groups with half-lives less than 0.05 second, the response curve would shift and the break point would occur at periods shorter than those observed. The dotted line in Figure 15 shows the curve expected with a delayed neutron group with a half-life of 0.05 sec and abundance of 0.04 present. Very short delayed neutron groups, and, of course, prompt neutrons, die away

completely before reaching the detector at the sample speeds used in this experiment.

Besides statistical uncertainty, discrepancies between theory and experimental data can arise from two sources; uncertainties in the delayed neutron parameters used to generate the theoretical curve, errors in period determination, which could appear to shift the break point, and non-uniformity of the beam and errors in determining the fractions of a period for activation, decay, and detection, which could affect both break point period and curve shape.

In the generation of the theoretical curve a single half-life (the shortest group half-life) of 0.230 second for uranium-235 and 0.257 second for plutonium-239 were assumed for the shortest lived group. These half-lives were statistically derived by Keepin[35] and, in reality, the sixth delayed neutron group probably has several discrete contributors with different half-lives. Figures 16 and 17 both indicate a slight deviation from such a theory. The data tend to fall below the theoretical curve and define a slightly less sharp break in the region of 0.4 second to 1.0 second. This indicates that there were delayed neutron emitters present with half-lives less than 0.230 second for uranium-235 and 0.257 second for plutonium-239 and/or that more than one half-life in the region of 0.2 second was present. The deviation, however, is only slightly greater than a standard deviation of the data, indicating that most of the 0.2 second group is generated by precursors with half-lives near 0.23 second. There appears to be no statistical deviation between theory and data for periods between 0.1 and 0.3 second, implying no appreciable contribution from delayed neutron precursors with half-lives between 0.04 and 0.12

second and no precursors with shorter half-lives of sufficient magnitude to have a detectable effect at 0.1 second.

One standard deviation of each point in the sets of data used to look for short half-life delayed neutron groups is about 1.0 percent. A discrepancy of one standard deviation at 0.1 second, corresponding to a delayed neutron group of 0.04 second half-life and a relative abundance of 0.01, should be observable as a change of slope in the 0.1 to 0.5 second period region. A discrepancy of three standard deviations at a 0.3 second period would affect observably the slope of the signature in the 0.2 to 0.7 second period region. This would correspond to a delayed neutron group of half-life 0.12 second and relative abundance of 0.03. The exponential slope as a function of period for short half-life groups is, itself, a function of half-life. The slope for shorter half-lives is steeper. Therefore, the sensitivity of these data to delayed neutron groups with half-lives less than 0.04 second decreases rapidly with decreasing half-life. A 1 σ discrepancy from theory at 0.1 second period would imply a response three standard deviations above the observed saturation level (response at 0.1 second period) at a period of 0.06 second. This corresponds to a delayed neutron group of half-life 0.025 second and a relative abundance of 0.03. From these data, then, it can be inferred that there are no delayed neutron groups with half-lives between 0.025 second and 0.12 second with relative abundances as large as the smallest group relative abundance reported by Keepin.

Errors in determining the fractions of a period that the sample spends in the beam, waiting, and in the detector are not particularly important in the signature analysis experiment because both the standards

and the unknowns were run with the same experimental configuration and theoretical curves were not used to separate the signatures of uranium and plutonium. In looking for short half-life delayed neutrons, however, errors in the values of experimental parameters used to generate the theoretical curve could introduce discrepancies between experimental and theoretical curves that might give rise to the apparent existence of non-existent delayed neutron groups. It was assumed that errors in the activation, wait, and detection fractions of a cycle, non-uniformities of the beam, and variations of detector geometry did not significantly affect experimental results. In Figures 19 and 20, the theoretical and experimental points for the complete curves of delayed neutrons as a function of cycle time for uranium-235 and plutonium-239, respectively, indicate by the agreement between experimental data and theory that this is a valid assumption. If searching for short half-life delayed neutron groups had been the primary thrust of this experiment or if such groups had been indicated by the data the experimental parameters affecting the theoretical curves would necessarily have received more attention.

CHAPTER VII

CONCLUSIONS

The purpose of this experiment, as stated in Chapter I, was to show the validity of the theory developed in Chapter III with an isotopic analysis using cyclic activation of delayed neutrons and to evaluate the applicability of the method to safeguards and nuclear material control situations. Figures 16 to 22 all contain theoretical plots as well as experimental points. Agreement between experimental data, the points in Figures 19 and 20, and the curve resulting from using Keepin's delayed neutron groups and abundances in Equation (3-28) is within statistical deviations at most points along the curve. Discrepancies at the high cycle frequency knee are small and are in the direction expected considering the theoretical curve was generated with a single delayed neutron half-life for each delayed group, and each group actually represents several delayed neutron precursors of similar, but slightly different, half life. Data taken at short cycle times showed no evidence of short-half-life delayed neutron groups. The delayed neutron groups of 73.9 ms and 4.02 ms half lives reported at VPI[44] were, as they surmised, gamma-induced photodisintegrations of deuterium.

Like other non-destructive assay methods, the method of isotopic analysis developed in this experiment has virtues and weaknesses that recommend it to some accountability situations and not to others. The property measured by this method is a result of fission--the property of

interest in special nuclear materials. Use of neutron interrogation and consequent neutron response allows assay in the presence of ambient gamma radiation. Results of the assay include the quantity and isotopic composition of the fissionable material present. On the other hand, this method counts delayed neutrons, which occur after a small percentage of fissions, so to obtain reasonable levels of accuracy, the assay must be done with long count times, in a high interrogation flux, and/or for large samples. The equations of Chapter III, however, hold for any interrogation source that can be pulsed, and which produces a delayed response. Fast or thermal neutrons could have been used to induce fissions resulting in delayed neutrons. Use of thermal neutrons had the advantage of expedience and high reaction cross sections, and the disadvantage, due to the high absorption cross sections, of limited penetration in the samples.

In the nuclear fuel cycle this assay method should find use where non-destructive analysis is necessary, and where there is a need to distinguish between the various fissioning isotopes as well as for measuring the overall quantity of fissionable material. The input and discharge of fuel at the reactor, and various stages of the reprocessing process, are logical materials to be assayed with this method.

Fresh fuel fed to light-water reactors will normally be low enrichment uranium (less than five percent enriched) or plutonium mixed with natural uranium. When it is necessary to identify the fissioning isotope, this delayed neutron assay method could find use. Fuel rods are too large to conveniently move into and out of a fixed neutron beam; a chopper would have to be used to pulse the neutron beam, keeping the sample steady or

moving it only slowly through the assay station. Neutron generators or some means of chopping a neutron source, such as californium-252, could be employed if sufficient flux intensities could be obtained.

Fuel pellet diameters for light water reactors are about one centimeter. This is comparable to the mean free path for thermal neutrons in slightly enriched fuel, so that self-shielding effects are significant. However, the assumption of homogeneity is warranted in fresh reactor fuel and the system can be calibrated with a known standard in the same physical form as the material to be assayed to compensate for self-shielding. Such a calibration would also compensate for self-shielding of the epithermal delayed neutrons and prompt neutrons from fissions caused by delayed neutrons. However, these latter two effects have been shown[47] to be small and to cancel each other in samples with diameters similar to fuel rods.

A light water reactor fuel rod is about four meters long and contains about 130 grams of fissionable material. The error analysis in Chapter VI shows that a gram of uranium-235 can be assayed to a precision of two percent (one sigma) in about an hour. In an hour, 10 grams of uranium-235 can be assayed to a precision of about 0.6 percent. Ten grams of uranium-235 are contained in a segment of LWR fuel rod about 30 cm long. Nuclear Regulatory Commission and International Atomic Energy Agency safeguards requirements are that the limit of error of the material unaccounted for (LEMUF) be not more than 0.2 percent of the total material balance. Ten one hour assays of 30 cm segments of fuel rod would have a total assayed material precision of 0.2 percent. A large number of rods could be counted for 10 minutes or so, each achieving

the same result, but the assay of each rod might not be good enough to detect the single out-of-specs fuel rod. Using a chopper or pulse generator to produce the required activation cycle, a rod could be moved slowly through an assay station while an assay was being done to assay the whole rod in one pass. An hour count with an assay station active volume containing about 30 cm of fuel rod would produce an assay with a precision of 0.6 percent but no information on the axial concentration of fissionable material.

Plutonium bearing fuel rods could be assayed for plutonium-241 content, and from that, an estimate of plutonium-240 made. An hour's assay on a 30 cm segment of fuel rod would yield plutonium-239 and plutonium-241 quantities with standard deviations of three percent. Thirty or thirty-five such measurements would be required to meet safeguard requirements of 0.5 percent standard deviation in the LEMUF.

Some plutonium assay is done by calorimetry. Accurate use of calorimetry requires that the isotonic composition of the plutonium be known since plutonium-240 and plutonium-241 content changes the heat of decay.[13] Use of the assay method developed in this experiment to assay plutonium for plutonium-239 and plutonium-241 content and calculating plutonium-240 content from the plutonium-241 present can improve calorimetric assay precisions. Isotopic assays with precisions of three percent allow calorimetric assay for total plutonium better than 1.0 percent.

Spent fuel assay is of interest to the reactor operator, who owns the plutonium and uranium in the fuel, and the reprocessor, who needs the assay to evaluate the operating parameters of his process, such as how much neutron absorber to add to prevent an accidental cricitality.

Materials balance at the reprocessor is also important because the plutonium output of the plant is in a form that would be potentially useful to a diverter of limited sophistication. Assay of spent fuel is complicated by the fission product gamma-rays that accompany the fuel and the difficulty of obtaining representative samples from remotely operated dissolver tanks.

The mean free path of thermal neutrons is similar in spent fuel to what it is in fresh fuel. There is less fissionable material with high capture cross sections, but there is some added neutron absorption by fission products. Thermal neutron absorption resulting in fissions is less in spent fuel than in fresh fuel.

Intense gamma-ray fields are associated with spent fuel at discharge from a reactor and at all early stages of reprocessing. In this experiment the gamma discrimination of BF_3 detectors was found to be insufficient to handle these fields. However, with gamma-ray shields for the BF_3 or ^3He detectors and pulse rise-time discrimination it should be possible to assay spent fuel by delayed neutrons.

The plutonium in spent fuel contains both plutonium-239 and -241. Composition for LWR discharge fuel is about 60 percent plutonium-239, 24 percent plutonium-240, and 16 percent plutonium-241 depending on burnup, reactor design, and reactor operation.[45] The plutonium-240 contributes a neutron background from spontaneous fission decay, which is increased further from (α,n) reactions due to transuranic elements. The results in Chapter VI were obtained with low neutron backgrounds; however, the effect of a large background can be considered in the error analysis. A neutron background equal to the count rate would increase

the standard deviation of the count rate by the square root of two. Indications from the literature[46] are that the neutron background from spent fuel is not large enough to preclude analysis by delayed neutrons. When plutonium-240 is present in the samples, increased interrogation flux is more efficient in bettering assay precision than increased sample size because statistics gained by more fissions in a larger sample are partially offset by increased plutonium spontaneous fission background.

LWR spent fuel will contain three fissionable isotopes, uranium-235, plutonium-239, and plutonium-241. The analysis done in Chapter VI was for two fissioning isotopes. To accommodate three fissioning isotopes a three parameter curve fitting numerical analysis could be applied to the data, or the analysis equipment could be calibrated with plutonium containing the approximate plutonium-239 to plutonium-241 ratios expected and a two parameter analysis done for uranium and total plutonium. Considering only delayed neutron fractions the results in Table 8 indicate that standard deviations of two percent for uranium-235 and 11 percent for plutonium-239 may be obtained after one hour of counting with a 30 cm length of spent fuel rod containing uranium-235 and plutonium in about equal atom percents at one percent enrichment. Interference from plutonium-241 delayed neutrons--the plutonium-241 delayed neutron contribution makes the total plutonium response more like the response of uranium-235 than plutonium-239--and neutron background from plutonium-240 spontaneous fission would increase these standard deviations. The IAEA requires a standard deviation of 0.8 percent for the reprocessing uranium material balance and 1.0 percent for plutonium. If a 30 cm sample of spent fuel would yield a total Pu assay with a standard devia-

tion of 11 percent in an hour, the IAEA requirements could be met with 100 samples. The spent fuel from an HTGR contains uranium-233 and uranium-235, which have delayed neutron signatures that are more separable than the signatures of uranium-235 and plutonium-240. HTGR fuel must be crushed and burned to get the fissionable material out of the carbon and silicon carbide microspheres and precision is lost in these processes. A non-destructive assay using the method developed here could make an assay on HTGR fuel as well as current wet chemical and mass spectrographic methods, with one to five percent accuracy, in less time and at less cost.

The objectives of this project were to develop an assay method based on cyclic activation of delayed neutrons and to assess its applicability to assay of nuclear materials. The equations developed in Chapter III describe a cyclic activation technique that is useful in activation analysis situations beyond those explored in these experiments. The shape of the activation response as a function of activation cycle frequency can be used to determine half lives and abundances of activation products. Activation cycle frequencies can be predicted from Chapter III equations to enhance or discriminate against certain half lives in a gamma-ray spectrum analysis.

Testing of the assay method was done with the experiments conducted in the GTRR thermal neutron beam from H-1. These experiments indicated that the equations of Chapter III did predict the response to cyclic activation adequately and that a useful assay of nuclear fuel can be obtained from differences in delayed neutron group abundances and half lives. The assay method developed here is not superior to currently

available methods for total fissile material assay--counting at only very short cycle time is comparable to other delayed neutron assay methods; but for isotopic assay of fissile materials there do not seem to be other non-destructive methods available that are more precise. The method developed here seems to be most suitable for the isotopic assay of fresh and spent reactor fuel, where its non-destructive nature and potential resistance to fission product gamma-rays are a significant advantage. Count times may be too long to consider seriously 100 percent throughput for fresh or spent fuel from a reactor, but current safeguard regulations can be met with less sampling problems than would be encountered with wet chemical or mass spectrographic analysis. A significant disadvantage of the method is the need for a strong source of thermal neutrons. However, the equations developed in Chapter III hold for a pulsed neutron generator or chopped isotopic neutron source as well as for cyclic activation in a reactor beam, if the source is sufficiently strong to produce enough delayed neutrons for good statistics. A reactor neutron beam may well be made available at the power plant where the fuel is used if such a feature is incorporated into the plant design.

The programs written for these experiments handle only two fissioning isotopes. This is sufficient for the assay of HTGR fuel, uranium-233 and uranium-235, or the isotopic assay of plutonium, plutonium-239 and plutonium-241. To establish this assay method as a useful tool in the assay of LWR spent fuel the effect of plutonium-241 on the assay of plutonium-239 and uranium-235 will have to be investigated. Further work should also be done to determine the practicality of using a pulsed

neutron source or a chopped-beam isotopic source to make the assay equipment more portable.

APPENDIX A

CHARACTERISTICS OF THE BF_3 NEUTRON DETECTORS

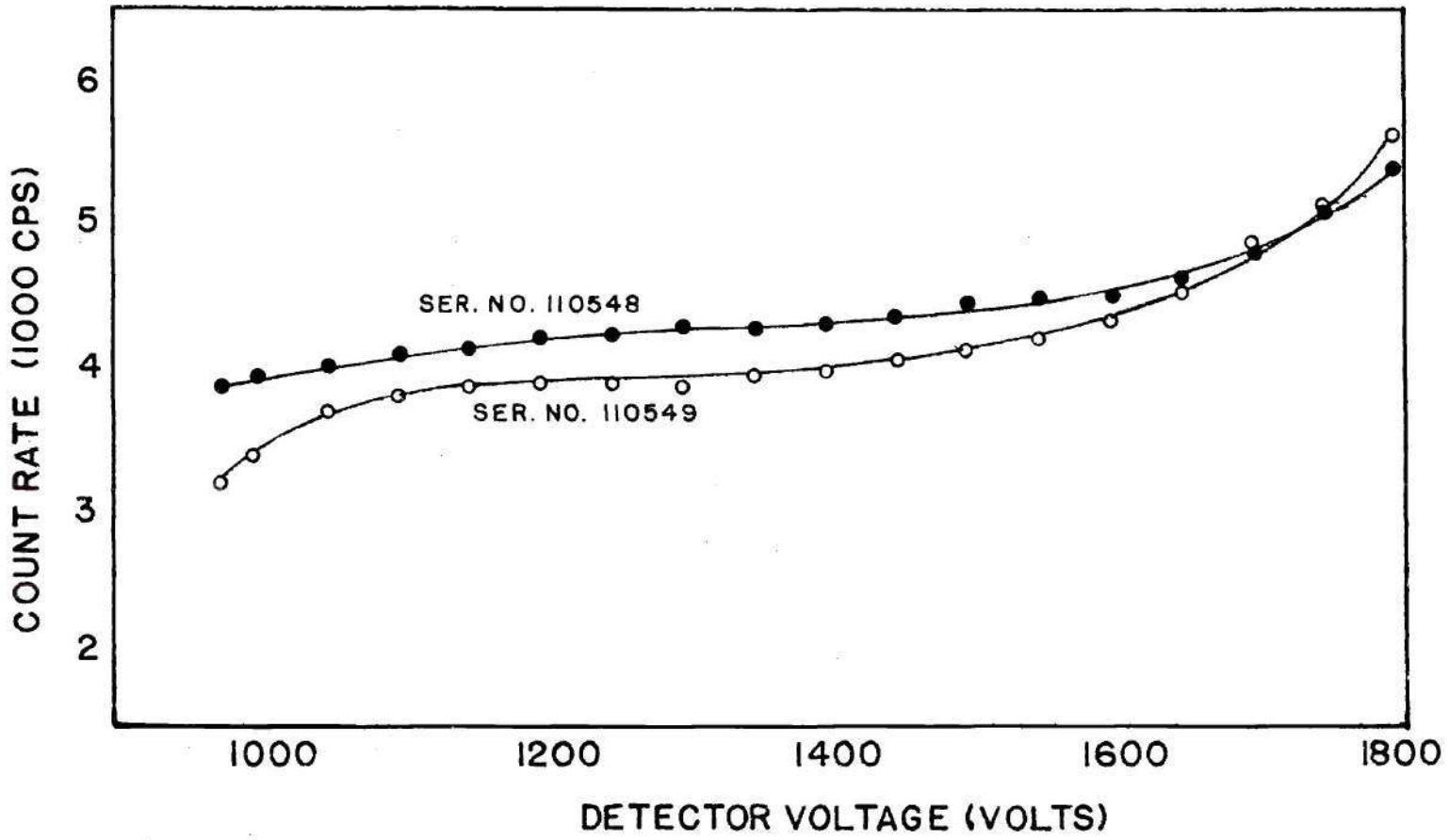

Figure 28. Count-Voltage Curves for PF_3 Filled LND Detectors Serial Numbers 110548 and 110549

REUTER-STOKES

UTER-STOKES ELECTRONIC COMPONENTS, INC.

18530 South Miles Parkway
Cleveland, Ohio 44128

MODEL NO. RSN-7A

SERIAL NO. K-723

PLATEAU CURVE

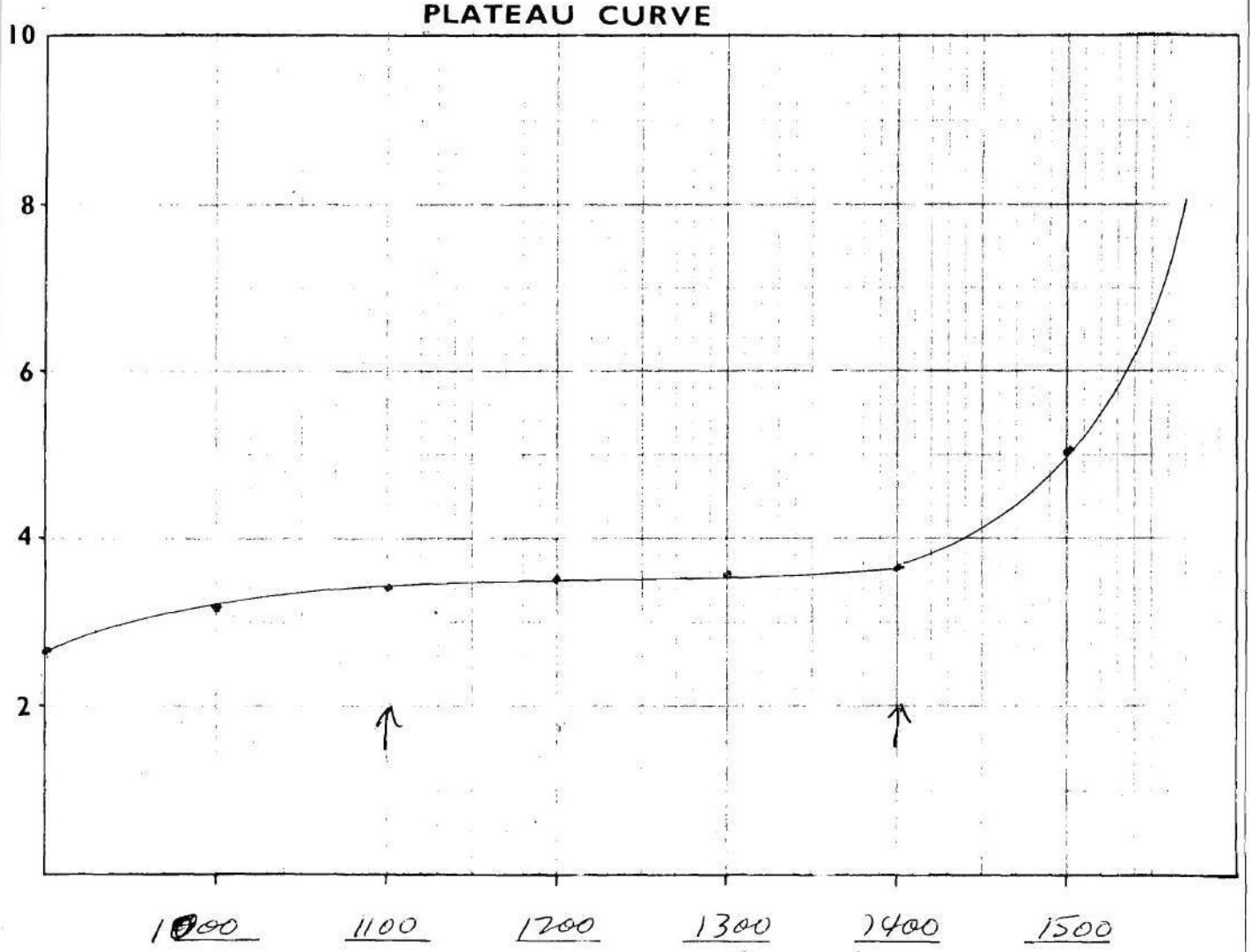

ATEAU LENGTH 300 VOLTS

SLOPE 2.1 % 100 VOLTS

OLTAGE SENSITIVE SYSTEM

AIN 32,500

SCRIMINATOR INPUT 0.28MV

IPUT CAPACITANCE 22.0 pf

ETECTOR CAPACITANCE 7.0 pf

ESTED BY RLB DATE 6/5/68

SOURCE PuBe

PARAFFIN MODERATOR

SENSITIVITY 4.7 CPS/NV

RESOLUTION FWHM 3.0%

FILL GAS BF_3

PRESSURE 40 CM OF Hg

st results quoted are reference values for REUTER-STOKES Quality Control Department age. Actual values will vary somewhat with test geometry and electronics employed.

TEST FORM 20

APPENDIX B

FLOW CHART FOR THE DATA ANALYSIS

COMPUTER PROGRAM DELTAR

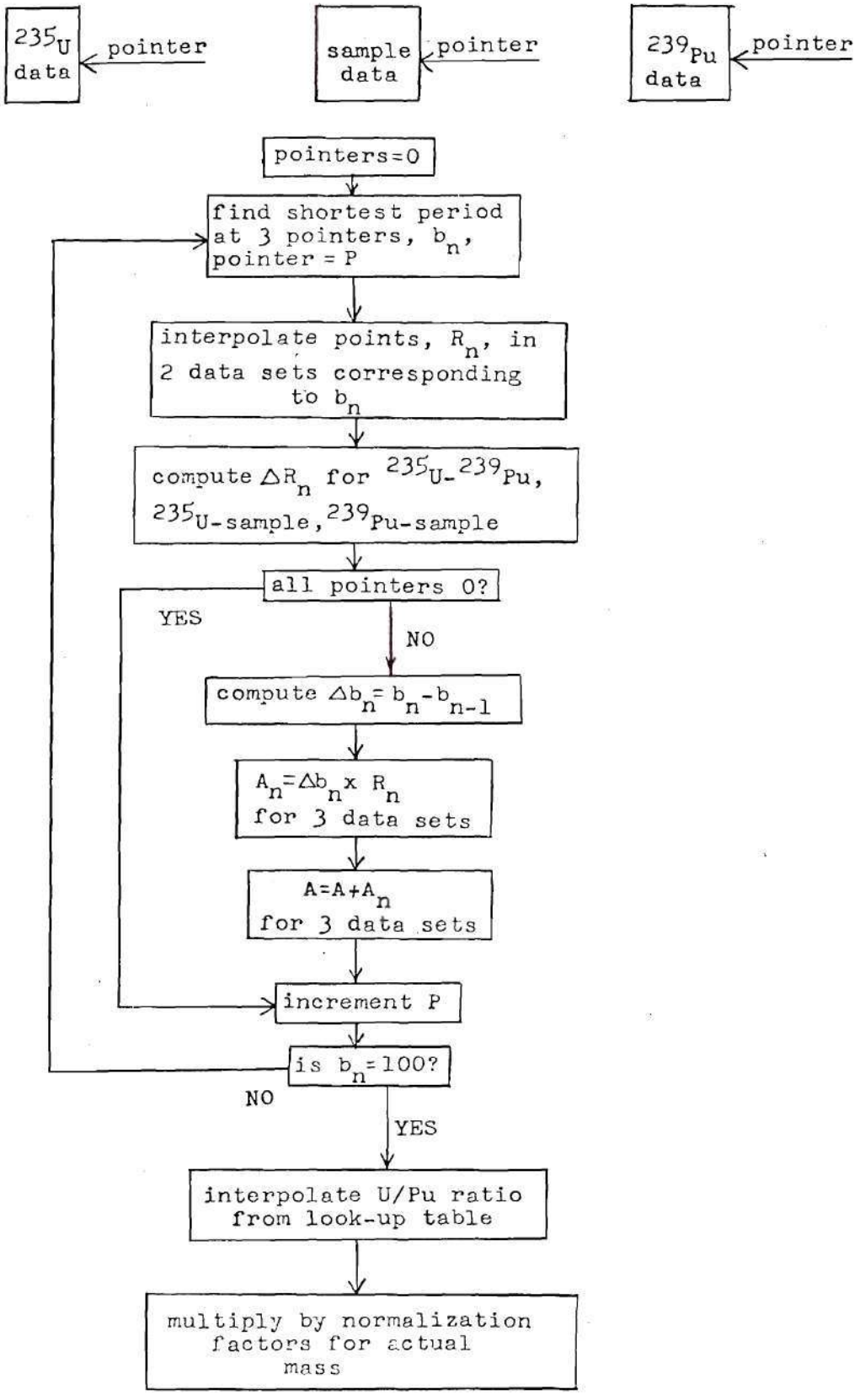
^{235}U data
pointer
sample data
pointer
^{239}Pu data
pointer
pointers=0
find shortest period at 3 pointers, b_n, pointer = P
interpolate points, R_n, in 2 data sets corresponding to b_n
compute ΔR_n for ^{235}U-^{239}Pu, ^{235}U-sample, ^{239}Pu-sample
all pointers 0?
YES
NO
compute $\Delta b_n = b_n - b_{n-1}$
$A_n = \Delta b_n \times R_n$ for 3 data sets
$A = A + A_n$ for 3 data sets
increment P
is b_n=100?
NO
YES
interpolate U/Pu ratio from look-up table
multiply by normalization factors for actual mass

BIBLIOGRAPHY

1. H. A. Bethe, "The Necessity of Fission Power," Scientific American, 234, 21-31 (1976)

2. Safeguards Dictionary, Brookhaven National Laboratories, WASH-1173 (1973).

3. H. C. Paxton, J. T. Thomas, D. Callihan, and E. B. Johnson, "Critical Dimensions of Systems Containing U^{235}, Pu^{239}, and U^{233}," Los Alamos Scientific Laboratory and Oak Ridge National Laboratory, TID-7028 (1964).

4. H. C. Paxton, "Los Alamos Critical Mass Data," Los Alamos Scientific Laboratory, LAMS-3067 (1964).

5. M. Willrich (Ed.), International Safeguards and Nuclear Industry, Johns Hopkins University Press, Baltimore, Md., 1973.

6. Fuel Trac, Nuclear Assurance Corporation, Atlanta, Ga., 1975.

7. A. E. Evans, Jr., "Non-destructive Assay of Fissile Material Samples in Support of Nuclear Safeguards," Los Alamos Scientific Laboratory, LA-UR-73-1595 (1973).

8. Code of Federal Regulations 10 CFR 70, Federal Register 38, No. 21 (1973).

9. Treaty on the Non-Proliferation of Nuclear Weapons Review Conference, International Atomic Energy Agency Bulletin 17, No. 2, 15 (1975).

10. "Fuel," Nuclear News, 18, 50 (1975).

11. G. R. Keepin, "Non-Destructive Detection, Identification, and Analysis of Fissionable Material," USAEC Rept. LA-3741 (1967).

12. J. E. Lovett, Nuclear Materials Accountability Management Safeguards, Monograph, American Nuclear Society, Hinsville, Illinois 1974.

13. F. X. Haas and W. W. Strohm, "Gamma-Ray Spectrometry for Calorimetric Assay of Plutonium Fuels," IEEE Trans. on Nuc. Sci., NS-22 734-378 (1975).

BIBLIOGRAPNY (Continued)

14. R. T. Jones (Ed.), "Selected Measurement Methods for Plutonium and Uranium in the Nuclear Fuel Cycle," USAEC Report TID-7029 (1963).

15. C. J. Rodden (Ed.), "Selected Measurement Methods for Plutonium and Uranium in the Nuclear Fuel Cycle," USAEC Report TID-7029 (2nd Edition) (1972).

16. H. Berger and N. P. Lapinski, "Improved Sensitivity and Contrast, Track Etch Thermal Neutron Radiography," Trans. Amer. Nuc. Soc., 15, 213-214 (1972).

17. G. R. Keepin (Ed.), "Nuclear Analysis Research and Development Program Status Report," Los Alamos Scientific Laboratory, LA-5091-PR (1972).

18. N. C. Rasmussen, "A Review of Passive Methods," USAEC Report WASH-1147, 96-108 (1970).

19. J. E. Lovett and D. B. James, "Plant Instrumentation Program, Second Quarterly Report, July-September 1970," USAEC Report BHO-69-2 (1970).

20. C. H. Englemann and J. E. Pettit, "Non-Destructive Determination of Nuclear Fuel Burnup Using Gamma Spectrometry," Centre Etudes Nucléaires, Saclay, France (1964).

21. J. A. Sovka and N. C. Rasmussen, "Nondestructive Analysis of Irradiated MITR Fuel by Gamma Ray Spectrometry," Massachusetts Institute of Technology, MITNE-64 (1965).

22. A. J. Fudge, R. Causer and L. Murphy, "Nondestructive Examination of Nuclear Fuel for Burnup by Gamma Scanning," International Symposium on Working Methods in High Activity Hot Laboratories, 1, 101-110 (1966)

23. M. M. Sawan and R. W. Conn, "Neutron Pulse Slowing Down in Heavy Media, Analysis with Application of the Lead Spectrometer," Nucl. Sci. Eng., 54, 127 (1974).

24. R. W. Conn, F. Beranek, J. Darby and W. F. Vogelsang, "Progress with the Lead Spectrometer for Fissile Materials Assay," Trans. Am. Nucl. Soc., 21, 489-490 (1975).

25. J. E. Foley, "Random Source Interrogation System for Nondestructive Assay of Fissionable Materials," Trans. Am. Nucl. Soc., 15, 670-671 (1972).

BIBLIOGRAPHY (Continued)

26. G. R. Keepin (Ed.), "Nuclear Safeguards Research and Development," Los Alamos Scientific Laboratory, LA-4315 (1969).

27. J. E. Strain, W. J. Ross, G. A. West and J. W. Landry, "The Design and Evaluation of a Delayed-Neutron Leached-Hull Monitor," Oak Ridge National Laboratory Report ORNL-4135 (1967).

28. F. F. Dyer, J. F. Emery and G. W. Leddicotte, "A Comprehensive Study of the Neutron Activation Analysis of Uranium by Delayed-Neutron Counting," Oak Ridge National Laboratory Report ORNL-3342 (1962).

29. J. M. Jamieson, "Determination of Multiple Half-Lives by Cyclic Activation," 12th Annual ANS Student Conf. Trans., Georgia Tech, Atlanta, 88 (1969).

30. C. F. Masters, M. M. Thorpe and D. B. Smith, "Measurement of Absolute Delayed-Neutron Yields from 3.1 and 14.9 MeV Fission," Nucl. Sci. Eng., 36, 202-209 (1969).

31. G. R. Keepin, R. H. Auguston and R. B. Walton, "Los Alamos Scientific Laboratory Safeguards Research and Development Program," USAEC Report WASH-1147, 110-131 (1970).

32. C. N. Henry, H. O. Menlove and R. H. Auguston, "Delayed Neutron Kinetic Response Methods for Nondestructive Analysis of Reactor Fuel Materials," Los Alamos Scientific Laboratory, LA-DC-9758 (1967).

33. R. B. Roberts, R. C. Meyer and P. Wang, "Further Observations on the Splitting of Uranium and Thorium," Physical Review, 55, 510-511 (1939).

34. G. R. Keepin, T. F. Wimett and K. R. Ziegler, "Delayed Neutrons from Fissionable Isotopes of Uranium, Plutonium, and Thorium," Physical Review, 107, 1044-1049 (1957).

35. G. R. Keepin, Physics of Nuclear Kinetics, Addison-Wesley, Reading, Mass., 1965.

36. G. R. Keepin, "Interpretation of Delayed Neutron Phenomena," J. Nucl. Eng., 7, 13-34 (1958).

37. E. C. Campbell, "Semi-Annual Progress Report for the Period Ending March 20, 1955," Oak Ridge National Laboratory Report ORNL-1879 (1955).

BIBLIOGRAPHY (Concluded)

38. W. W. Givens, W. R. Mills, Jr. and R. L. Caldwell, "Cyclic Activation Analysis," Proc. Int'l. Conf. on Modern Trends of Activation Analysis, 139 (1968).

39. W. W. Graham and D. M. Walker (Eds.), "Safety Analysis Report for the 5 Mw Georgia Tech Research Reactor," Georgia Institute of Technology, Atlanta (1966).

40. G. R. Keepin, "Prediction of Delayed-Neutron Precursors," Physics Review, 106, 1359-1360 (1957).

41. Signetics Digital, Linear, and MOS Data Book, Signetics Corporation, Sunnyvale, California (1972).

42. W. J. Price, Nuclear Radiation Detection, McGraw-Hill, New York, 2nd Edition, 1964.

43. R. A. Forster, H. O. Menlove and D. L. Matthews, "A ^{124}Sb Photoneutron System for Fissile Material Assay," Trans. Am. Nucl. Soc., 30, 80 (1974).

44. R. J. Onega, P. W. Forbes, A. K. Furr and A. Robeson, "Measurement of Short-Lived Delayed Photoneutrons from Fission-Fragment Gamma Rays of ^{235}U in Heavy Water," Nucl. Sci. Eng., 32, 49-55 (1968).

45. M. Willrich and T. B. Taylor, Nuclear Theft: Risks and Safeguards, Ballinger Publishing Company, Cambridge, Mass., 1974.

46. T. Gozani, "On the Measurement of Fissile Material Content in LWR Spent Fuel," Trans. Am. Nucl. Soc., 21, 488 (1975).

47. G. R. Keepin, "Nondestructive Detection, Identification, and Analysis of Fissionable Material," USAEC Report WASH-1076, 150-171 (1967).

VITA

John McCloskey Jamieson was born in Phoenix, Arizona on August 8, 1944. He graduated from Jenkins High School in 1962 and entered the co-operative program in electrical engineering at Georgia Tech.

In 1967, Mr. Jamieson received a Bachelor of Electrical Engineering degree from Georgia Institute of Technology and began graduate studies in Nuclear Engineering at Georgia Tech. During his studies toward a Master's degree, he received a NDEA fellowship. He married Barbara Harper in 1968.

Mr. Jamieson received a Master's degree in Nuclear Engineering in 1969 and continued his studies toward a Doctorate in Nuclear Engineering at Georgia Tech. During this time, Mr. Jamieson supported himself by teaching physics labs at Georgia State University, writing computer programs, and doing electrical engineering work for Technical Analysis Corporation. He is currently working for Technical Analysis Corporation as Director of Engineering.